The Indo-Pacific drivers of the Indian Summer Monsoon-Decadal Variability and Prediction

A thesis submitted during 2021 to the University of Hyderabad in partial fulfilment of the award of a Ph.D. degree in Earth and Space Sciences

by

Feba Francis

Reg. No: 15ESPE01

Under the supervision of

Prof. Karumuri Ashok



Centre for Earth, Ocean and Atmospheric Sciences School of Physics

University of Hyderabad
(P.O.) Central University, Gachibowli,
Hyderabad-500 046
Telangana
India



This is to certify that the thesis entitled "The Indo-Pacific drivers of the Indian Summer Monsoon-Decadal Variability and Prediction", submitted by Feba Francis bearing Reg. No. 15ESPE01, in partial fulfilment of the requirements for the award of the degree of Doctor of Philosophy in Earth Sciences, is a bonafide record of the work that has been carried out by him under my supervision and guidance.

This thesis has not been submitted previously in part or in full to this or any other University or Institution for the award of any degree or diploma.

Prof. Karumuri Ashok

Supervisor

Head

Head Atmospheric Sciences

University of Hyderabad

Centre for Earth Ocean and Atmospheric Sciences

Dean

School of Physics

School of Physics
University of Hyderahad
Hyderahad-500 046, INDIA



CERTIFICATE

This is to certify that the thesis entitled "The Indo-Pacific drivers of the Indian Summer Monsoon-Decadal Variability and Prediction" submitted by Feba Francis bearing registration number 15ESPE01 in partial fulfilment of the requirements for the award of Doctor of Philosophy in the School of Physics is a bonafide research work carried out by her under my supervision and guidance.

The thesis is free from plagiarism and has not been submitted previously, either in part or in full, for the award of any academic degree or diploma to this or any other university or institution.

Further, the student has the following publication(s) before submission of the thesis for adjudication and has produced evidence for the same in the form of acceptance letter or the reprint in the relevant area of his research:

- Feba, F., Ashok, K. & Ravichandran, M. "Role of changed Indo-Pacific atmospheric circulation in the recent disconnect between the Indian summer monsoon and ENSO", Climate Dynamics (2018). https://doi.org/10.1007/s00382-018-4207-2
 This publication appears in Chapter 3 of the dissertation
- K. Ashok, <u>F. Feba</u> and C T Tejavath. "The Indian Summer Monsoon Rainfall and ENSO: A review", *Mausam*, 70, 3 (July 2019), 443-452.
 This publication appears in **Chapters -1 & 3** of the dissertation
- 3. <u>Feba F</u>, Ashok K, Collins M and Shetye SR (2021) Emerging Skill in Multi-Year Prediction of the Indian Ocean Dipole. *Frontiers in Climate* 3:736759. doi: 10.3389/fclim.2021.736759

This publication appears in Chapters – 4 & 5 of the dissertation

and has made presentation in the following conferences:

- Feba, F., K Ashok & M Collins., 'Decadal Prediction of Indian Ocean Dipole.'
 European Geophysical Union (EGU)- EGU General Assembly 2020, Vienna, Austria
 & online from 4 8 May 2020 (Poster Presentation)
- Feba, F., K K Vikas & K Ashok, 'Indian Summer Monsoon impacts on Bay of Bengal Cyclones through River Water Discharge.' The Australian Meteorological and Oceanographic Society Annual Meeting and the International Conference on Tropical Meteorology and Oceanography (AMOS-ICTMO 2019), Darwin, Australia from 11-15 June 2019. (Poster Presentation)
- Feba, F., K Ashok & M. Ravichandran 'Decadal Variability of Winds over Tropical Indian Ocean' and 'Decadal Prediction of Indian Summer' CLIVAR Open Science Conference Qingdao, China 2016. (Poster Presentations)
- 4. <u>Feba, F.</u>, K Ashok & M. Ravichandran, "Returning to The Weakening Teleconnections of Tropical Pacific and Indian Summer Monsoon Rainfall" in National Conference at Indian Institute of Science, Bengaluru, July, 2015.

Further, the student has passed the following courses towards the fulfilment of the coursework required for a Ph.D.

Course code	Course	Credit	Pass/Fail
ES801	Earth System Sciences	4	Pass
ES805	Research Methodology	3	Pass
ES806	Mathematics for Earth Sciences	4	Pass
ES807	Interdisciplinary Course	3 -	Pass
AP811-830	Special paper on specific research topic	2	Pass
	Total	16	

Prof. Karumuri Ashok

frami APhl

Supervisor

Head Centre for Earth, Ocean &

Centre for Earth Ocean and Atmospheric Sciences

Hyderabad-500 046, INDIA.

Dean

School of Physics

DEAN

School of Physics
University of Hyderahad

vderabad-500 046, INDIA

DECLARATION

I, Feba Francis, hereby declare that the thesis entitled "The Indo-Pacific drivers of the Indian Summer Monsoon-Decadal Variability and Prediction" submitted by me under the guidance and supervision of Prof. Karumuri Ashok is a bonafide research work. I also declare that it has not been submitted previously in part or in full to this University or any other University or institution to award any degree or diploma.

Date:22/11/2021

Feba Francis

Reg. No. 15ESPE01

Jams 1301 31/5/12

UNIVERSITY OF HYDERABAD NOTIFICATION OF RESULTS

Course Work: Ph.D., Centre for Earth and Space Sciences,

Month & Year: April'2017 Semester -II

Sl. No	Regn.No.	Name of the Student	CORE/COMPULSORY COURSES & NO OF CREDITS AND GRADES				
No			ES 801 Credits 4	ES 805 Credits 3	ES 806 Credits 4	ES 807 Credits 3	ES 811- 830 Credits 2
1	13ESPE01	KONETI SUNITHA	Pass	Pass	Pass	Pass	Pass
2	13ESPE03	DEBASHRI GARAI	Pass	Pass	Pass	Exempted	Pass
3	15ESPE01	FABA FRANCIS	Pass	Pass	Pass	Pass	Pass
4	15ESPE02	HEMADRI BHUSHAN AMAT	Pass	Pass	Pass	Fail	Pass
5	15ESPE03	K. MALLESH	Pass	Pass	Pass	Exempted	Pass
6	15ESPE04	CHENNU RAMU	Pass	Pass	Pass	Pass	Pass
7-	15ESPE05	GOVARDHAN DANDU	Pass	Pass	Pass	Pass	Pass
8	15ESPE07	BOYAJ ALUGULA	Pass	Pass	Pass	Pass	Pass
9	15ESPE09	TEJAVATH CHARAN TEJA	Pass	Pass	Pass	Pass	Pass
10	15ESPE10	BILLINGI TARUN KUMAR	Pass	NA	Pass	NA	Pass
11	16ESPE01	RESHMA M.R.	Pass	NA	Pass -	Exempted	Pass
12	16ESPE02	SEEDABATTULA V BALAJI MANASA RAO	Pass	NA	Pass	NA	Pass
13	16ESPE04	SUNIT MOHANTY	Pass	NA	Pass	NA .	Pass
14	16ESPE05	TARUN THOMAS T.	Pass	NA	Pass	NA	Pass

Course No. Title of the Course

ES 801 Earth system sciences -4

ES 805 Research Mehtodology -3

ES 806 Mathematics for Earth Sciences -4

ES 807 Interdisciplinary course -3

ES 811-830 Special Paper on Specified Research Topic -2

NA - NOTAPPEARED

Dated: 29.05.2017

Controllof Examination 30-3

To

Head, Centre for Earth and Space Sciences Dean School of Physics

2 1000

Dedicated to

Charan, Vikas and My Family

Acknowledgements

I must begin by thanking my supervisor **Prof. K. Ashok**, University of Hyderabad for his patient guidance, understanding disposition, valuable advices and consistent inspiration, throughout my PhD.

I am grateful for my co-authors, Prof. **Mat Collins**, University of Exeter, **Dr. M Ravichandran**, MOES Secretary and **Prof. Satish S Shetye** and for their valuable insights in every step and helping me improve my work further.

I wish to express my gratitude to my doctoral committee members, **Dr. S Srilakshmi**, **Dr. Syed**Maqbool Ahmed and **Dr. Vijay Kanawade** for their constant support and incessant encouragement.

I am grateful to the Head of the Centre for Earth, Ocean and Atmospheric Sciences, **Prof. K. S. Krishna**, and former Heads, **Prof. M. Jayananda**, **Prof. V C Chakravarthi** and **Prof. A C Narayana**for providing the facilities and support in the centre.

I would like to acknowledge Council of Scientific & Industrial Research-Junior Research Fellowship for providing financial support.

I wish to thank all my teachers for the many lessons; academic and otherwise. I wish to thank my friends and workmates Charan, Vikas, Boyaj, Mathew, Abin, Hemadri, Vijay, Bidya, Fousiya, Govardhan and Yagnesh for their company, support and fruitful scientific discussions. I want to thank my friends Vivek, Rama Krishnan, Devender, Rohit, Basha, Archit, Anupriya and Nisha for their moral and emotional support. Last but not least; I am deeply indebted to my family, who have always stood by me.

Feba Francis

Contents

	Page No.
Certificate	
Course certificate	
Declaration	
Acknowledgements	
List of Figures	i
List of Tables	iii
Abbreviations	iv
List of publications/conferences	v
Abstract	vii
Chapter-1 Introduction	1
1.1 The Indian Summer Monsoon	1
1.2 The El Niño Southern Oscillation	9
1.3 The El Niño Southern Oscillation and the Indian Summer Monsoon	12
1.4 The Indian Ocean Dipole	17
1.5 The Indian Ocean Dipole and the Indian Summer Monsoon	19
1.6 Decadal Prediction	21
1.7 Aims and Objectives	22
Chapter-2 Data and Methods	25
2.1 Datasets	25
2.1.1 Observational and Reanalysis Datasets	25
2.1.2 Model Datasets	27
2.1.3 Preprocessing of Model Output	29
2.2 Climate Indices	30
2.2.1 NIÑO3 and NIÑO4 indices	30

2.2.2 Warm Water Volume	30
2.2.3 Dipole Mode Index	31
2.3 Statistical Methods	31
2.3.1 Composite Analysis	32
2.3.2 Linear Correlation	32
2.3.3 Linear Regression	33
2.3.4 Determination of Statistical Significance	34
2.3.5 Empirical Orthogonal Function (EOF) analysis	35
Chapter-3 Recent changes in the Indian Summer Monsoon	37
associated Indo Pacific atmospheric circulation	
1.1 The ENSO indices	37
1.2 The weakening ENSO-ISM relations	38
1.2.1 The concurrent relation between ENSO indices and ISMR	39
1.2.2 The lead-lag relation between ENSO indices and ISMR	40
3.3 Analysis of the surface winds over the tropical Indo-Pacific	42
3.4 Conclusion	49
Chapter-4 Exploring the Decadal prediction skills of Indo-	51
Pacific drivers of the Indian Summer Monsoon	
4.1 Decadal Prediction	51
4.2 Preprocessing of Model Output	53
4.3 Lead Prediction skills for ENSO	54
4.4 Lead Prediction skills for IOD	55
4.5 Fidelity of the Simulated IOD	58
4.6 Conclusion	61
Chapter-5 Source of Decadal Predictability of The Indian	62
Ocean Dipole	
5.1 Sources of Decadal Prediction	62
5.2 Source of the IOD Predictability on a decadal scale	63
5.3 Source of IOD as predicted in the models	68

5.4 Conclusion	71
Chapter-6 Conclusions and Future Scope	72
6.1 Summary	72
6.2 Future Scope	74
List of References	76

List of Figures

		Page No
Chapter 1		
Figure 1.1	Monthly means of rainfall over India	2
Figure 1.2	Indian Summer Monsoon Onset Dates over different regions	3
Figure 1.3	The mean monsoon rainfall over India during June to September	4
Figure 1.4	A Schematic representation of the Semi-permanent features	6
	of the Indian summer monsoon	
Figure 1.5	The mean sea level pressure during June to August overlayed	7
	with the wind vectors	
Figure 1.6	The interannual variability of the Indian summer rainfall	8
Figure 1.7	A schematic representation of SST, thermocline, Walker	10
	circulation, and precipitation over the Pacific Ocean during	
	different phases of ENSO	
Figure 1.8	The Indian Summer Monsoon Rainfall composites during	13
	El Niño and La Niña years	
Figure 1.9	Linear simultaneous correlation between NINO3.4 index with	14
	the Indian Summer Monsoon Rainfall	
Figure 1.10	A schematic representation of SST and thermocline in the	18
	equatorial Indian Ocean during positive and negative phases	
	of the IOD	
Figure 1.11	The Indian Summer Monsoon Rainfall composites during	20
	positive and negative phases of IOD	
Figure 1.12	Decadal prediction as both, initial value problem and forced	22
	boundary problem	
Chapter 2		
Figure 2.1	The SST indices Niño4, Niño3, Niño 3.4, and Niño 1+2 and	31
6	The WWV index	

Chapter 3

Figure 3.1	Correlation of ENSO Indices (WWV, NINO3, and NINO4)	39
	with ISMR during JJAS	
Figure 3.2	Correlation of ENSO Indices (WWV, NINO3, and NINO4)	4(
	with ISMR during FMAM	
Figure 3.3	Correlation of ISMR with surface winds (1000 mb) during JJAS	43
	with zonal correlations	
Figure 3.4	Correlation of ISMR with surface winds (1000 mb) during JJAS	44
	with meridional correlations	
Figure 3.5	Regression of ISMR with surface winds (1000 mb) during JJAS	45
	with zonal regressions	
Figure 3.6	Regression of ISMR with surface winds (1000 mb) during JJAS	46
	with zonal regressions	
Figure 3.7	Difference of regression of ISMR with surface winds (1000 mb)	47
	during 1978–2008 from 1958–2008	
Figure 3.8	Sea level pressure variability of Mascarene High	48
Chapter 4	!	
Figure 4.1	Pre-processing of the output data from all the models	53
Figure 4.2	Anomaly correlations between observed NINO3 index with	54
	the corresponding predicted NINO3 index at different lead	
	years for various models	
Figure 4.3	Anomaly correlations between observed IODMI with	55
	the corresponding predicted IODMI at different lead years	
	for various models	
Figure 4.4	Evolution of persistence skills	56
Figure 4.5	The second mode from the EOF analysis of the tropical Indian	58
	Ocean SST, from a) HadISST b) MIROC5 and c) CanCM4	
Figure 4.6	The direct comparisons of predicted IODMI with the observations	59
	from various models	

Chapter 5

Figure 5.1	Spatial distribution of the anomaly correlation of HadISST derived	63
	IODMI with vertically averaged subsurface temperatures from	
	ORAS4 (over 300m to 800m depth)	
Figure 5.2	Vertical distribution of anomaly correlation of IODMI with	65
	previous years' subsurface temperatures, averaged annually	
Figure 5.3	Same as Figure 5.1 but vertically averaged annually over the surface	66
	to 100m depth	
Figure 5.4	A schematic representation of the pathway of the signals from	67
	the Southern Ocean to the Equatorial Indian Ocean	
Figure 5.5	Spatial distributions of the anomaly correlation of MIROC5	68
	and CanCM4 derived IODMI with vertically averaged subsurface	
	temperatures annually-averaged from the same respective models	
	from 10 years before the occurrence of the IOD event.	
Figure 5.6	Spatial distributions of the anomaly correlation of MIROC5 and	69
	CanCM4 derived IODMI with vertically averaged subsurface	
	temperatures annually-averaged from the same respective models from	
	4 years to 1 year before the occurrence of the IOD event.	

List of Tables

Chapter 2

Table 2.1 The analyzed models with the initialization techniques, number of the ensemble- members, institution, and references

Abbreviations

ACC Antarctic Circumpolar Current

AISMR All India Summer Monsoon Rainfall

BCC-CSM Beijing Climate Center Climate System Model, Version 1.1

CanCM4 Canadian Coupled Global Climate Model, Fourth Generation

CMIP5 Coupled Model Intercomparison Project- Phase 5

EMUC East Madagascar Undercurrent

EOF Empirical Orthogonal Function

ENSO El Niño Southern Oscillation

EQUINOO Equatorial Indian Ocean Oscillation

FMAM February, March, April and May

GFDL Geophysical Fluid Dynamics Laboratory Climate Model, Ver 2.1

Hadley Centre Sea Ice and Sea Surface Temperature dataset

IMD India Meteorological Department

IOD Indian Ocean Dipole

IODMI Indian Ocean Dipole Mode Index

ISM Indian Summer Monsoon

ISMR Indian Summer Monsoon Rainfall

ITCZ Inter-Tropical Convergence Zone

JJAS June, July, August and September

MIROC5 Model for Interdisciplinary Research on Climate, Version 5

PDO Pacific Decadal Oscillation

SLP Sea-Level Pressure

SODA Simple Ocean Data Assimilation Reanalysis 2.1.6 dataset

SON September, October and November

SST Sea Surface Temperature

TIO Tropical Indian Ocean

WWV Warm Water Volume

List of publications/conferences

Publications from the thesis

- Feba, F., Ashok, K. & Ravichandran, M."Role of changed Indo-Pacific atmospheric circulation in the recent disconnect between the Indian summer monsoon and ENSO", Climate Dynamics (2018). https://doi.org/10.1007/s00382-018-4207-2
- 2. K. Ashok, **F. Feba** and C T Tejavath. "The Indian Summer Monsoon Rainfall and ENSO: A review", *Mausam*, 70, 3 (July 2019), 443-452.
- 3. <u>Feba F</u>, Ashok K, Collins M and Shetye SR (2021) "Emerging Skill in Multi-Year Prediction of the Indian Ocean Dipole". *Frontiers in Climate* 3:736759. doi: 10.3389/fclim.2021.736759

Other publications related to thesis

- Book Chapter: <u>Feba F</u>, D Govardhan, C T Tejavath and K Ashok (2021) "ENSO Modoki Teleconnections to Indian Summer Monsoon rainfall A Review". 10.1016/B978-0-12-822402-1.00003-X.
- Vikas Kumar Kushwaha; S. Prasanna Kumar; <u>F Feba</u>; Karumuri Ashok- "Findlater Jet Induced Summer Monsoon Memory in the Arabian Sea" Under review in *Climate Dynamics*

Conferences/Symposiums

- Feba, F., K Ashok & M Collins., 'Decadal Prediction of Indian Ocean Dipole.'
 European Geophysical Union (EGU)- EGU General Assembly 2020, Vienna, Austria
 & online from 4 8 May 2020 (Poster Presentation)
- Feba, F., K K Vikas & K Ashok, 'Indian Summer Monsoon impacts on Bay of Bengal Cyclones through River Water Discharge.' The Australian Meteorological and Oceanographic Society Annual Meeting and the International Conference on Tropical Meteorology and Oceanography (AMOS-ICTMO 2019), Darwin, Australia from 11-15 June 2019. (Poster Presentation)
- 3. **Feba, F.,** K Ashok & M. Ravichandran 'Decadal Variability of Winds over Tropical Indian Ocean' and 'Decadal Prediction of Indian Summer' CLIVAR Open Science Conference Qingdao, China 2016. (Poster Presentations)
- 4. <u>Feba, F.</u>, K Ashok & M. Ravichandran, "Returning to The Weakening Teleconnections of Tropical Pacific and Indian Summer Monsoon Rainfall" in National Conference at Indian Institute of Science, Bengaluru, July, 2015.

Abstract

The El Niño Southern Oscillation (ENSO) is the primary tropical climate driver impacting almost all over the globe. We study the teleconnection from tropical Pacific to the Indian summer monsoon rainfall (ISMR) using various observational and Reanalysis datasets. In confirmation with the earlier findings, we find that the interannual correlations between the various SST indices of ENSO and ISMR have continued to weaken. Interestingly, we find that even the robust lead correlations of the tropical pacific warm-water-volume with ISMR have weakened since late 1970s. Our analysis suggests that there is a relative intensification of the cross-equatorial flow from the southern hemisphere into the equatorial Indian Ocean associated with ISMR due to strengthening of Mascarene High. Further, a shift in the surface wind circulation associated with monsoon over the northern pacific since late 1970s has resulted in a strengthened cyclonic seasonal circulation south-east of Japan. These changed circulation features are a shift from the known circulation-signatures that efficiently teleconnect El Niño forcing to South Asia. These recent changes effectively weakened the teleconnection of the El Niño to ISMR.

The Indian Ocean Dipole (IOD) is the other leading phenomenon of climate variability in the tropics, which affects the global climate. However, the best lead prediction skill for the IOD, until recently, has been limited to ~six months before the occurrence of the event. Here we show that multi-year prediction has made considerable advancement such that, for the first time, two general circulation models have significant prediction skills for the IOD for at least two years after initialization. This skill is present despite ENSO having a lead prediction skill of only one year. Our analysis of observed/reanalysed ocean datasets shows that the source of this multi-year predictability lies in sub-surface signals that propagate from the Southern Ocean into the Indian Ocean. Prediction skill for a prominent climate driver like the Indian Ocean Dipole has wide-ranging benefits for climate science and society.

1

INTRODUCTION

Humans have studied climate for several thousands of years, even as far back as 40,000 years ago as can be understood from some cave paintings. A detailed text on climate and weather was written by Hippocrates around 400 BC. A more modern scientific approach to climate research began probably about a few centuries ago (Edmund Halley mapped an early version of the trade winds in 1686). There are two primary reasons for studying climate (or weather). One is to understand its variability and then the second, to try to predict it on various scales. This thesis is an attempt to expand the understanding of the impact of two major climate drivers on the Indian Summer Monsoon and their prediction, on interannual and decadal scales.

1.1 The Indian Summer Monsoon

For several centuries, seafarers and traders have crossed the Arabian Sea with a great understanding of the seasonal reversal of winds (Rawlinson, 1916). This seasonal reversal of winds, accompanied by rainfall, was called Mausam –the Arabic term for 'season'- and later came to be known as Monsoon. The general character of the monsoons and their inter-regional variations reflect the juxtaposition of continents and oceans. Hence arises the difference in pressure, resulting from the difference in temperature between land and sea. The response to this contrast is the seasonal change of winds joined with a copious amount of rainfall (Ramage, 1971; Rao, 1976).

The Indian Summer Monsoon (ISM), also called the Indian Southwest Monsoon is the life source of over a billion people living in the sub-continent. Every year, from June to September, the ISM provides about 70% of annual rainfall (Figure 1.1). The maximum rainfall is observed during the month of July, followed by August. The ISM winds reach the Indian mainland in two flanks. During the pre-monsoon period, a cross-equatorial pressure gradient develops from the Mascarene islands to the Indian mainland due to the thermal contrast developed as a result of differential heating of land and sea. The trade winds flowing along the equatorial Indian Ocean recurve off the Somali coast due to the pressure gradient and south-westerlies flowing towards India.

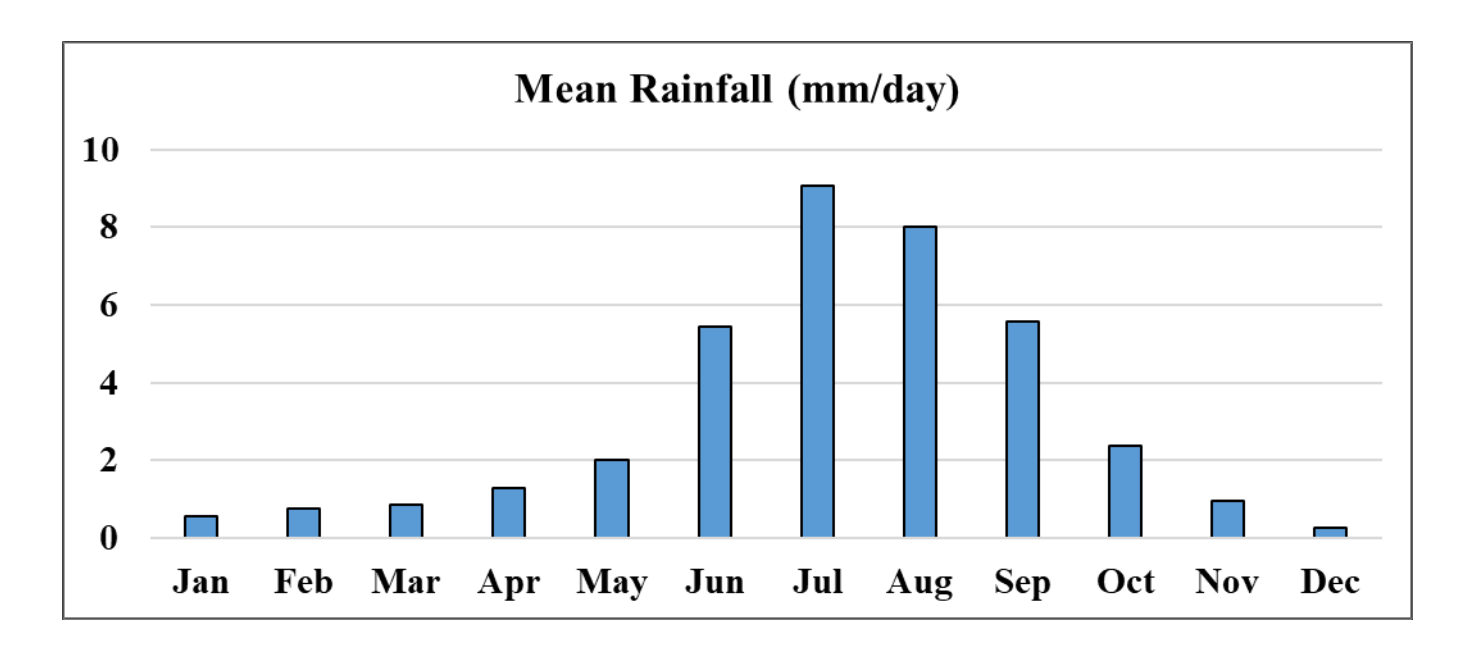


Figure 1.1: Monthly means of rainfall over India (All India rainfall averaged over the period of 1901-2019)

This southwest extent of ISM winds makes its entry into the Indian mainland, along the Kerala coast on June 1st with a standard deviation of 8-9 days (IMD, 1943; Joseph et al., 1994) and thus beginning a four-month long wet season, lasting till September. In the meanwhile, the eastern extent of the ISM winds reaches Andaman & Nicobar Islands by 20th May and then advances across the Bay of Bengal.

After the onset over the Kerala coast, the ISM advances rapidly from the south to the north till about 23°N. Beyond 23°N, the ISM advances from east to west. Within 3-4 pentads (15-20 days) following onset, the ISM sets over most of the Indian subcontinent (Figure 1.2). Once set in, the summer monsoon is sustained by the latent heat released from its own vapour. As the dry land cools after the onset, the latent energy forms a heat source in the mid-atmosphere maintaining the pressure gradient (Webster.1998; Gadgil., 2018).

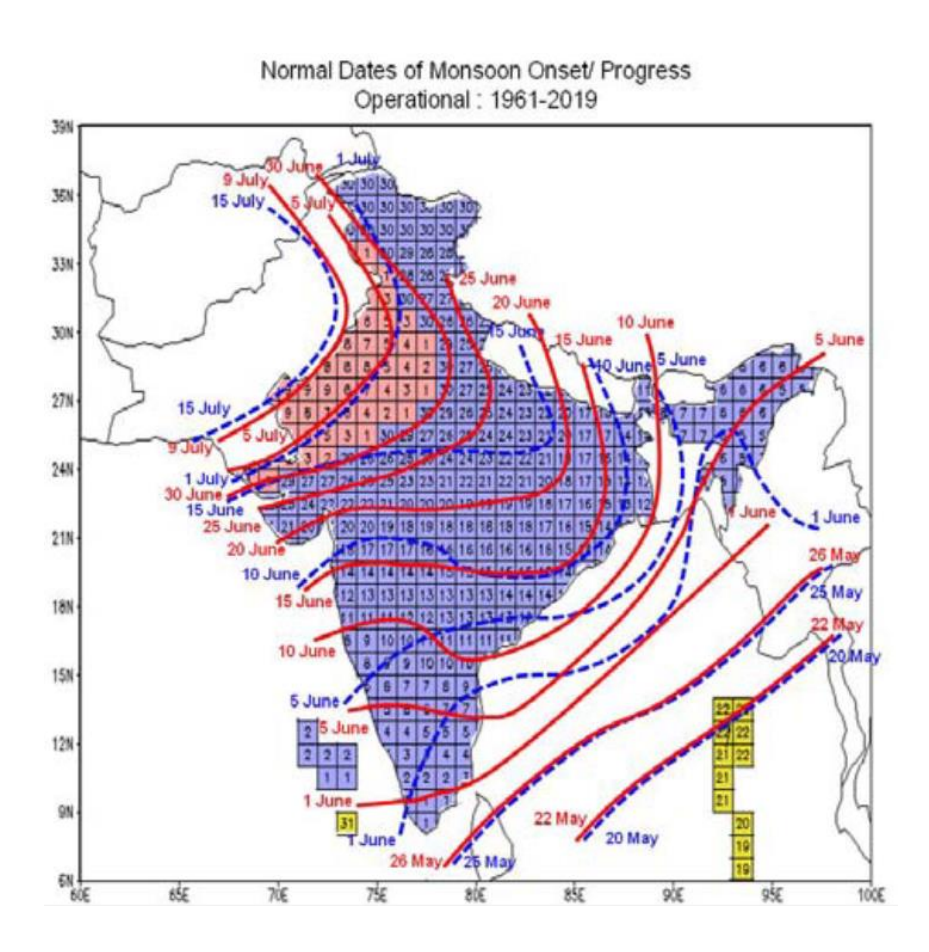


Figure 1.2: Indian Summer Monsoon Onset Dates (Source – Pai et al., 2020). The map shows the normal dates of monsoon onset/progress based on the IMD declared operational dates for events during the period of 1961-2019 along with existing normal dates (base period: 1901-40). The new and old onset dates are shown using solid-red and dotted-blue isochrones, respectively. Grids with climatological dates pertaining to May, June, and July are shaded yellow, blue, and orange respectively.

The ISM rainfall, also, shows great spatial variability (Figure 1.3) with the highest rainfall along the western coast of India, due to the orographic effects and over the head of the Bay of Bengal with a northwest-ward stretch along the monsoon trough. This north-westward stretching region is called the Monsoon Zone (Sikka and Gadgil, 1980). An alternate hypothesis suggests that the ISM is a manifestation of the Inter-Tropical Convergence Zone (ITCZ; Charney, 1969; Gadgil., 2018). Once the onset takes place, the land-sea thermal contrast may not be as important as the diabatic processes (Goswami and Chakravorty, 2017).

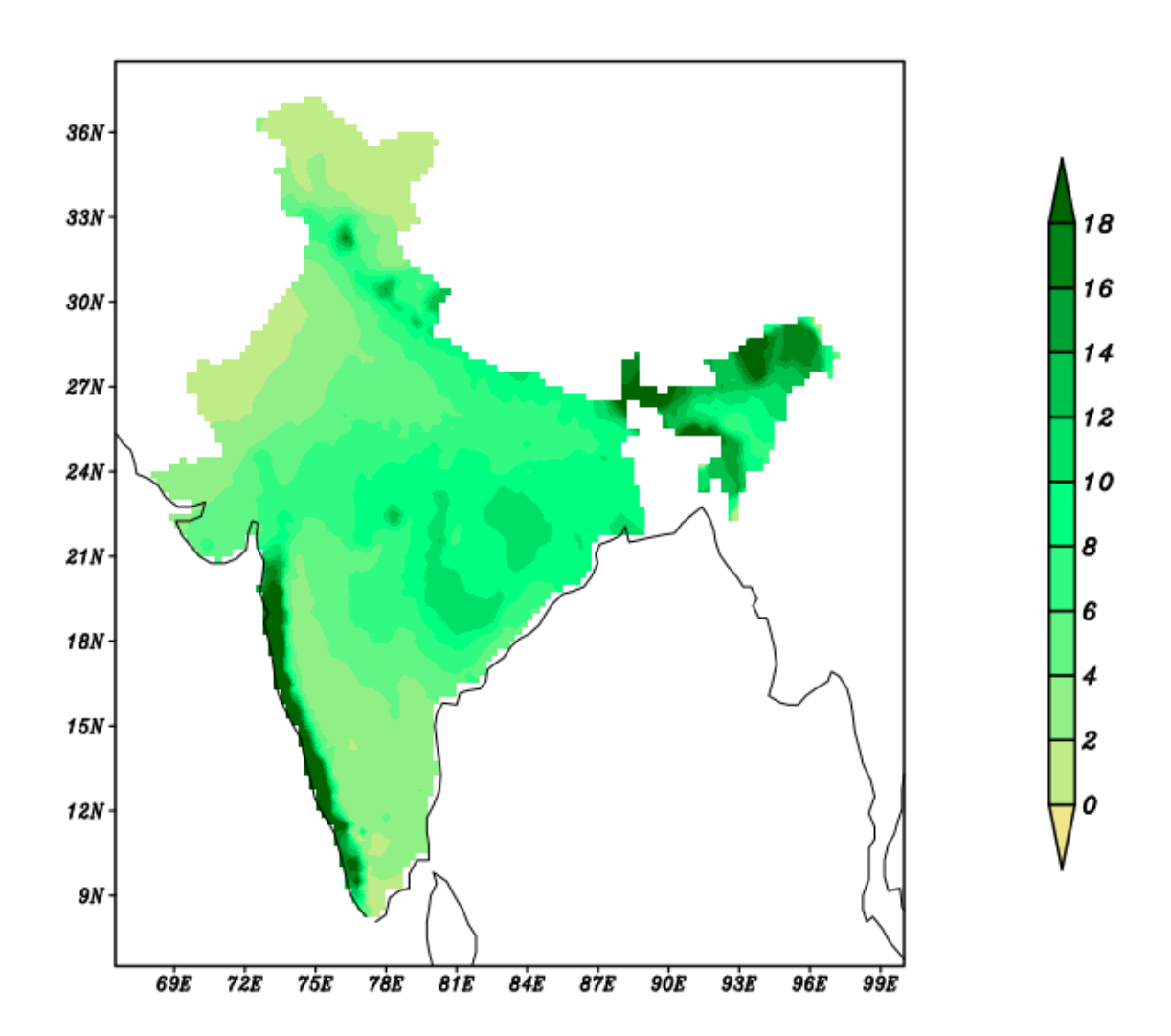


Figure 1.3: The mean monsoon rainfall over India during June to September averaged over 1901-2019.

Units: mm/day.

The dynamic ISM system has several characteristic patterns that are semi-permanent in nature, i.e., they are present throughout the summer monsoon season with varying positions and intensities, on various scales. These inter-related patterns are defined by the unique physiographical and geographical land features. The major semipermanent features associated with the ISM are 1. Monsoon Trough, 2. Mascarene High, 3. Heat Low, 4. Low-Level Jet, 5. Tibetan high and 6. Tropical Easterly Jet. A schematic representation of these features is depicted in figure 1.4 (Krishnamurthy and Bhalme, 1976).

- i. The **Monsoon Trough** is the zone of convergence of winds of the two hemispheres also called the Intertropical Convergence Zone (ITCZ, Riehl, 1954). The highest rainfall activity is observed along the axis of the trough. The north-south shifts of the monsoon trough axis are associated with dry-wet spells of monsoon activity.
- ii. The **Mascarene High** is a region of high sea level pressure in the south-western Indian Ocean (~50°E, 30°S) and plays a huge role in the cross-equatorial flow of ISM (Figure 1.5). The mean monthly sea level pressure over the Mascarene high is about 1025 hPa (Ananthakrishnan, et al., 1968).
- iii. The monsoon winds release most of the moisture on the south of the Himalayas as they flow over the orography. This causes subsidence over north-western India causing a **Heat Low** (Figure 1.5). The Heat low is shallow extending to about 1.5 Km in height and forms an inversion layer in the atmosphere which further sustains the low.
- iv. The **Low-Level Jet** also called the Somali Jet or the **Findlater Jet** (Findlater, 1969), is a narrow jet along the Somali coast over the Indian Ocean (Figure 1.5). It accounts for over 50% of the cross-equatorial flow of the monsoon in the lower atmosphere.

- v. The **Tibetan High** is a feature over the Tibetan plateau during the ISM (Murakami., 1987). The Tibetan plateau has a dual role with respect to the ISM. It acts as a physical barrier to the atmospheric flow and also as a mid-atmosphere heat source. An anticyclone forms over the plateau during the ISM, as a result of the sensible heating at an altitude of 4500 m.
- vi. The **Tropical Easterly Jet** is a band of strong upper atmospheric easterlies flowing from Southeast Asia to the Atlantic, across the Indian Ocean (Koteswaram, 1958). During the ISM, the jet is present over south Indian between 120 and 150N.

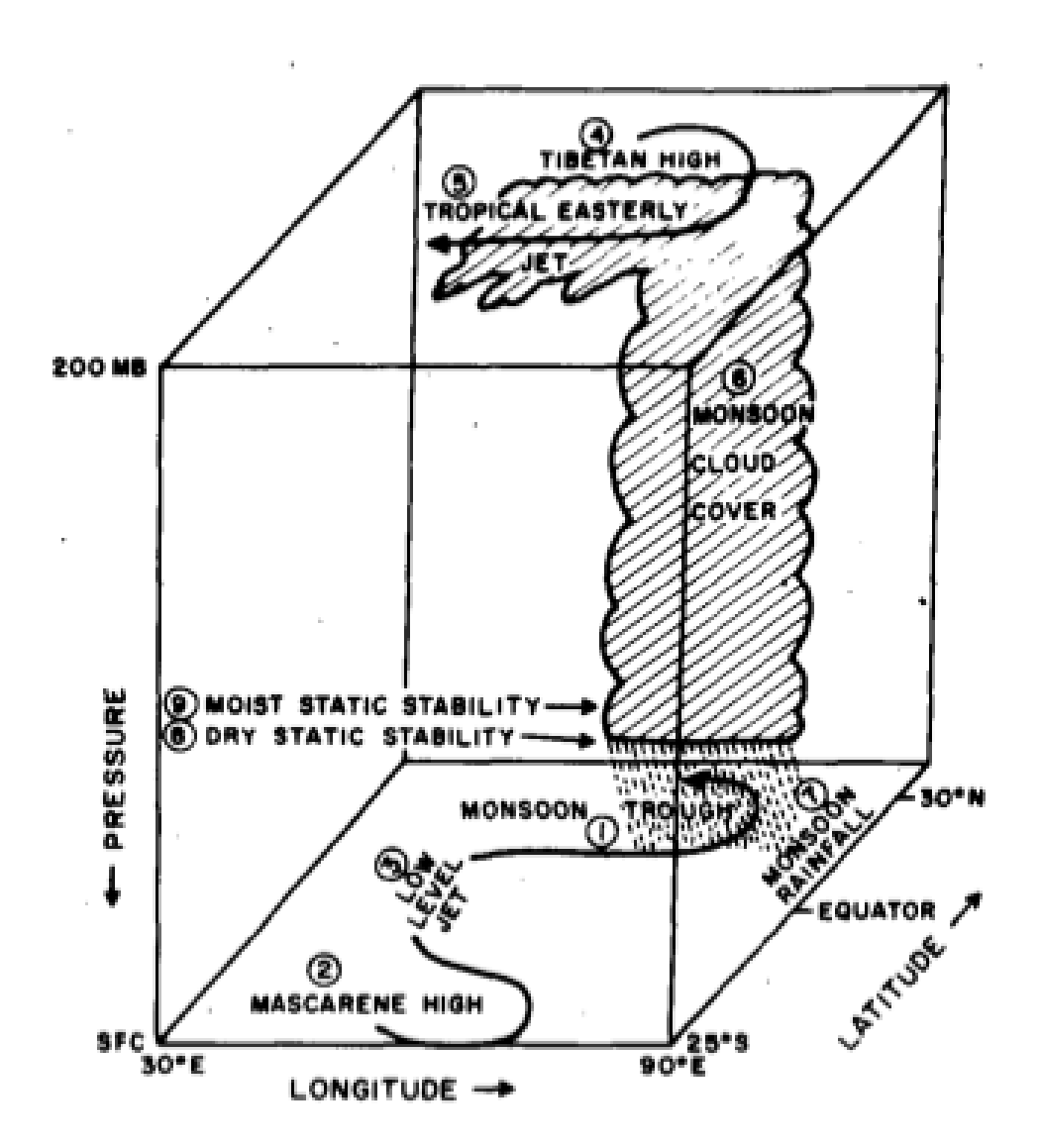


Figure 1.4: The Semi-permanent features of the Indian summer monsoon. A schematic representation adapted from Krishnamurti and Bhalme, (1976).

The variability of each of these features affects, and is, in turn, is also closely linked, to the intensity of monsoon circulation and the spatial and temporal rainfall distribution. The variability of these features is associated with intra-seasonal to interannual variability of the ISM. Further details can be found in Rao (1976), Pant and Kumar (1997), and the Monsoon Monograph series (Tyagi et al., 2012) which provide comprehensive summaries of these aspects of the monsoon.

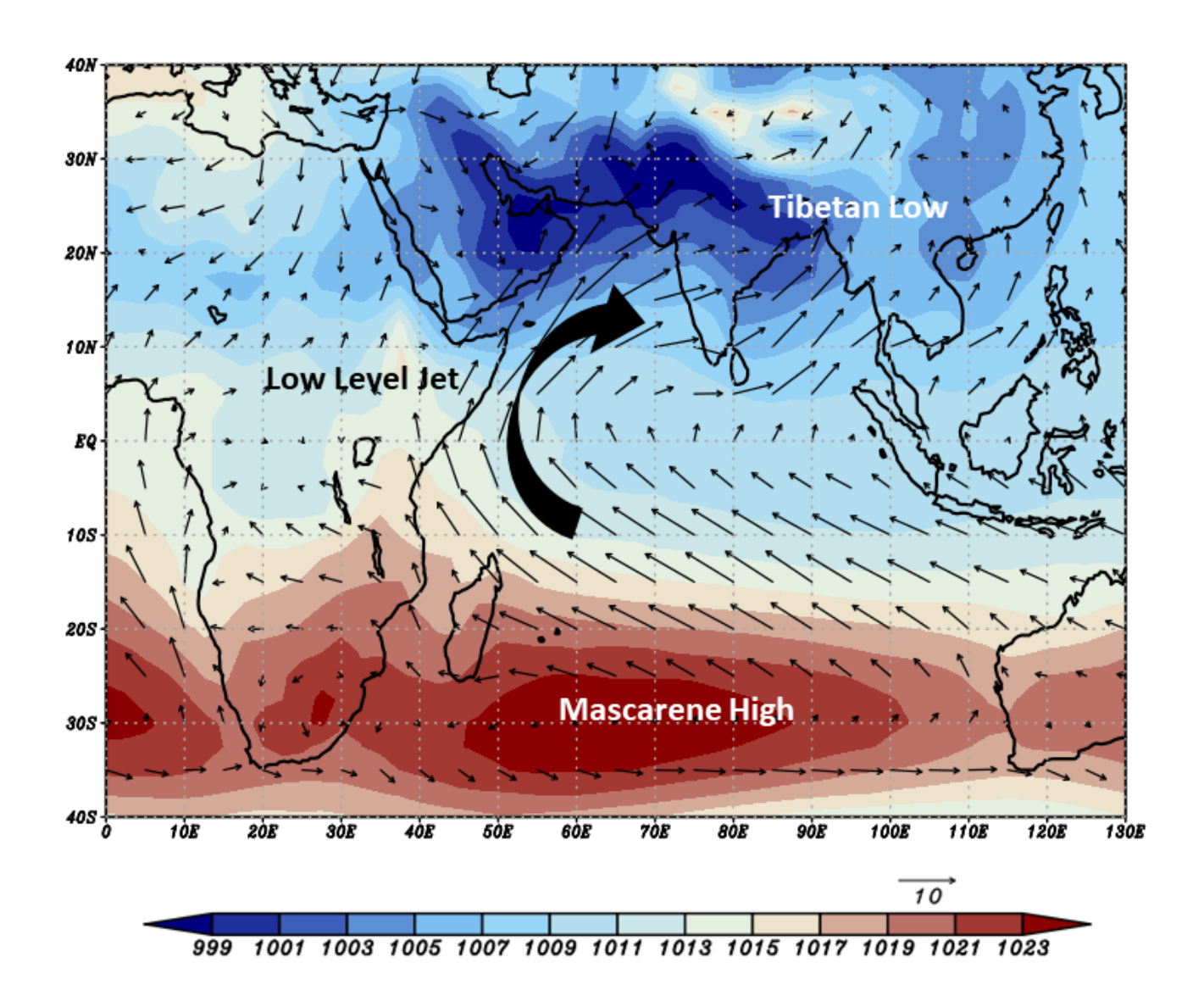


Figure 1.5: The mean sea level pressure during June to August overlayed with the wind vectors. Units for pressure- mb and wind vectors-m/s. All the datasets are averaged over the years, 1948-2019.

The ISM is a potent system occurring with reassuring regularity. Yet, the ISM is influenced by the interplay of several factors including but not limited to the thermal state of the oceans, snow cover over Eurasia and over the Himalayas, etc. These factors cause ISM to exhibit a wide range of spatial and temporal variabilities on intraseasonal, interannual, decadal, and centennial scales. For this study, we focus on the interannual variability of ISM (Figure 1.6) and the factors that attribute to this variability.

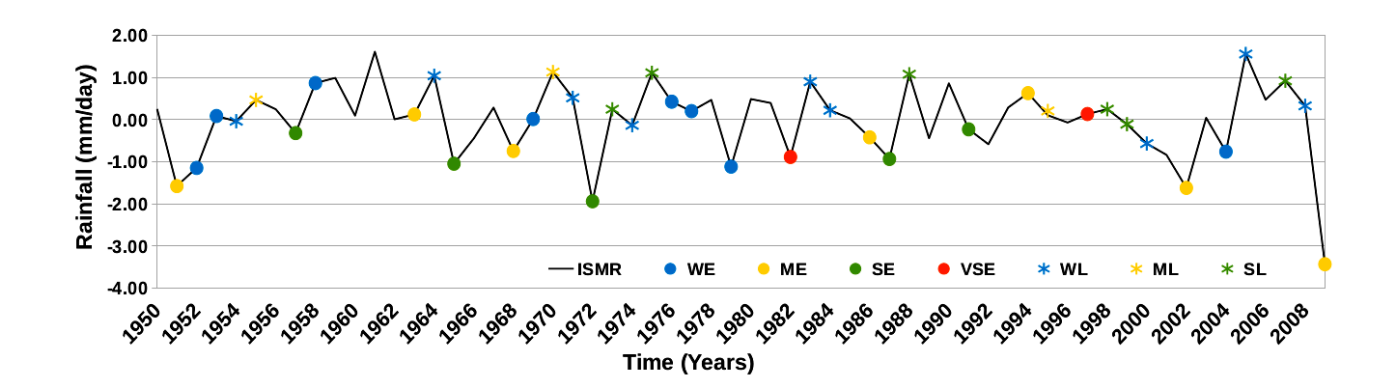


Figure 1.6: The interannual variability of the Indian summer rainfall area-averaged over the Indian land region (66.5° E-101.5° E; 6.5° N-39.5° N) during the 1951-2009 period. Here WE, ME, SE, and VSE stand for weak, moderate, strong, and very strong El Niños, respectively. WL, ML, and SL stand for Weak, Moderate and Strong La Niñas, respectively, as per https://ggweather.com/enso/oni.htm

The interannual variability of ISM is characterised by a standard deviation of 10% (Parthasarathy et al., 1994; Kothawale and Rajeevan, 2017). Although the variation seems small, the departures from the mean have large impacts on agriculture and the economy. The flood and drought years are identified as the departure of ISM beyond the ± 1 standard deviation. As shown in figure 1.6, the number of drought years exceeds the number of flood years over the 1901-2019 period. Several early studies (Sikka 1980; Pant and Parthasarathy 1981; Shukla and Paolino, 1983; Webster, 1992; Soman

and Slingo, 1997) have shown the drought years to co-occur with El Niño, the negative phase of a leading mode of climate variability – The El Niño Southern Oscillation (ENSO).

1.2 The El Niño Southern Oscillation

Gilbert Walker's attempts to find lead predictions skills for the Indian summer monsoon rainfall have resulted in the discovery of what has been later known as the Southern Oscillation, the atmospheric component of the El Niño Southern Oscillation (ENSO; Walker, 1923, 1924, 1928). The ENSO is a quasi-periodical coupled ocean-atmospheric phenomenon in the tropical Pacific. This is also referred to as an 'oscillation' with a periodicity ranging from 2-7 years (Philander, 1990; Sarachik and Cane., 2010). The tropical Pacific is a region of pronounced Walker Circulation. The eastern equatorial Pacific is characterised by higher Sea-Level Pressures (SLPs) and cooler Sea Surface Temperatures (SSTs) in relation to the western Pacific. The difference of SLPs between the eastern and western equatorial Pacific is called the Southern Oscillation Index (Bjerkenes, 1969). This SLP gradient and the resultant trade winds drive an upwelling in the East and hence a shallower thermocline. Superimposing on these *normal* conditions is an irregular and interannual cycle of the SLP gradient and warming or cooling episodes. The warm phase-the El Niño is associated with anomalous warming in the eastern pacific with a causatum of weakened trades and decreased upwelling, deepening the thermocline (Gill, 1980; Lindzen and Nigam, 1987). The cool phase – the La Niña, is associated with anomalous cooling and weakened trades, and increased upwelling. During an El Niño, the persistent precipitation normally seen over the western Pacific extends eastward and vice versa during the La Niña phase as shown schematically in figure 1.7. These changes over the equatorial pacific have far-reaching ramifications for the climate all over the globe.

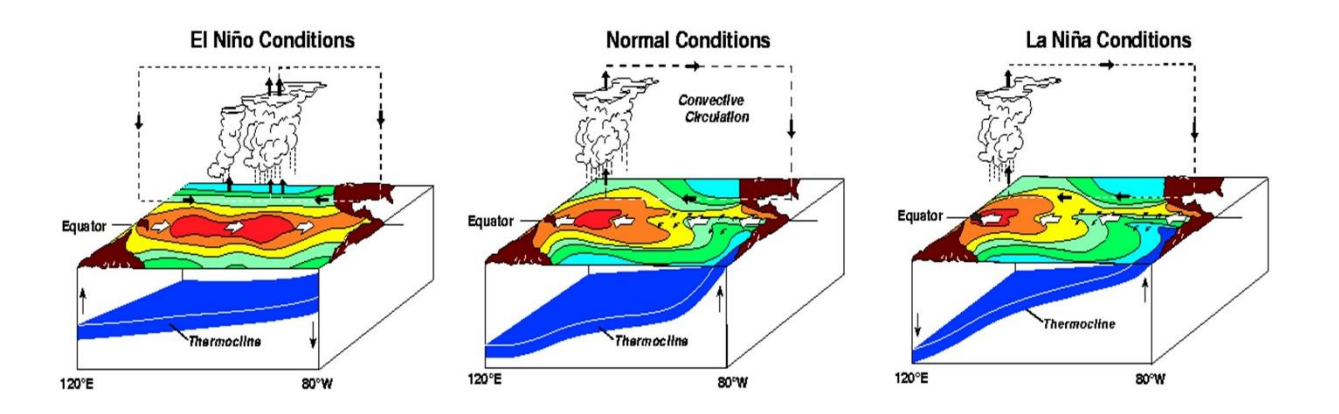


Figure 1.7: A schematic representation of SST, thermocline, Walker circulation, and precipitation over the Pacific Ocean during different phases of ENSO, i.e., during El Niño, Normal, and La Niña Conditions. The figures are sourced from < https://www.pmel.noaa.gov/elnino/schematic-diagrams>

The ENSO events are not limited to the SSTs in the eastern equatorial Pacific Ocean. As depicted in the schematic figure 1.7, the Walker circulation shifts eastward during an El Niño and westward, during a La Niña. The slope of the thermocline tilts downward in the east during an El Niño whereas the slope becomes steeper with an upward tilt in the east during a La Niña. With changes in the atmospheric circulation and ocean subsurface, ENSO is a large-scale phenomenon impacting almost all over the world.

To a significant extent, the ENSO can be deemed as self-sustaining positive ocean-atmosphere feedback (Bjerkenes, 1969). An ENSO event is normally seasonally phase-locked from boreal spring through ensuing boreal winter (December to February) when it peaks and then decays thereafter. The delayed oscillator theory explains that the Rossby waves generated in the eastern Pacific propagate west and reflect from the western boundary returning as Kelvin waves and reverse the ENSO effect (Zebiak and Cane, 1987; Suarez and Schopf, 1988; Battisti and Hirst, 1989). From another

perspective, the divergence by Sverdrup transport discharges the equatorial heat content which gets recharged by climatological upwelling. This is known as the recharge-discharge oscillator theory (Jin, 1997). Another hypothesis is that off-equatorial SST anomalies induce equatorial easterly wind anomalies (off-equatorial anomalous anticyclones), causing upwelling and subsequent cooling. This mechanism is called the western Pacific oscillator mechanism (Weisberg and Wang, 1997; Wang et al., 1999). In addition, external land heating and interaction with the previously coupled anomalies play a role (Masumoto and Yamagata, 1991).

Besides the well-known canonical El Niño, a new type of El Niños with anomalous warming in the central tropical pacific straddled by cooling of SST anomalies on its both flanks, have been occurring with increased frequency since the mid-1970s (Ashok et al., 2007; Kao and Yu, 2009; Kug et al., 2009; Marathe et al., 2015). These events, which occurred recently are seasonally phase-locked from boreal summer through ensuing winter and are named the El Niño Modoki, (also as the central pacific El Niño or Warm Pool El Niño). During the Modoki events, the maximum anomalous heating persists in the central tropical pacific for more than three consecutive seasons (Ashok et al., 2007; 2017; Marathe and Ashok, 2021), distinguishing itself from the transitory component of the canonical El Niño (e.g., Larkin and Harrison, 2005). The teleconnections of both types of El Niños differ in the phase and magnitude of the responses in temperature and rainfall (e.g., Weng et al., 2007; Yeh et al., 2009; Ashok et al., 2009a, b; Cowan and Cai 2009, to name a few). Indeed, the location of the heat source has relevance on the domain of its impacts (Matsuno, 1966; Gill, 1980; Keshavamurty, 1982; Soman and Slingo, 1987; Larkin and Harrison, 2005; Annamalai and Liu, 2005). This is particularly applicable to the ISM as well.

1.3 The El Niño Southern Oscillation and the Indian Summer Monsoon

Most severe summer monsoon droughts over India are associated with the El Niño events. In the simplest terms, the ISM tends to be anomalously weaker during El Niño years and to intensify during the La Niña years as can also be seen in the composite analysis (Figure 1.8). However, as Rajeevan (Monsoon Monographs, Ed. Tyagi et al., 2012) mentions, there is no one-to-one relationship between them. The relationship between ISM and ENSO has been studied extensively for the past few decades (Sikka, 1980; Keshavamurty, 1982; Shukla and Paolina, 1983; Rasmussen and Carpenter, 1983; Ropelewski and Halpert, 1987; Webster and Yang, 1992; Nigam, 1994; Ju and Slingo, 1995; Yang, 1996; Zhang et al., 1996; Kawamura, 1998; Navarra et al., 1999; Slingo and Annamalai, 2000; Lau and Nath, 2000; Wang, 2000; Ashok et al., 2004; Ashok and Saji, 2007; Hrudya et al., 2021). A simultaneous linear correlation between the NINO3.4 (an ENSO index, discussed later) and local rainfall anomalies over India (Figure 1.9) during the summer monsoon season from June-September (JJAS), shows that most of the correlations are negative, implying that the anomalously warm conditions during boreal summer over the eastern tropical pacific can result in anomalously deficit summer monsoon rainfall over India.

Given the intimate connection between the tropical pacific SST with the Walker circulation/southern oscillation, it is reasonable to consider that a mechanism of how the SST changes in the eastern tropical pacific transmit into the Indian summer monsoon region involves through Walker circulation changes. Bhalme and Jadhav (1984), analysing Indian rainfall datasets for the 1875-1980 period, reported a drier Indian Ocean and large monsoon rainfall deficiency occurring concurrently with weak Walker circulations. Shukla and Paolino (1983), through an analysis of Indian summer monsoon rainfall and the Darwin pressure associated intimately with ENSO datasets for 1901-1950, suggested that an anomalously high (low) Darwin pressure coincides with anomalously low (high) monsoon rainfall. Pant and Parthasarathy (1981) also have documented the relevance of the southern

oscillation changes for the Indian summer monsoon. Webster et al. (1998) indicated that boundary anomalies, such produced by ENSO, produce a temporal persistence and spatially large-scale descent over the Indian monsoon region, reducing rainfall either by producing a displacement of the seasonal mean rainfall patterns. All these studies imply that changes in the Walker Circulation with ENSO are considered to affect the ISM.

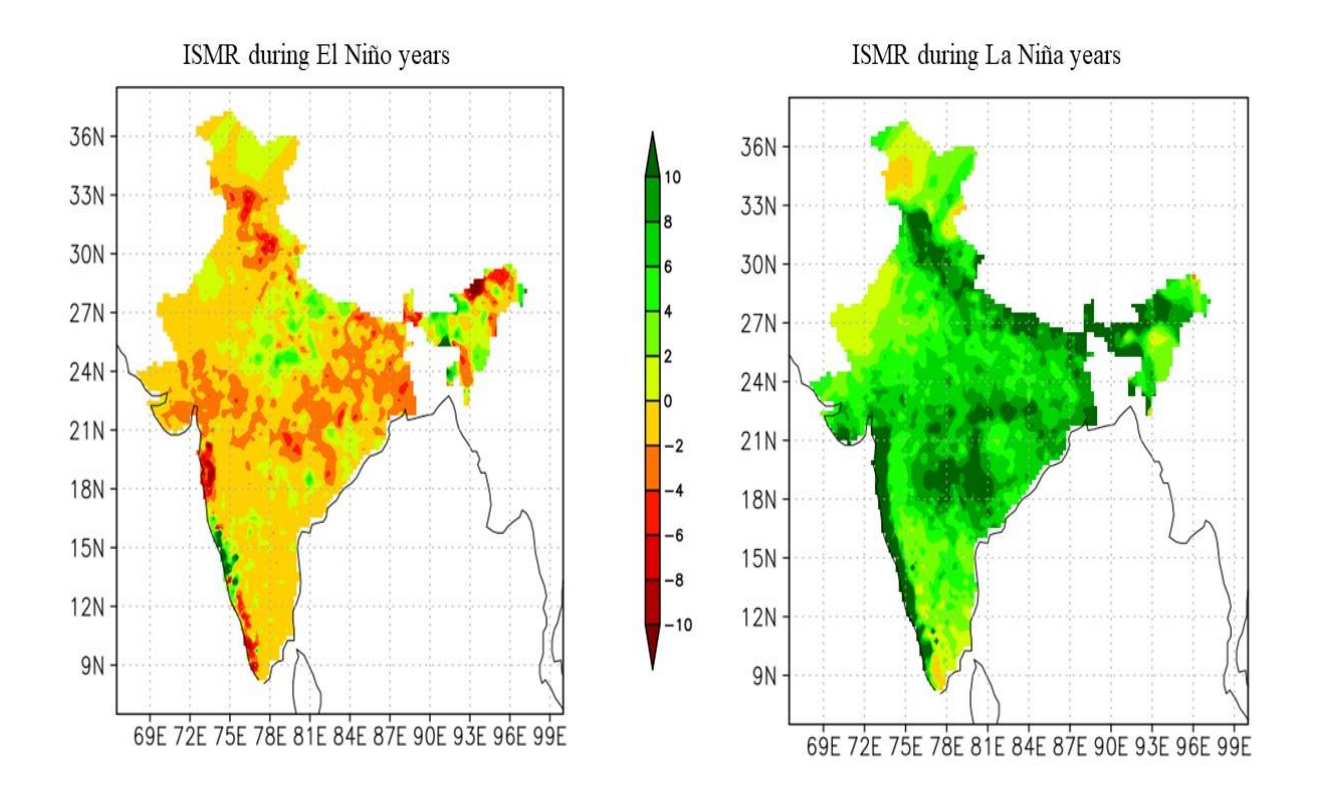


Figure 1.8: The ISMR composites during El Niño and La Niña years. Units for rainfall are mm/day. El Niño years show a deficit rainfall whereas La Niña years show a surplus amount of rainfall.

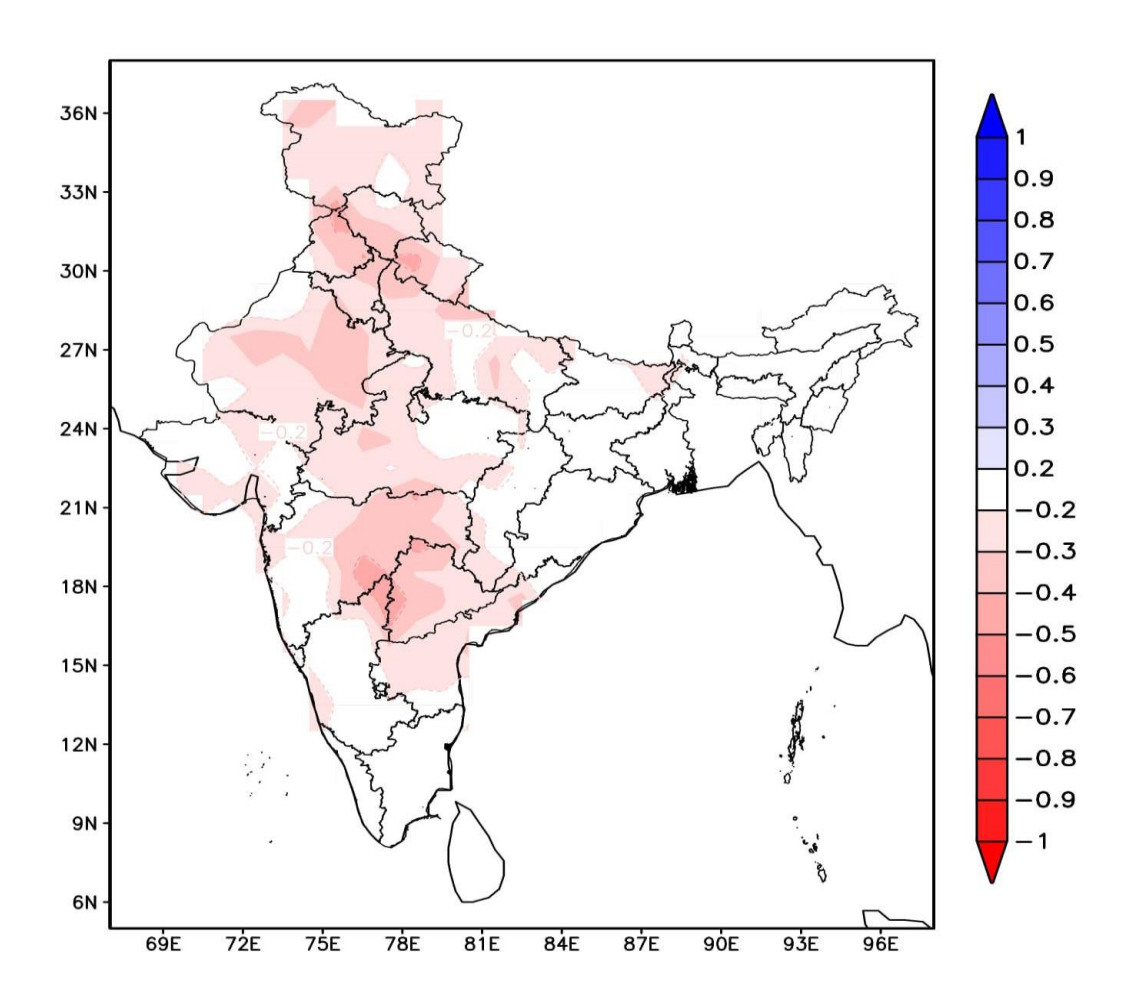


Figure 1.9: Linear simultaneous correlation between NINO3.4 index with the ISMR for 1901-2009 period. Only significant correlation values have been plotted (0.05 significance level from a 2-tailed Student's t-test).

Atmospheric general circulation model experiments by Keshavamurty (1982); Palmer et al. (1992); Shukla and Wallace (1983); Navarra et al. (1999); Ju and Slingo (1995); Soman and Slingo (1997); Dai and Wigley, 2000; Ashok et al. (2004), etc. demonstrate that the tropical pacific SST anomalies associated with ENSO indeed influence the Indian summer monsoon through modulation of zonal circulation cells. Broadly, these studies suggest that large-scale circulation changes due to the eastward shift of Walker Circulation and decreased equatorial divergence over the tropical Indian Ocean during El Niño years (Figure 1.7). Meanwhile, for a La Niño, the Walker circulation shifts westward and thereby causing an equatorial convergence over the Indian Ocean. The anomalous convergence in the tropical Indian Ocean results in the modulation of the cross-equatorial meridional

circulation, which causes an anomalous divergence over the Indian region and thereby a drier (wetter) than normal ISM. Indeed, this type of signals can be seen in the Indian Region and the Indian Ocean to its south, in years such as 1987 (Ashok et al., 2001) when the El Niño event does not co-occur with any other tropical oceanic climate driver such as the strong Indian Ocean Dipole (IOD, discussed in section 1.4) - which can interfere with the anomalous signal of ENSO.

Apart from the southern oscillation index, other equatorial SST-based indices, such as the NINO3 or NINO3.4 indices (See Section 2.2: Climate Indices) are routinely used to represent the variability of the canonical ENSO and have been used as a major predictor in the statistical forecast of the ISM (Mohanty et al., 2019). Many teleconnection studies such as Kumar et al. (1999), Gadgil et al. (2004), Ashok et al. (2012), Marathe et al. (2021), etc., also use the SST-based index while studying the tropical teleconnections to the ISMR. Interestingly, a study by Meinen and McPhaden (2000) shows that the magnitude of SST anomalies of ENSO is directly related to warm water volume (WWV) of the equatorial Pacific Ocean for the 1980 to 1999 period. Later, Rajeevan and McPhaden (2004) show, using both observed and reanalysed datasets, that WWV is an improved ENSO-related predictor of ISM as the WWV has a lead predictive skill of 3-4 months during February to May (FMAM), for the following ISM

Notably, the observed ENSO-ISMR link has apparently weakened in the last two decades of the twentieth century (Kumar et al. 1999; Chang et al. 2001; Krishnamurthy and Kirtman 2003; Ashok et al., 2001; Kawamura et al. 2005; Horii et al. 2012). Background and circulation changes associated with global warming have been proposed as a potential reason for the weakening by Kumar et al. (1999) and Ashrit et al. (2001). Kumar et al. (1999) attribute, through a running correlation analysis, that the weakening observed in the late 1990s due to a shift in background circulation associated with global warming. Chang et al. (2001) show that on removing two years, 1983 and 1997, the

correlations remain robust. Ashok et al. (2001, 2004), and Ashok and Saji (2007) suggest that this weakening is owing to the increased positive IOD events (see section 1.4)., which, when strong, anomalously increases the Indian summer monsoon rainfall. In other words, the weakening is just apparent and associated with the neutralizing impact of the co-occurring IOD events. Sreejith et al. (2015) argue that the air-sea coupled interaction over the tropical Indian ocean is the reason for the weakening of the ENSO-ISMR links.

On the other hand, Gershunov et al. (2001) suggest that the monsoon-ENSO relationship is less variable on decadal scales. In other words, even though many physical processes may be partially responsible for the modulation of the interannual correlation, it is not possible to distinguish their effects from stochastic noise in running correlation analyses, and therefore, it could just be an issue of sampling (Cash et al., 2017).

At the same time, the interannual manifestations of the tropical Pacific variability are also undergoing significant changes over the recent period. Specifically, we see more and more of El Nino Modoki events, with anomalous warming along the central Pacific with anomalous cooling on both sides (Kug and Kang 2006; Ashok et al. 2007; Yeh et al. 2014) since the late 1970s. On the other hand, the frequency of the canonical El Nino events, typified by anomalous warming (cooling) in the eastern (western) tropical has reduced since then. Interestingly, the tropical Pacific also witnessed hitherto unseen anomalous basin-wide warming from May 2009 through April 2010 and then in 2014 (Ashok et al. 2012; Jadhav et al. 2015). The Pacific Decadal Oscillation (PDO) also affects the ENSO-ISM by enhancing (suppressing) ENSO impacts on the ISM when they both are in the same (opposite) phase (Krishnamurthy and Krishnamurthy, 2014).

These conditions make it interesting to take a relook at the decadal variability of the teleconnections of the Pacific basin to the ISM. It will be particularly worthwhile to see if there are any recent internal changes in the pacific atmosphere, which have a bearing on the monsoon teleconnections. This forms the very first objective of this thesis.

1.4 The Indian Ocean Dipole

The year 1997 posed a challenge to the monsoon prediction community as India received a good summer monsoon despite the year being a strong El Niño year. Coincidentally, research into the tropical oceans of the year led to the discovery of the Indian Ocean Dipole (Saji et al., 1999; Webster et al., 1999; Murtugudde et al., 2000). The IOD is an inherent manifestation of interannual variability in the tropical Indian Ocean. It is a coupled ocean-atmospheric phenomenon. It initiates sometime during April-May, peaking during the boreal fall season from September to November (SON), and dissipates later (Saji et al., 1999). During the positive phase, the western equatorial Indian ocean shows anomalously higher SST than the eastern equatorial Indian Ocean (Figure 1.10). This creates a zonal gradient across the equatorial Indian Ocean changing the surface winds to easterlies from westerlies. The change is quite evident in the sea surface level as the eastern region is anomalously lowered while the western region is raised. The opposite of this is seen during the negative phases, though positive events are stronger than negative events with respect to their amplitudes (Cai et al., 2013). The growth of IOD also involves the coupled Kelvin and Rossby wave propagation akin to the ENSO (Rao et al., 2002). While many positive IOD events co-occur with ENSO, it is mainly due to the seasonal phase-locking of the two different phenomena in the two neighbouring basins (Yamagata et al., 2004). Of course, strong IOD and ENSOs have inter-basin connectivity through an atmospheric bridge, particularly the triggering (e.g., Ashok et al., 2003; Saji et al., 2018; Izumo et al., 2013; Marathe et al., 2021).

Though ENSO explains about 25% of IOD variance and they are both highly correlated, they both are inherently different with significantly distinct wave spectra as understood by a wavelet analysis (Saji and Yamagata, 2003). IOD and ENSO can co-occur in some years, in-phase, like 1972, 1982, or 1997 with both the positive phase of IOD and El Niño occurring together or in 1996 or 2010 with negative IOD co-occurring with La Niña. The opposite is also true where there have been instances of IOD events with no ENSO in the years such as 1967, 1994, or 2006. On removing the co-occurring years, the correlation value shows a fast drop. The co-occurrence is partly the reason for a high correlation between the two phenomena. Moreover, the proximity of the Pacific and Indian ocean basins renders a propensity to interact across the Indonesian throughflow or through atmospheric pathways.

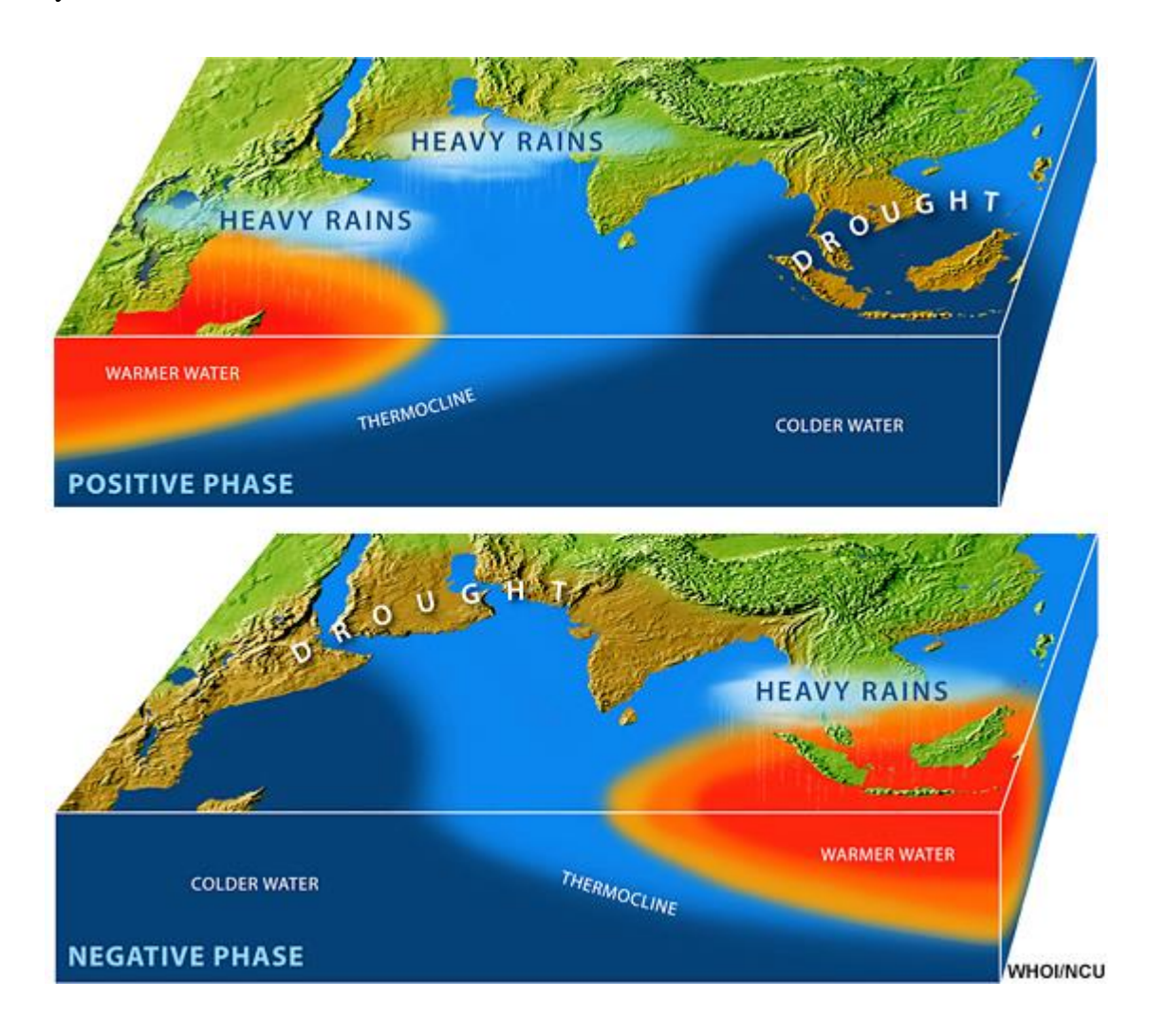


Figure 1.10: A schematic representation of SST and thermocline in the equatorial Indian Ocean during positive and negative phases of the IOD. Also shown are impacts on rainfall over different

regions on different phases of IOD. The figure is sourced from the book, Introduction to Tropical Meteorology, The COMET program.

1.5 The Indian Ocean Dipole and the Indian Summer Monsoon

The IOD impacts can be seen globally. A positive IOD is associated with decreased rainfall in the western and southern regions of Australia (Ashok et al., 2003b), increased forest fires across Australia, droughts across Indonesia (Saji and Yamagata, 2003) increase in rainfall and floods in East Africa (Behera et al., 2005) and the increase of ISM (Ashok et al., 2001; 2007). IOD also causes an anomalous dipole-like rainfall pattern across the east-west of South America during the austral spring (Chan et al., 2008).

The impact of IOD on ISM can modulate the ENSO-ISM teleconnections. A positive IOD is associated with higher-than-normal ISM rainfall and a negative IOD, with a lesser than normal ISM rainfall (Figure 1.11). A positive IOD can even negate the impacts of a co-occurring of El Niño as in 1997 (Behera et al., 1999. On the other hand, a negative IOD can debilitate an already weak ISM when co-occurring with an El Niño (Ashok et al., 2001; Pokhrel et al., 2012). During a positive IOD, the colder SST anomaly in the eastern equatorial Indian Ocean induces a reduction in convection and hence anomalous subsidence and divergence. Meanwhile, a strong convergence is observed over the Bay of Bengal, indicating an enhanced meridional circulation and thereby a stronger ISM (Ashok et al., 2001). The equatorial Indian Ocean oscillation (EQUINOO; Gadgil., 2003; Francis and Gadgil, 2013) is the atmospheric component of the IOD. EQUINOO is an oscillation of enhanced (suppressed) convection over the western (eastern) Indian Ocean in its positive phase and vice-versa in the negative phase. The EQUINOO index called EQWIN is derived from the zonal component of the equatorial surface wind averaged over the central Indian Ocean and seems to have a higher

correlation with the ISM (Gadgil, 2004). It is mostly synonymous with the atmospheric signature of the IOD.

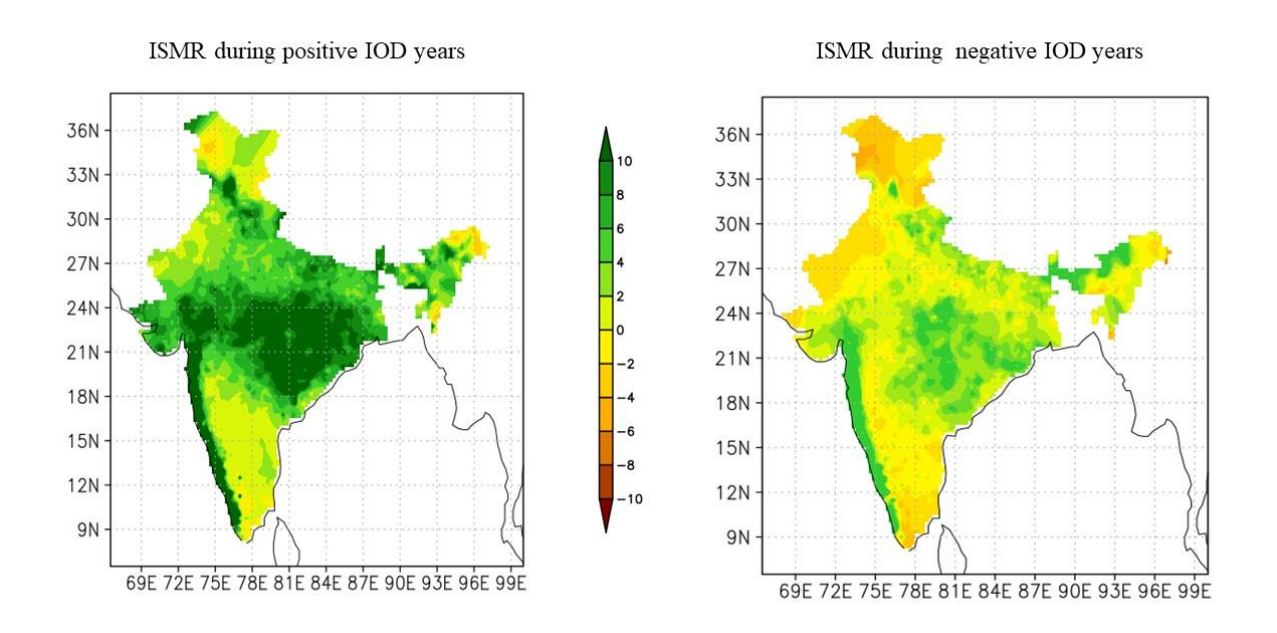


Figure 1.11: The ISMR composites during positive and negative phases of IOD. Units for rainfall are mm/day. Positive IOD years show a surplus rainfall over the western coast and the central region of India, whereas the negative IOD years show a deficit rainfall.

The impacts of the IOD on the Indian monsoons are shown statistically to be more and more prominent relative to that from the ENSOs (e.g., Krishnaswamy et al., 2014). Some companion research by us also indicates that the IOD events in the recent two decades facilitate extreme rainfall events in the northwest states of Gujarat, etc. (Boyaj, personal communication). The IOD and ENSO events have been shown to impact the Kharif rice production in the Indian states of Bihar, Haryana, Karnataka, Kerala, Madhya Pradesh, Odisha, Punjab, United Andhra Pradesh (UAP), Uttar Pradesh,

and West Bengal (Amat and Ashok, 2018; Amat et al., 2021). The 2019 IOD is an example of how a strong IOD is associated with heavy rains over India during the summer monsoon (e.g., Ratna et al., 2020). Interestingly, the June-July months of the year witnessed El Niño Modoki like conditions, which resulted in a weak monsoon during these months. The pacific conditions reached neutral by August, but a strong positive IOD was seen from August, due to which the rainfall deficit during June-July was wiped off (Ratna et al., 2020). All these emphasize the importance of the IOD.

In addition, recent studies such as Kucharski et al., (2007; 2008), Pottapinjara (2015), Yadav et al. (2018), and Venugopal (2020) show that the Atlantic can also influence the Indian summer monsoon. However, given the stronger inter-connections between the ISM, ENSO, and IOD (e.g., Meehl and Alablaster, 2001; Ashok et al., 2014; Borah et al., 2021), I henceforth mainly focus on the variability of the tropical Indo-pacific and its relevance to the Indian summer monsoon.

1.6 Decadal Prediction

Decadal Prediction i.e., prediction of climate information for the near future (5-20 years) is an emerging discipline. It has great promise for societal needs and economic policymakers (Meehl et al., 2009). Decadal prediction falls in the niche between weather prediction and climate prediction. Therefore, the decadal prediction has to resolve both the initial value problems such as in weather or seasonal prediction and also the boundary conditions as in long-term climate forecasts (Figure 1.12; Boer et al., 2016). The source of the decadal predictability lies in decadal climate variability, including slow varying oceanic processes, snow cover, and anticipated changes in anthropogenic greenhouse gases and aerosols. Studies have shown that there is some *skill* in decadal prediction over regions where the temperatures can be strongly modulated by oceans (Branstator and Teng, 2010; Gaetani and Mohino, 2013), mainly in regions of low-frequency ocean variability like the north Atlantic (Yeager et al., 2012; Robson et al., 2013). Some prediction skills on a decadal scale were

found for temperatures over the North Atlantic, a zone of the ocean overturning circulation, for 3-8 years (Zhang and Zhang., 2015; Borchert, 2018). The source of predictability was found to lie in the upper ocean heat content (upper 700m).

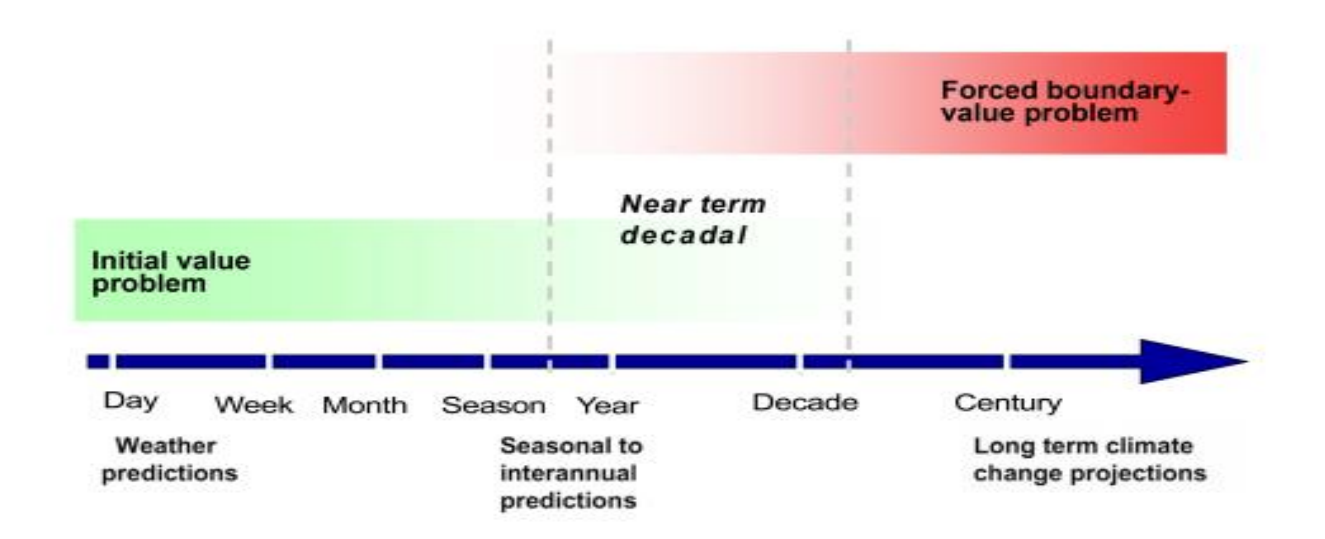


Figure 1.12: Interannual to decadal climate predictions have to resolve both, initial value problems and forced boundary problems (Figure from Boer et al., 2016).

Interestingly, the inter-annual ENSO and the IOD can also be modulated by decadal processes (Ashok et al., 2004; Schott et al., 2009) or slow changes in the interannual processes (Tozuka et al., 2007). The presence of such low-frequency variability shows a promise for the possibility of such a prediction skill. Attempts to predict ENSO have shown a 12-17 months lead prediction skill (Sun et al., 2018; Pal et al., 2020). Whereas, the prediction of IOD has met with a relatively shorter lead time skills, the highest being of 4 months (Wu and Tang, 2019; Zhao et al., 2020)

1.7 Aims and Objectives

Though earlier studies, as mentioned above, show the weakening of ENSO-ISM skills, the cause for this apparent weakening in the recent two to three decades is not yet fully understood. Further, the weakening has so far been observed with respect to the SST indices of ENSO and ISM. As mentioned earlier, for the 1950-2000 period, the WWV shows a significant lead prediction skill for ISM at least for one season ahead. The present state the robustness of association of this index with ISM has not been explored. Also, the mechanisms of the weakening on a decadal scale and potential roles of naturally occurring decadal phenomena within the Indo-pacific are not fully understood. These aspects need further study

Decadal prediction, which shows impressive skill in the north Atlantic, motivates us to explore for prediction in the Pacific and Indian Ocean drivers beyond interannual timescales, potentially on decadal time scales. Specifically, that both ENSO and IOD contain their inherent decadal variabilities, shows some promise and needs to be explored. It would be interesting to take a look at their respective decadal prediction skills.

Considering these gaps in the studies so far, I have set the objectives of the thesis as,

- Understanding the decadal variability of Indo-Pacific teleconnections to Indian Summer Monsoon.
- 2. Exploring the mechanisms for the weakening of the ENSO-ISM links.
- Exploring the multi-year to decadal prediction skills of the tropical Indo-Pacific drivers, and finding a potential source for any significant predictability on a multi-year scale.

The entire thesis is divided into six chapters, including this introduction., Chapter 2 describes the data sources and methods in detail. In Chapter 3, I present my results from the study of ENSO-ISM links on a decadal scale. Chapter 4 consists of the results from the analysis of decadal prediction skills of ENSO and IOD. Chapter 5 suggests a possible mechanism for the source of the prediction skill. Finally, Chapter 6, the concluding chapter, comprises a summary of the entire work, and briefly portrays the scope for future work.

2

DATA AND METHODS

2.1 Datasets

The thesis reports my results from the analysis of various aspects of climate. The results presented in this thesis are based on different datasets covering varying distinct time periods, each of which is defined clearly. This non-uniformity arises depending on the availability of the data at the time of the study. Nevertheless, we have presented the results with explicit mentioning of the time period to avoid any confusion. Here we describe the sources of the data along with the statistical and the data processing techniques employed on the data.

2.1.1 Observational and Reanalysis Datasets

Rainfall

We use the All India Summer Monsoon Rainfall (AISMR) rain gauge dataset by Parthasarathy et al. 1994. This dataset has been prepared using in-situ observations from a distributed network of 306 rain gauge stations over India with proper area weightage. We also use the daily gridded rainfall dataset generated by the India Meteorological Department (IMD) with a spatial resolution of 0.25° X 0.25° (Pai et al., 2014). This rainfall dataset is developed by using rainfall measurements from a

network of 6995 rain gauge stations spread across 36 meteorological subdivisions of India. The data are interpolated using a two-dimensional interpolation method as described by Shepard (1968). These data are openly accessible from the Climate Data Service Portal of IMD (IMD - CDSP (imdpune.gov.in)).

Ocean Temperature

For Sea Surface Temperature (SST), we use the Met Office Hadley Centre Sea Ice and Sea Surface Temperature dataset (HadISST; Rayner et al. 2003) at a spatial resolution of 1^o X 1^o. The HadISST dataset is reanalyzed from the Met Office Marine Data Bank (MDB), the Global Telecommunications System (GTS), and the Comprehensive Ocean-Atmosphere Data Set (COADS, now ICOADS). The data were gridded by using the Reduced Space Interpolation technique (Kaplan et al., 1997). This dataset is freely available at https://www.metoffice.gov.uk/hadobs/hadisst/data/download.html.

For the subsurface data, we use the Simple Ocean Data Assimilation (SODA) Reanalysis 2.1.6 dataset (Carton and Giese 2008; available at SODA 2.1.6 datasets - NOAA Data Catalog), which are available at a gridded spatial resolution of 0.5° X 0.5° with 40 vertical levels. We also use Ocean Reanalysis data from the European Centre for Medium-Range Weather Forecasts (ORAS4; Balmaseda et al., 2013; available at Ocean Reanalysis/analysis | ECMWF). This gridded data has 42 vertical levels and a spatial resolution of 1° X 1°.

Winds and Sea Level Pressure

We use the atmospheric circulation data and sea level pressure (SLP) from Derived National Centers for Environmental Prediction (NCEP) Reanalysis data, provided by the NOAA/OAR/ESRL PSD, Boulder, Colorado, USA (Kalnay et al. 1996; <u>Datasets- NCEP/NCAR Reanalysis: Pressure: NOAA</u>

<u>Physical Sciences Laboratory</u>), and those from the first atmospheric reanalysis, (ERA-20C; Poli et al., 2016) from European Centre for Medium-Range Weather Forecasts (ECMWF; <u>ERA-20C | ECMWF</u>).

2.1.2 Model Datasets

For the study of decadal prediction, we use the decadal runs of Coupled Model Intercomparison Project- Phase 5 (CMIP5). The experimental setup and design of CMIP5 experiments are detailed in Taylor et al., (2009). We have accessed and downloaded the data from CMIP5 - Home | ESGF-CoG (Ilnl.gov). These data are available from multiple other sources as well. The CMIP5 includes a new additional experiment, near-term climate change modeling experiments: Decadal Climate Prediction (Meehl et al., 2009). Observed ocean and sea ice conditions were used to initialize the Atmospheric and Ocean General Circulation Models (AOGCMs) in the decadal prediction experiments. The core experiments are designed in two sets. The first set is of 10-yr hindcasts initialized from observations for the years 1960, 1965, and every 5 years (with an option of initializing every year) till 2005. These 10-year simulations, give a possibility to assess the prediction skill of the climate system where the initial climatic state has an ascertainable influence. The other set extends the 10-year simulations to 30 years, initialized in 1960, 1980, and 2005. In our study, we use the first set of hindcasts with 10-year simulations and select only the models initialized every year.

We analyze the decadal hindcasts of four models (detailed in Table 2.1), the Canadian Coupled Global Climate Model, Fourth Generation (CanCM4; Merryfield et al., 2013), the Model for Interdisciplinary Research on Climate, Version 5 (MIROC5; Watanabe et al., 2010), the Beijing Climate Center Climate System Model, Version 1.1 (BCC-CSM; Wu et al. 2013), and the Geophysical Fluid Dynamics Laboratory Climate Model, Version 2.1 (GFDL; Delworth et al., 2006; Zhang et al., 2007). Each of the model runs has anthropogenic and natural forcing in them and

comprises several independent decade-long ensemble-runs by each model. CanCM4 is assimilated with ERA-40 and ERA-Interim for the atmospheric component nudged with observed SSTs. For its oceanic component, SODA and GODAS (NCEP Global Ocean Data Assimilation System) subsurface ocean temperature and salinity are used and adjusted to retain the model T–S relationship. For MIROC5, the Coupled model is integrated using observation-based ocean temperature and salinity datasets. The BCC-CSM is a coupled model integrated with ocean temperature nudged to SODA data above 1500 m. GFDL is a Coupled model assimilated using the Ensemble Kalman filter. In GFDL, the atmosphere is constrained by reanalysis datasets, and the ocean is assimilated with observed temperatures and salinity.

Table 2.1: The analyzed models with the initialization techniques, number of the ensemble- members, institution, and references.

Model	Initialization	Ensemble Members	Institution	Reference
CanCM4	Full-field	10	Canadian Centre for Climate Modelling and Analysis	Merryfield et al 2013
MIROC5	Anomaly	6	The University of Tokyo Center for Climate System Research; National Institute for Environmental Studies; Japan Agency for Marine-Earth Science and Technology Frontier Research Center for Global Change	Watanabe et al., 2010
GFDL	Full-field	10	Geophysical Fluid Dynamics Laboratory, The National Oceanic and Atmospheric Administration (NOAA)	Delworth et al., 2006; Zhang et al., 2007
BCC-CSM	Full-field	3	Beijing Climate Center	Wu et al. 2013

Full-field and Anomaly initializations are two techniques used in seasonal to decadal climate prediction. In the Full-field approach, the model is initialized using observations. This approach removes model biases by constraining the model to be as close as feasible to the observations. But, for a forecast prediction, as the model cannot be constrained any longer, the model drifts back to its biased climate state. This drift/bias needs to be considered and corrected. The correction techniques still retain some non-linear biases as residual errors. An alternate method is to use the model mean state along with observed anomalies. This Anomaly initialization method reduces the model biases but there is a chance of the model anomalies being inconsistent with the observations. Comparison studies of both methods show very little to insignificant differences in most regions. Over the Indian Ocean Basin, Smith et al., (2013) show that Full-field initialization shows greater skill, and Hu et al., (2019) show Anomaly initialization as having a greater skill for the Indian Ocean basin mode.

2.1.3 Preprocessing of Model Output

In a chaotic system, the deterministic prediction is limited by the rapid growth of the initial condition errors (Lorenz, 1963; Lai et al., 1999; Carriuolo, 2006; Warner, 2010). The errors, beyond a deterministic point, affect the predictability of any model. Ensemble prediction is a feasible way of estimating forecast predictability beyond the range limited by the initial errors (Palmer and Hagedorn, 2006; Collins, 2007) Models are initialized for the same time periods with varying initial states to account for the uncertainties in the initial data. Different parameterization schemes or multiple models are used to reduce model limitations. The model hindcast data from CMIP5 decadal runs are initialized with different initial conditions for different ensemble members (Table 2.1). I calculated the ensemble-mean of each model for all the analyses.

2.2 Climate Indices

For the study of the ENSO (Section 1.2) and IOD (Section 1.4), we use both sea surface and subsurface temperature indices as defined below.

2.2.1 NIÑO3 and NIÑO4 indices

The Niño3 and Niño4 are SST indices used as an indicator of the tropical Pacific El Niño conditions. They are calculated as anomalies of monthly mean SSTs area-averaged in the boxes 150°W - 90°W; 5°S - 5°N and 160°E - 150°W, 5°S - 5°N respectively. The Niño3 index lies over the eastern end of the tropical Pacific, whereas the Niño4 index lies to the west of the Niño3 index as shown in Figure 2.1. Both the indices are negatively correlated with the Indian Summer Monsoon as explained in Section 1.3. There are other SST indices also, like the Niño1+2 index (90°W - 80°W, 10°S - 0°) at the eastern end of the Pacific or the Niño3.4 index (170°W - 120°W, 5°S - 5°N) in the central Pacific. In this study, I consider only Niño3 and Niño4 indices.

2.2.2 Warm Water Volume

Following Meinen and McPhaden (2000), we define the tropical pacific warm water volume, henceforth referred to as the WWV, as the integrated volume of water above the 20°C isotherms in 5°N-5°S; 120°E-80°W (Figure 2.1). The magnitude of ENSO SST indices is directly related to the magnitude of the zonal mean of WWV anomalies. Rajeevan and McPhaden (2004) show that the WWV has a lead predictive skill of a season earlier for the Indian Summer Monsoon.

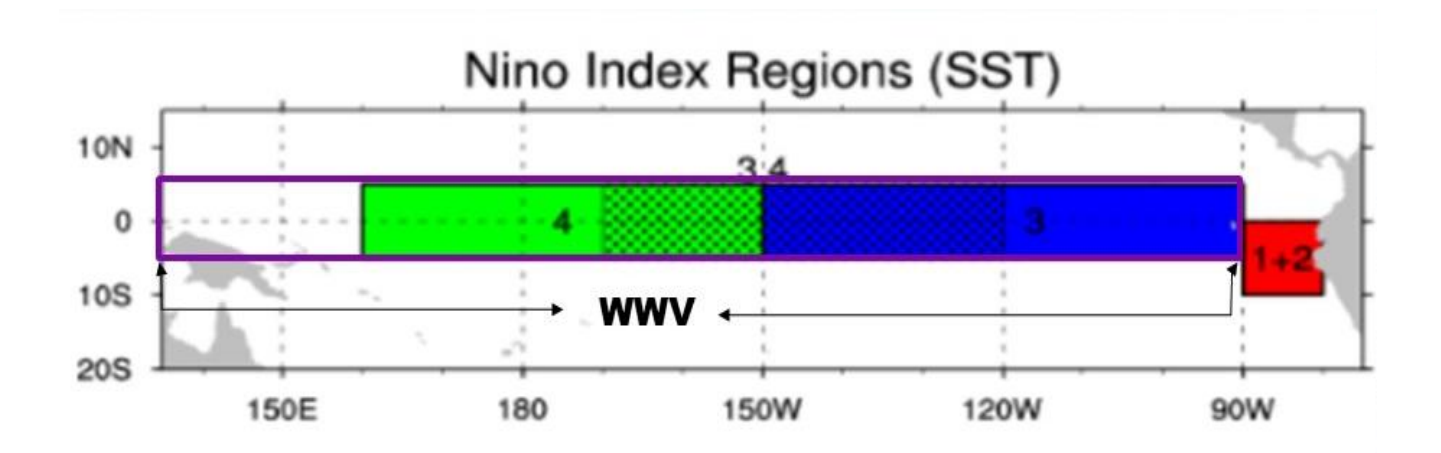


Figure 2.1: The SST indices Niño4 (green), Niño3 (blue), Niño 3.4 (speckled), and Niño 1+2 (red) and the associated regions. The WWV index is over the entire equatorial box from 120E to 80W. Source: Modified from the figure from Climate Data Guide, National Center for Atmospheric Research (NCAR).

2.2.3 Dipole Mode Index

We calculate the Indian Ocean Dipole Mode Index (IODMI) as defined by Saji et al., (1999). To find the west-east gradient, the characteristic dipole pattern (Figure 1.10), we calculate the SST gradient between the western equatorial Indian Ocean (50°E 70°E and 10°S 10°N) and the south eastern equatorial Indian Ocean (90°E 110°E and 10°S-0°). We take into consideration the IODMI only during the months of September to November as the IOD peaks during this season.

2.3 Statistical Methods

For understanding the decadal variability of Indo-Pacific teleconnections to Indian Summer Monsoon (Chapter 3), I have detrended all the datasets used. This is to remove the linear trends and to emphasize only the interannual variability. Whereas, the observations and the model output to study decadal prediction (Chapters 4 and 5) have not been detrended, as the linear trends also help in

decadal prediction. The data are then processed using different statistical methods or tools such as composite analysis, correlation, and regression analyses (Von Storch and Zwiers, 1999).

2.3.1 Composite Analysis

The composite analysis is a useful technique used to determine some of the basic characteristics that are difficult to observe in total averages. The composite analysis is used in meteorology to explore the large-scale impacts of teleconnections from different modes of variability like the ENSO or the IOD. In composite analysis, similar cases of a given phenomenon under a certain criterion are segregated together as composites. For example, to study the effects of opposite phases of ENSO, composites of El Niño events and La Niña events for variables like temperature or precipitation are prepared (Figure 1.8). The average of each composite set gives an estimate of how the phenomenon affects the selected variables during a particular phase. The difference between these composites shows a contrast-comparison. The criteria for composite selection or the interpretation of the results should be carried with due caution, considering climate variability on various other scales around each composite, and therefore the composite may not be a true representative of the typical state. However, composite analysis is a simple and quite powerful tool to get an early estimate of the mean state of a variable during a particular phase of any climate mode, before other statistical methods are considered (e.g. Yamagata et al., 2004; Ashok et al., 2007).

2.3.2 Linear Correlation

Linear correlation is a method to assess the co-variance (varying together) of any two independent samples and to check a potential linear relation between them. I use Pearson's correlation coefficient throughout this thesis. For two samples x and y with standard deviations as s_x and s_y , respectively, the correlation is measured using a correlation coefficient value (r) and calculated as

$$r = \frac{\sum_{i=1}^{n} (x_i - \overline{x})(y_i - \overline{y})}{(n-1)s_x s_y}$$

$$= \frac{\sum_{i=1}^{n} (x_i - \overline{x})(y_i - \overline{y})}{\sqrt{\sum_{i=1}^{n} (x_i - \overline{x})^2 \sum_{i=1}^{n} (y_i - \overline{y})^2}}$$

The value of r ranges between -1 to +1. When r > 0, the independent samples are considered to be positively correlated, and when r < 0, the samples are considered to be negatively correlated (Von Storch and Zwiers, 1999; Ross, 2020).

The correlation analysis has a few limitations. The correlation analysis doesn't assume any causation for the observed relation. Also, correlation doesn't give a quantitative assessment of which variable affects the other and how much. Moreover, data outliers tend to cause a misinterpretation of results.

2.3.3 Linear Regression

Correlation analysis considers the co-relationship between two samples. Whereas, regression determines a relationship between a dependent (or called response) variable and one or more independent variables. A linear regression establishes a relationship trying to fit a straight line between all the data points. Hence the equation for regression is a straight line. For two random samples x and y, where y is dependent on x, then

$$y_i = \alpha + \beta x_i + e$$

Where α , β , and e are the intercept value, slope, and regression residual (or called the least error) respectively.

$$\beta = \frac{\sum_{i=1}^{n} (x_i - \overline{x})(y_i - \overline{y})}{\sum_{i=1}^{n} (x_i - \overline{x})^2}$$

$$\alpha = \overline{y} - \beta \overline{x}$$

Linear regression can be applied to more than two samples, i.e., more than two independent predictors called multi-linear regression (e.g. Ashok et al., 2007). In my study, I look only at simple linear regression with only one independent variable. The estimated regression line (\hat{y}) is used by assuming the least error to be ~ 0 .

Therefore,
$$\hat{y}_i = \alpha + \beta x_i$$

2.3.4 Determination of Statistical Significance

In Statistics, the interpretation of results is by testing an initial (or null) hypothesis with an alternate hypothesis. A statistical test is used to either reject or continue with this null hypothesis and the decision is based on the data sample. But there is always a possibility of errors, i.e., rejecting a true null hypothesis (Type I error) or accepting a false null hypothesis (Type II error). To reduce these errors, the results are interpreted using a level of statistical significance.

For the significance testing about the mean, I used Student's *t*-test. Student's *t*-test is used for smaller sample sizes and calculated using mean (\bar{x}) and standard deviation (s) of a sample of size (n).

$$t = \frac{\overline{x} - \mu}{s / \sqrt{n}}$$

For uni-directional (n-1) degrees of freedom) or bi-directional (n-2) degrees of freedom) variations of mean, one-tailed t-test or two-tailed t-test is used, respectively. As climate means can vary in either direction, I use the two-tailed t-test throughout this thesis.

To remove uncertainties regarding sample biases, variance, or confidence level, and to improve the robustness of our results, I use the Bootstrapping technique. Bootstrapping is a resampling procedure where random samples are generated which follow the same distribution function $F_X(x)$ as the actual data sample. Then, the random sample is analyzed and checked if the inferences from earlier statistical analysis hold true for the new random sample as well. The inferred results are approximate as the distribution of the parameter estimate is derived from the estimated distribution function of the actual sample. To reduce further uncertainties from bootstrapping, a large number of random bootstrap samples are generated.

2.3.5 Empirical Orthogonal Function (EOF) analysis

Empirical Orthogonal Functions (EOFs) or Principal Component Analysis is a multivariate analysis technique of decomposing one random vector into its empirically derived basis functions or orthogonal spatial patterns. EOFs are often used in climate science to study spatial patterns of climate variability and their temporal variability. EOFs help to find structures (or patterns) that explain maximum variance in space-time. EOFs are derived by computing the eigenvectors of a spatially weighted anomaly covariance matrix. The corresponding eigenvalues provide a measure of the percent variance explained by each spatial pattern. By definition of orthogonality, each of the EOFs is independent. The lower-order EOFs can be interpreted as natural modes of climate variability in the observed system where as higher-order EOFs tend to be incoherent and hence considered 'noise'.

Used frequently in the study of climate dynamics, EOFs are used to understand the dominant modes of long-term climate variability. Covarying spatial patterns can be observed with each of the EOFs. EOFs are sensitive to the time and space domain chosen and hence must be used with caution (e.g., Behera and Yamagata, 2003; Marathe et al., 2015).

3

Recent changes in the Indian Summer Monsoon associated Indo Pacific atmospheric circulation

In this chapter, I revisit the Indian Summer Monsoon teleconnections with the ENSO indices (both ocean surface and subsurface temperature indices) and show how there has been a significant weakening in the teleconnections in the recent decades, even with the subsurface index. I analyse the surface winds over the tropical Indo-pacific region find the changed circulation features are a shift from the known circulation signatures that efficiently teleconnect El Niño forcing to South Asia.

3.1 The ENSO indices

As introduced in Sections 1.2 and 1.3, the ENSO is one of the major factors affecting the ISM interannual variability. The discovery of ENSO was based on the gradient between Tahiti and Darwin sea-level pressure anomalies, called the Southern Oscillation Index (SOI). Meanwhile, SST indices were also used as an alternate way of looking at ENSO phases. A working definition of ENSO was suggested by considering only the SST anomalies [SCOR 1983]. The SST indices widely used are Niño 1 + 2, Niño3, Niño4 and Niño3.4. The indices are defined as monthly averages of SST anomalies over their respective regions (Section 2.2.1). I consider only Niño3 and Niño4 indices in this study as they are indicators for Eastern and Central Pacific respectively and are non-intersecting boxes. Time evolutions of SST anomalies for both El Niño and La Niña composites of Niño3 and Niño4 indices are comparable.

During the evolution of an ENSO event (eg., during the strong El Niño of 1997-98), the thermocline in the eastern equatorial Pacific deepened a few months before the peaking of the SST over the region. The Warm Water Volume (WWV; see section 2.2.2) and hence the heat content increases as the water piles up over the deepened thermocline. This accumulation up of WWV acts as preconditioning of the eastern equatorial Pacific before the peaking of an El Niño (Wyrtki 1985; Cane et al. 1986; Jin, 1997a, b; Meinen and McPhaden, 2000). Jin (1997a, b) found that the recharge-discharge mechanism of the ENSO variability is balanced by the thermocline, i.e., heat content in the subsurface. Later Meinen and McPhaden (2000) show that the amplitudes of WWV are correlated to the Niño3 index. Importantly, they show that the anomalies in SST were noticed months after the WWV anomalies and hence WWV could be used as a predictor for ENSO. The importance of the WWV index for ISM was found by (Rajeevan and McPhaden 2004). The tropical pacific WWV during February-May (FMAM) shows a statistically significant lead correlation with the following Indian summer monsoon rainfall.

3.2 The weakening ENSO-ISM relations

Recent studies have shown that ENSO-ISM links decades (see section 1.3) have weakened over the past few decades. The weakening has been attributed to several factors like the circulation changes due to global warming (Kumar et al. (1999); Ashrit et al. (2001) or the interaction over the tropical Indian ocean (Sreejith et al., 2015), etc. On the other hand, some studies have claimed the weakening as apparent only statistically due to noise or sampling issues (Gershunov et al., 2001; Cash et al., 2017). As part of this thesis, for my first objective, I revisit the ENSO-ISM links using both the SST and subsurface indices.

We use AISMR from IMD, HadISST, and SODA datasets (Section 2.1.1) for rainfall, SST, and subsurface temperatures, respectively. All the datasets have been de-trended for the 1958–2008 period in order to remove the linear trends and to emphasize only the interannual variability and then the datasets are divided into three partially overlapping 30-year periods starting from 1958, specifically, 1958–1987, 1968–1997 and

1978–2007. I calculated and show correlations between ISMR and the SST indices, and those between ISMR and WWV.

The significance of the correlation is calculated using Student's two-tailed test. The degrees of freedom have been ascertained as N = 2, where N is the number of samples. As we take the interannual boreal summer values that are largely independent of 1 year to the other, this is a reasonable supposition. Therefore, the threshold of the significant correlation stands at 0.36 (0.28) for 30 (51) years at a 95% confidence level. Further, we have ascertained the significance of the correlations between the ISMR and two NINO indices by a boot-strapping test (1000 simulations). For this, we used the bootstrapping subroutine "bootstrap_correl", from the NCAR Command Language (NCL) package. This routine takes, as inputs, two input time-series for which the correlations need to be obtained (the ISMR and Niño3 SST, for example, in our case). Based on these input series, it generates 1000 time-series pairs randomly and computes correlations between each pair. After that, the correlations are ordered as per magnitude. Once this is done, the 50th highest correlation among the 1000 correlations computed, for example, gives us the 0.05 significance level (i.e., 95% confidence level) for the correlations. In the case of correlation differences between two time-series, the differences of correlations are ordered as per magnitude to identify the significant threshold values. The results from the above bootstrapping test show that the correlations for the recent period (1978–2008) differ from the total period (1958–2008) at a 90% confidence level.

3.2.1 The concurrent relation between ENSO indices and ISMR

Figure 3.1 shows the simultaneous correlations of the ISMR with the various ENSO indices, i.e., WWV, NINO3, and NINO4, for June-September (JJAS) season for each 30-year overlapping period (1958–1987, 1968–1997, 1978–2007) and also for the total period (1958–2008). In accordance with the earlier findings (Kumar et al. 1999; Ashok et al. 2001; Rajeevan and McPhaden 2004), the results for JJAS show gradually weakening over time. The correlations with the Niño3 index particularly show a very rapid decrease, with

the correlations becoming insignificant during the recent period, i.e., 1978-2007. The Nino4 index, more relevant to the Indian summer monsoon rainfall owing to its relative proximity to the sub-continent (Kumar et al. 2006; Ashok et al. 2007), also shows gradually weakening association with the ISMR over the period, though the correlations are still significant at 95% confidence level even through the late 2000s. The multi-decadal correlation coefficient between the WWV and ISMR, also decreased from a high -0.44 in 1958–1987 to -0.36 in 1978–2007, though the recent correlations are still statistically significant at a 95% confidence level.

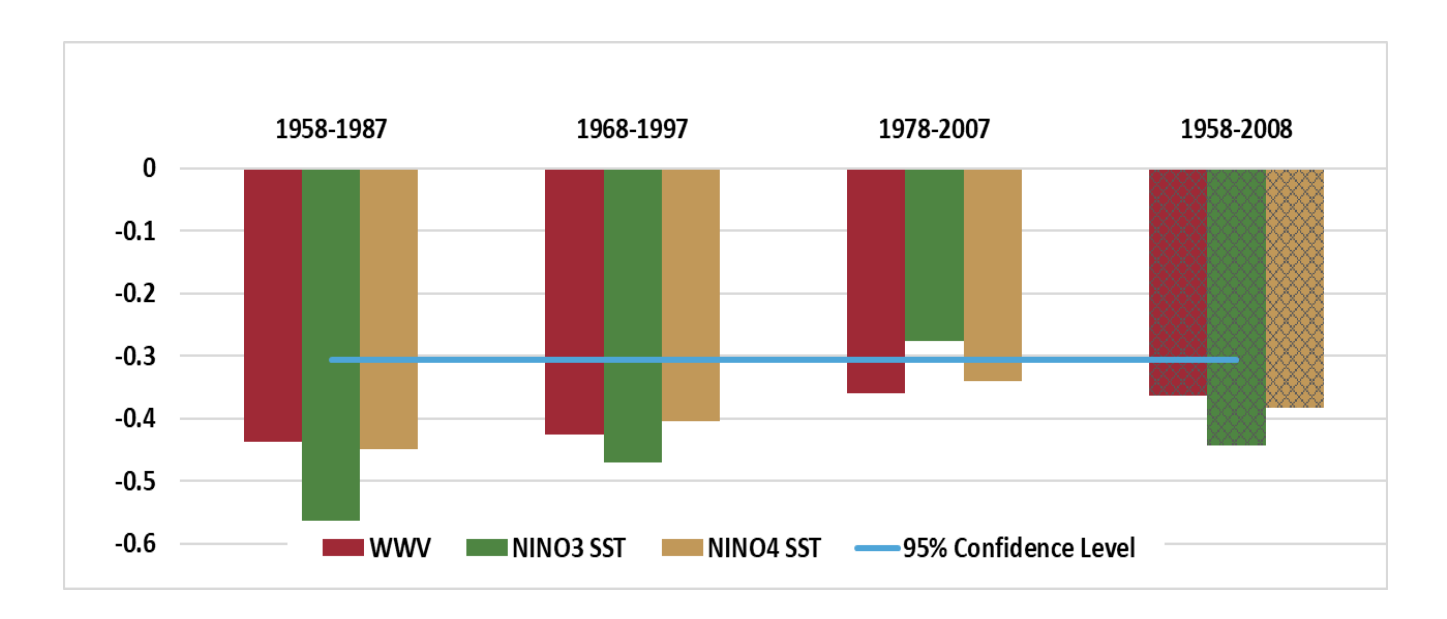


Figure 3.1: Correlation of ENSO Indices (WWV, NINO3, and NINO4) with ISMR during **JJAS**. The solid-coloured bars are for the three overlapping periods, i.e., 1958–1987, 1968–1997, and 1978–2007. The hatched bars are for the total period, 1958-2008.

3.2.2 The lead-lag relation between ENSO indices and ISMR

Following Rajeevan and McPhaden (2004), I present the lead correlations of the various Pacific indices during the pre-monsoon season (FMAM) with the subsequent (lag) ISMR in the different overlapping periods (Figure 3.2). Our results are in conformation with earlier findings in the sense that the lead correlations of the pre-monsoon WWV with the ISMR have been, all the while significant at a 95% confidence level. However, just as the weakening simultaneous correlations, the magnitude of the lead

correlation of the WWV with the ISMR has also steadily decreased. We also find that the lead correlation during FMAM has a significant lead predictive skill, though it has weakened further and is insignificant for the recent period, 1978–2007. For the 1958–2008 period as the seasonal correlations of ISMR with WWV show that these are maximum when computed simultaneously, just as that in the case of the ISMR correlations with any simultaneous tropical pacific SST index.

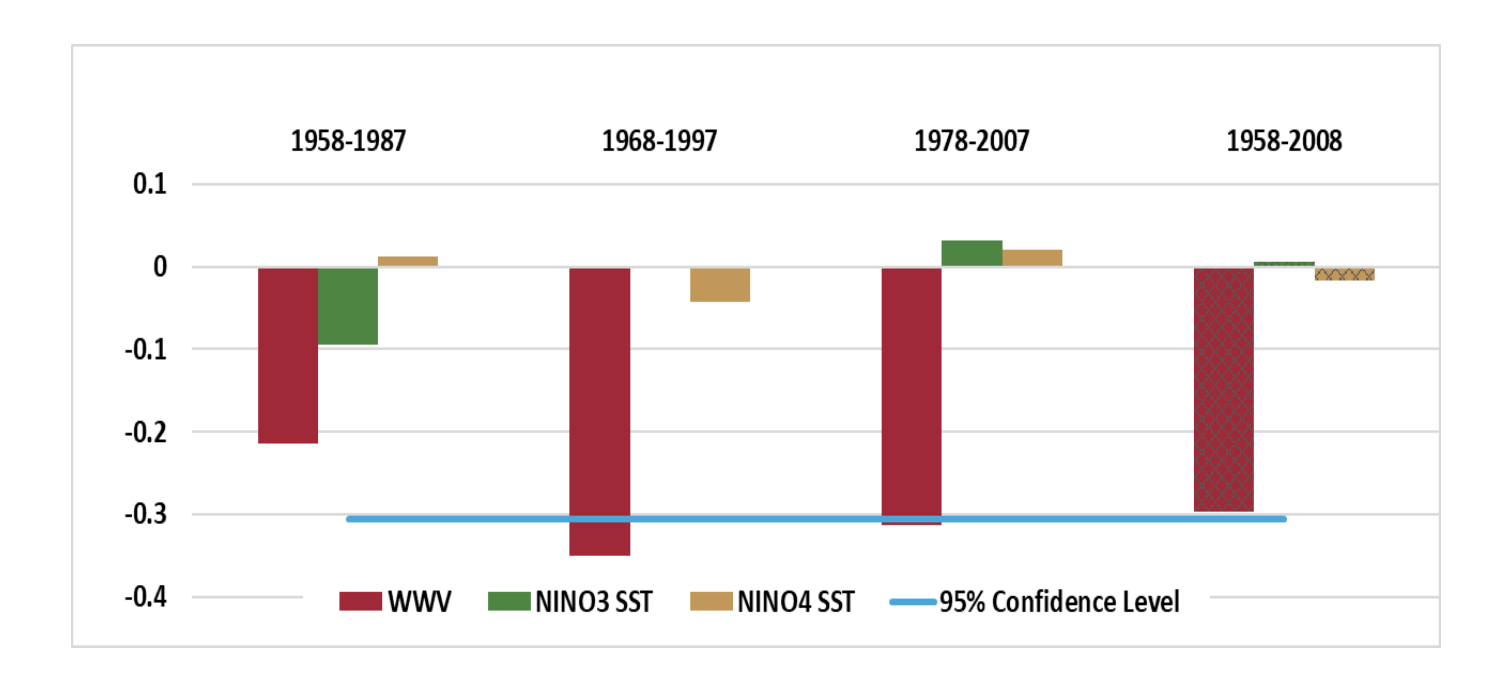


Figure 3.2: Correlation of ENSO Indices (WWV, NINO3, and NINO4) with ISMR during **FMAM**. The solid-coloured bars are for the three overlapping periods, i.e., 1958–1987, 1968–1997, and 1978–2007. The hatched bars are for the total period, 1958-2008.

Thus, our analysis shows that the weakening of the ENSO-Monsoon correlation in the recent period can be attributed to changes associated with ENSO characteristics or PDO. Having said that, one should be aware of the fact that such a weakening of correlation for the 1978–2008 period as compared to 1958–2008 period is potentially due to internal modulations in monsoon, and not necessarily related to any discernible external cause (e.g., Gershunov et al. 2001; Ashok et al. 2014; Wu et al. 2017), or in other words, just an issue of sampling (Delsole and Shukla 2012; Cash et al.2017). From this context, it is apropos to mention a recent analysis of PMIP3 simulations for the last millennium (Tejavath et al. 2018), which shows that, four of seven

models simulate statistically significantly weakened intra-annual ENSO-Monsoon correlations from Medieval Warm Period (1000–1199 AD) to Little Ice Age (1550–1749 AD) apparently due to changes in ENSO characteristics.

3.3 Analysis of the surface winds over the tropical Indo-Pacific

The second objective of my thesis is to explore the mechanisms for the weakening of the ENSO-ISM links. To find a potential cause for the observed weakening of ENSO-ISM links, we analyse the JJAS surface winds over the tropical Indian and Pacific Oceans. During the 51-year period, 1958–2008, the winds over the Tropical Indian Ocean (TIO) show a weakening correlation with ISMR (Figures 3.3; 3.4). By intercomparing these correlations over various sub-periods (Figures. 3.3a–c; 3.4a–c), we find that the surface winds during JJAS over the tropical Indo-Pacific basin show the strongest links over the Pacific basin during 1958–1977 and over the Indian subcontinent than anywhere else in the tropical region. Specifically, the eastern tropical Pacific circulation exhibits rather weak links to ISMR during the recent period.

Looking at the circulation patterns, the correlations show a shift in the circulation pattern during the recent period. There is a prominent weakening of the cyclonic circulation (observed in Figures 3.3a, b; 3.4a, b) associated with ISMR over the tropical Pacific during the recent period (Figures 3.3c; 3.4c). The corresponding correlations for the 1978–2007 period indicate a 'disconnect' in correlation vectors between the tropical Pacific and TIO. We believe that this is mainly due to a decadal change in the mean circulation over the Indo-Pacific region.

A linear regression analysis (Figures 3.5; 3.6) has been carried out to estimate and understand the apparent shift of dependence of ISMR. With the local zonal and meridional winds as independent variables and ISMR as the dependent variable, the regression analyses show similar patterns. We find that this link over the whole

period is mainly being contributed only from the early period. We notice a sudden increase of an apparent relevance of the circulation in TIO during 1978–2007 (Figure 3.6c). We also find strong regression vectors in the western Pacific at 25°N (Figures 3.5c; 3.6c) (Krishnamurthy and Krishnamurthy 2017). Some studies show that there is a westward shift of subtropical high (Hu 1997; Gong and Ho 2002; Zhou et al. 2009; Mujumdar et al. 2012; Preethi et al. 2016), we believe this shift might be arising mainly due to this westward intensification of subtropical high. This suggests a paramount relevance of the changes in the circulation over the western Pacific region for the weakening of the ENSO teleconnections to the ISMR. Indeed, a difference plot (Figure 3.7) obtained by subtracting the regressions for the 1958–2008 period from the recent decades of 1978–2008 indicates a strengthening in the cyclonic correlation/regression vectors associated with ISMR south-east of Japan in the recent period. In this context, it is pertinent to recall Figures 7 and 8 of a seminal study by Lau and Nath (2000) which shows an anticyclone southeast of Japan and an anomalous cyclone over the Bay of Bengal and the Indian region during boreal summer months in El Niño years. Evidently, the weakening of this anticyclonic circulation (or rather strengthening of the cyclonic circulation) is associated with ISMR effectively weakened the ENSO-ISMR links.

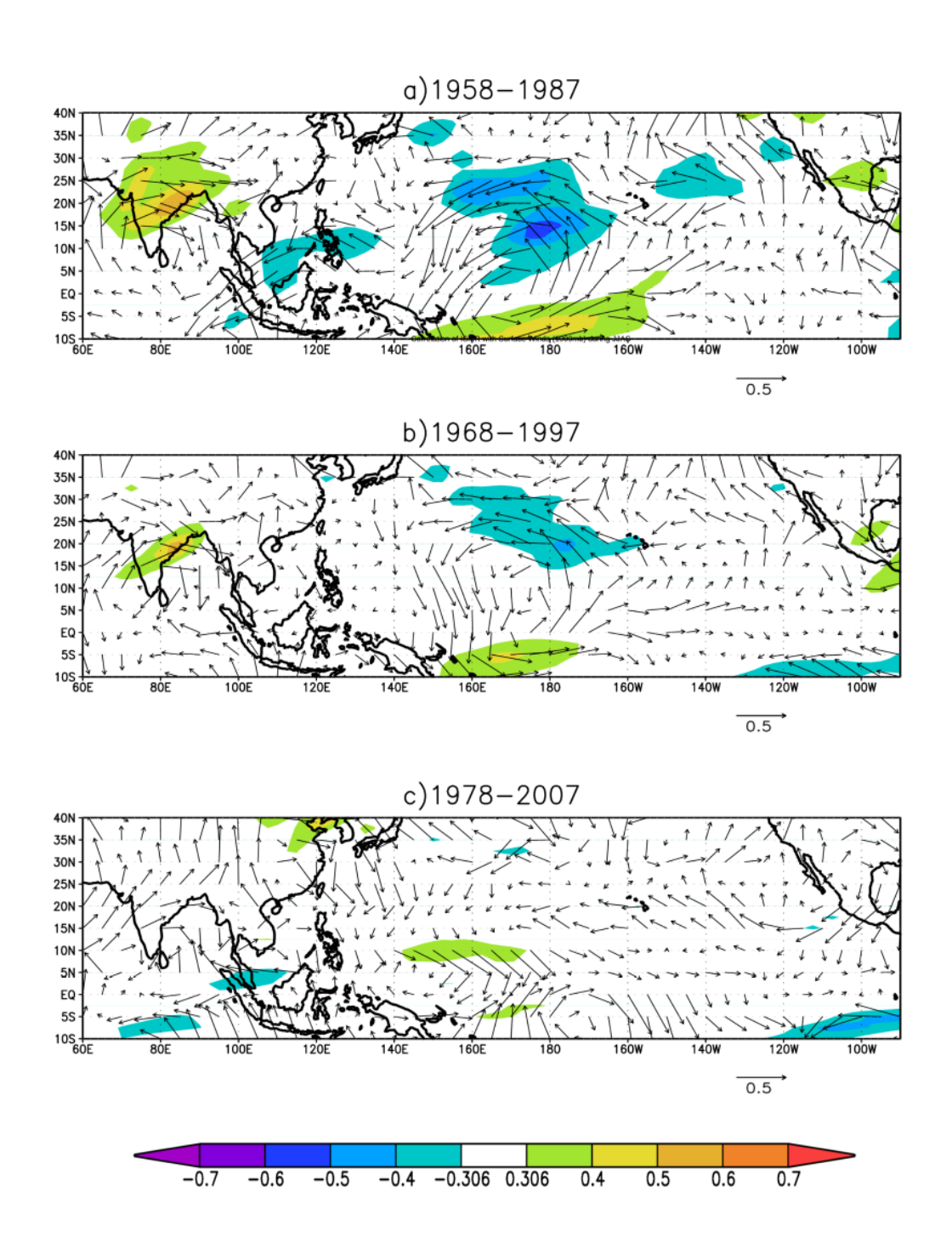


Figure 3.3: Correlation of ISMR with surface winds (1000 mb) during JJAS (zonal correlations at 95% significance in colour)

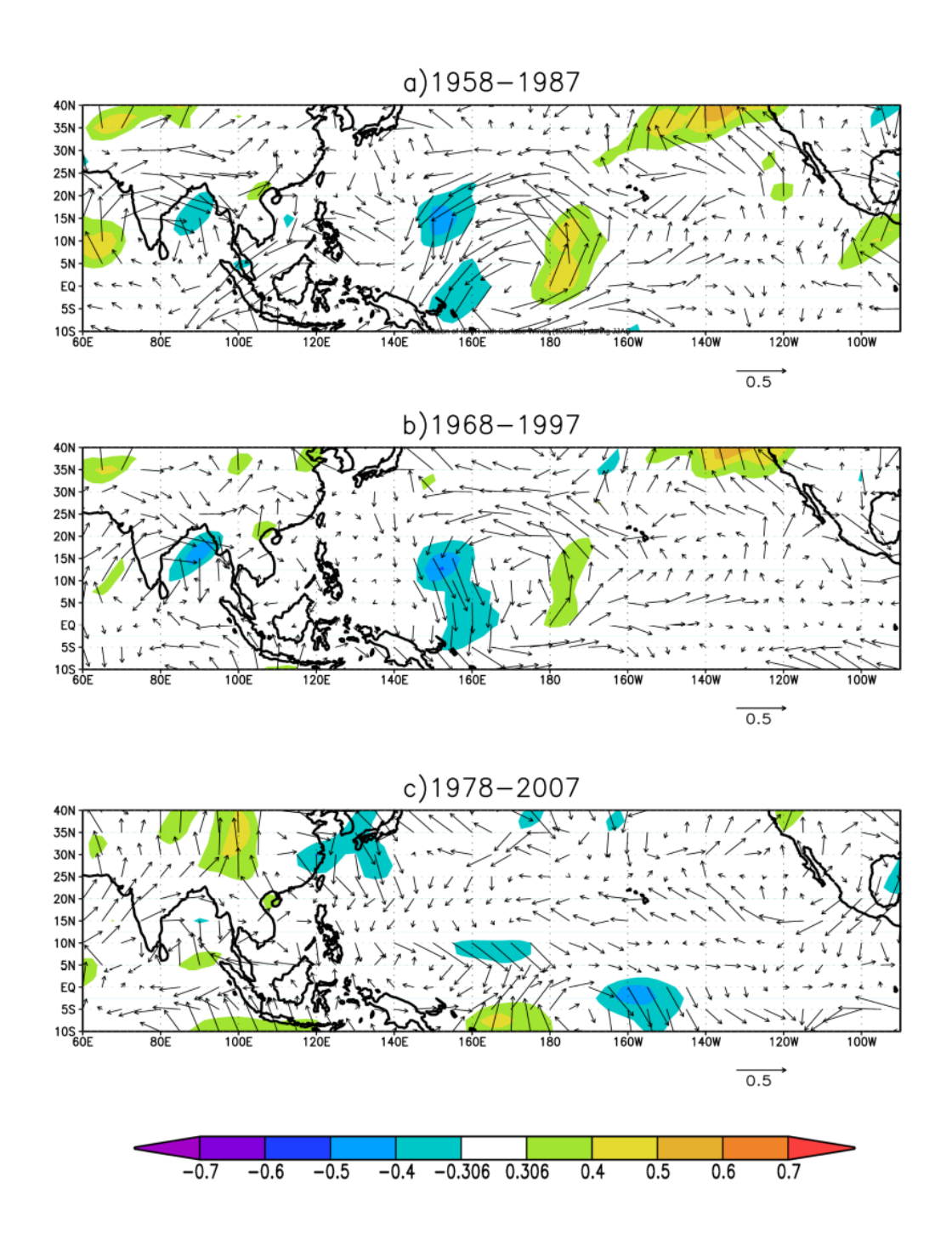


Figure 3.4: Correlation of ISMR with surface winds (1000 mb) during JJAS (meridional correlations at 95% significance in colour)

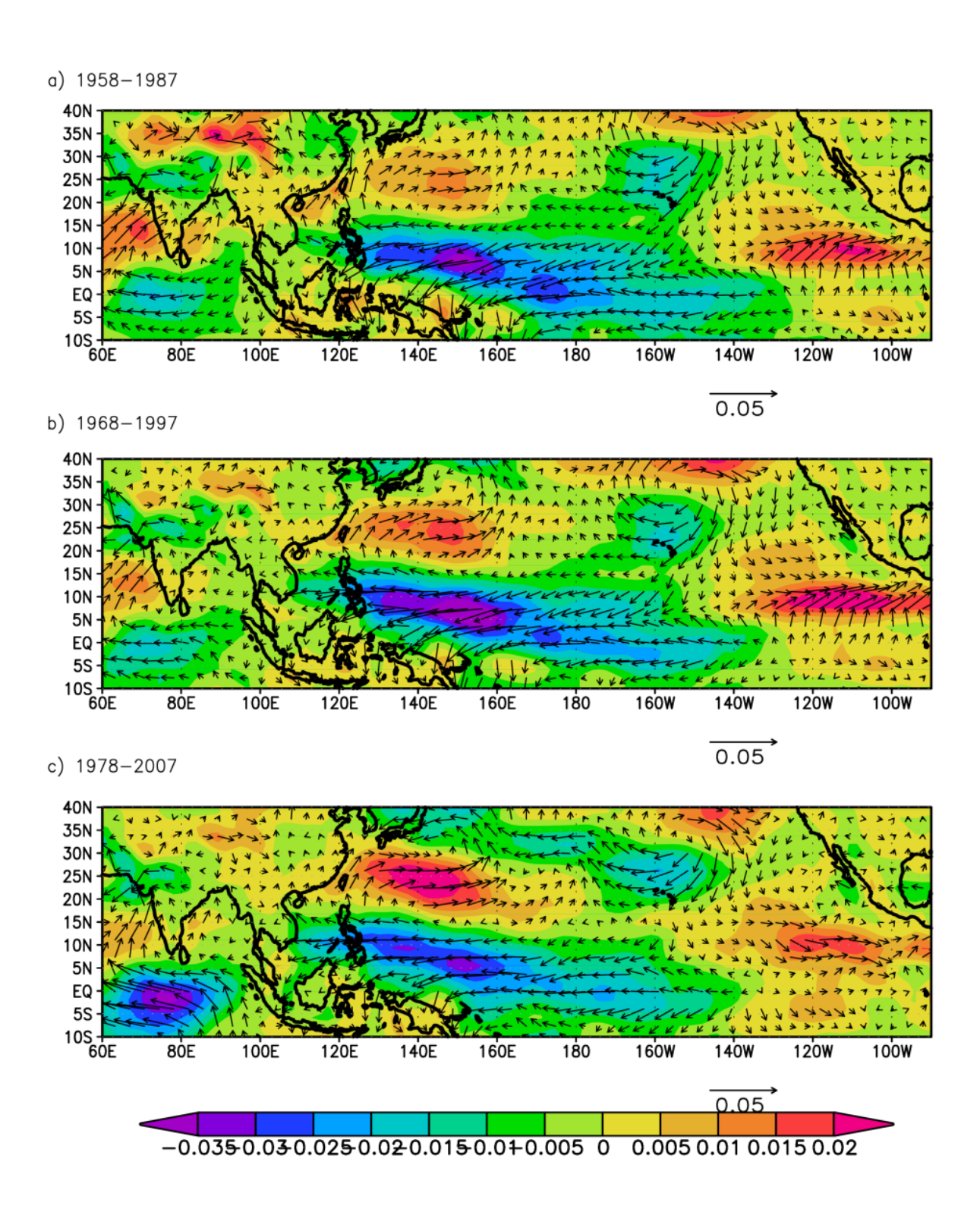


Figure 3.5: Regression of ISMR with surface winds (1000 mb) during JJAS (zonal regressions in colour)

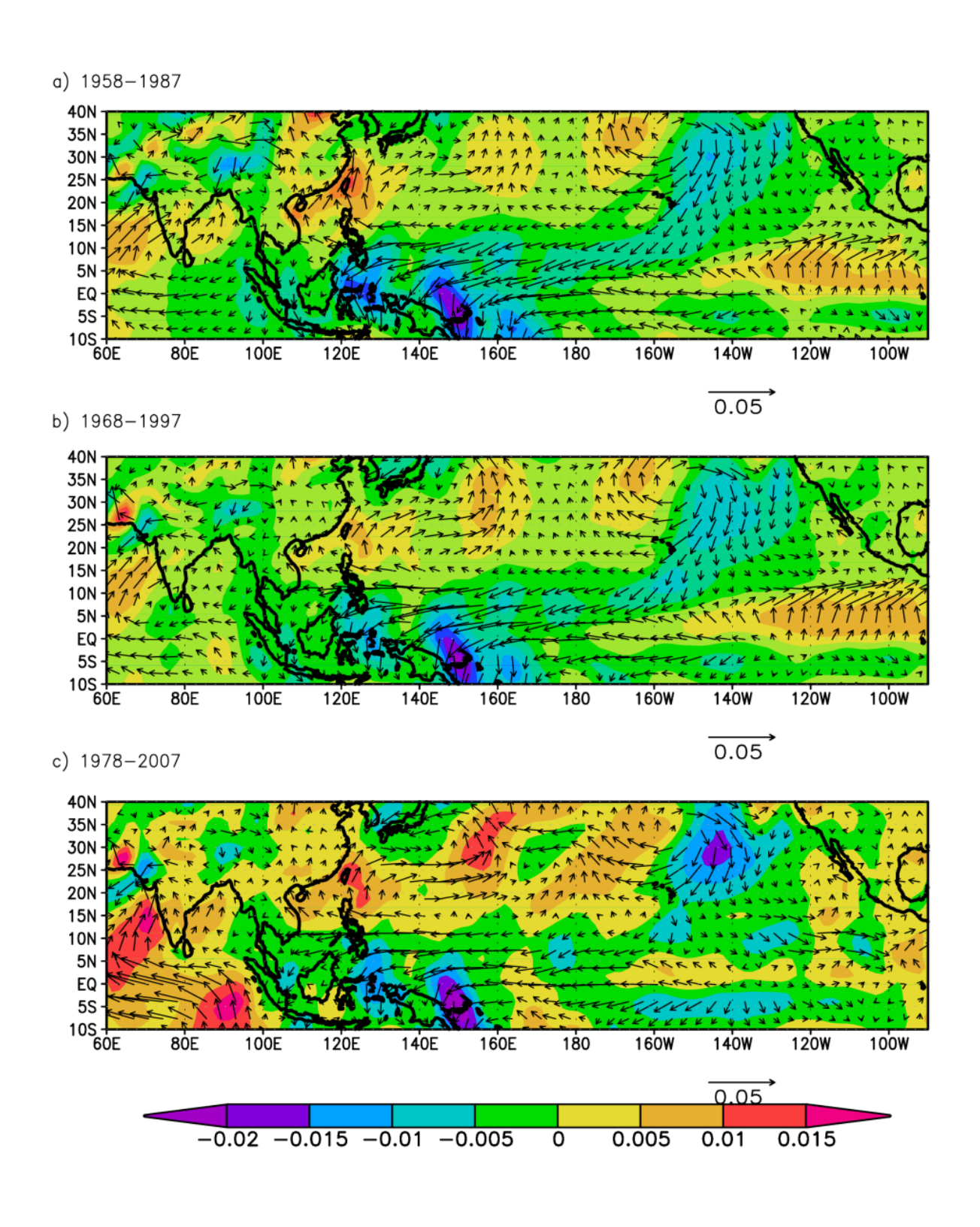


Figure 3.6: Regression of ISMR with surface winds (1000 mb) during JJAS (meridional regressions in colour)

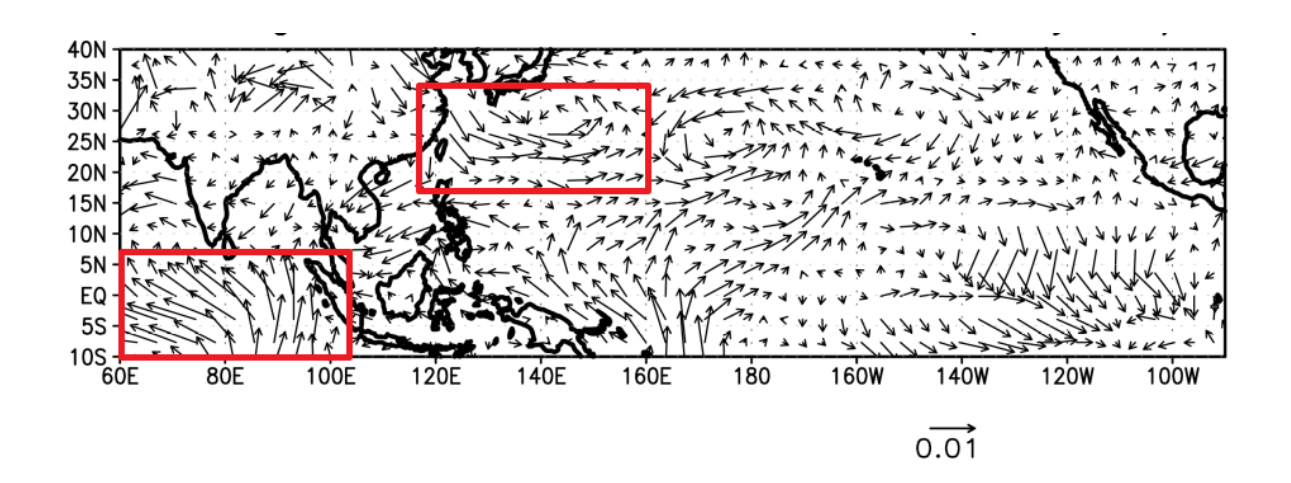


Figure 3.7: Difference of regression of ISMR with surface winds (1000 mb) during 1978–2008 from 1958–2008 (51 years). The region over the northeast Pacific shows an anomalous cyclonic circulation. The region over the equatorial Indian ocean shows an intensified cross-equatorial flow.

Interestingly, the correlation and regression analysis, shown in Figures 3.3, 3.4, 3.5, and 3.6, also suggest a low-level cross-equatorial strengthening of the regression vectors over the TIO and Bay of Bengal regions during the 1978–2007 period as compared to the previous decades, along with the correspondingly strengthened cyclonic circulation southeast of Japan. The winds over TIO seem to have a north-easterly directional shift post-1970s. The cross-equatorial flow which was limited to the west of the TIO has broadened eastwards, basin-wide, along with the TIO. A further investigation into this shows that the variability of Mascarene High is relatively more relevant to the ISMR variability in recent decades. The standard deviation of an SLP-based Mascarene high index (25°S:35°S; 40°E:90°E) for 1978–2008 is 6.68% higher than that for the 1951–2008 period, suggesting that there is a decadal change in the Mascarene High strength, and consequently the associated circulation (Figure 3.8). We believe that this has resulted in the observed relatively stronger association of monsoon rainfall with the cross-equatorial low-level circulation in TIO in recent decades. While further examination of this aspect is beyond the scope of the current study, it will be worth investigating a mechanism for this apparent decadal variability of Mascarene High.

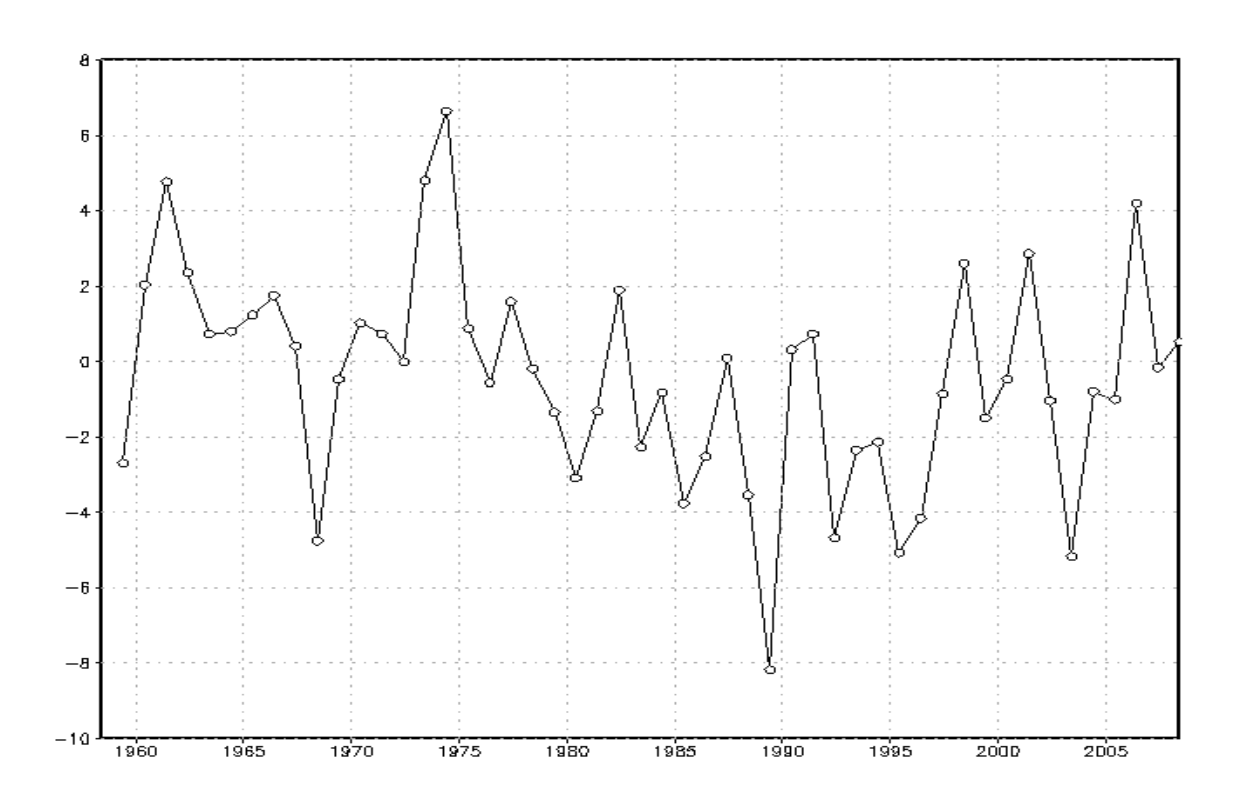


Figure 3.8: Sea level pressure variability of Mascarene High

3.4 Conclusion

This chapter concludes two objectives of my thesis. To understand the decadal variability of Indo-Pacific teleconnections to Indian Summer Monsoon and to explore the mechanisms for the weakening of the ENSO-ISM links. We find that irrespective of the choice of the indices, the teleconnections of Pacific and ISMR seem to weaken, though WWV still has significance. WWV has a lead prediction skill during the premonsoon season and the highest correlation was found to be during FMAM. Our study shows that there is a shift in the mean state of winds in the recent period of 1978–2007 (Figures 3.5; 3.6). Particularly, the winds over the north western Pacific show a cyclonic intensification during the same period. There is a weakening of anticyclonic circulation correlation vectors south-east of Japan which connected ENSO to ISMR.

A simultaneous strengthening of a cross-equatorial circulation in TIO as compared to the pre-1977 periods is also observed. This shows an increased relevance of the cross-equatorial flow due to the decadal variability

of Mascarene High. This is opposite to the circulation over Eastern TIO associating El Nino with ISMR. Such a change in the background state apparently disrupts the teleconnections of the ENSO impact which results in the weakening of the ENSO connections.

All these suggest that a shift in the ISMR associated surface wind circulation in recent decades over the Indo-Pacific region weakens the El Niño transfer mechanism in recent decades. We also plan to reconfirm the results reported in the current work through an analysis of various CMIP5 model outputs and by conducting some dynamical simulations.

4

Exploring the Decadal prediction skills of Indo-Pacific drivers of the Indian Summer Monsoon

4.1 Decadal Prediction

The future climate, at least for the next few decades, depends on natural climate variability as much as on anthropogenic forcing (Cane, 2010; Moss et al., 2010; Kushnir et al., 2019). Neither seasonal predictions nor study of climate projections, alone were sufficient anymore. Demand for near-term (5-30 years) predictions has increased among policy makers and stakeholders. Internal variability from climate drivers like ENSO has to be accounted for as in seasonal-interannual prediction, along with external forcings like greenhouse emissions or aerosol concentrations. Decadal prediction emerged intending to bridge this gap between seasonal-interannual prediction and long-term climate projections.

For a feasible decadal prediction, the general circulation models have to resolve two problems. First, the initial value problem of predicting the future state of climate by giving an estimate of its present state. Secondly, boundary condition problem of assessing potential changes in climate by external forces (Collins, 2002). Weather prediction or seasonal to inter-annual forecasts are initial value problems. Boundary conditions include anticipated changes in anthropogenic greenhouse gases and

aerosols. The decadal prediction has to account for both internal variability of the system by resolving initial value problems, and also external forcing by resolving the boundary conditions.

Early attempts of decadal prediction by Smith et al., (2007) and Keenlyside et al., (2008) were optimistic and showed promise, though contradicting in their results. Smith et al., (2007) showed an improved skill for prediction over Indian and Southern Oceans. Meehl et al (2009) state that decadal prediction could be feasible by model initialization with assimilation of persistent anomalies (mainly in upper-ocean heat content) to account for any lack of ability to simulate the climate natural variability, accurately. Several other studies also show that decadal prediction shows a higher skill for regions where the climate is strongly modulated by low-frequency variability in the oceans (Yeager et al., 2012; Robson et al., 2013). Along with ocean temperatures and salinity, assimilating other aspects of climate, like snow cover, sea ice, soil moisture, etc., may also have the potential to improve prediction skills beyond the seasonal to interannual time scales (Meehl et al., 2009). Skills in the decadal prediction of SSTs were observed over the north Atlantic (Dunstone et al., 2016; Borchert et al., 2012; Xin et al., 2021), tropical Pacific (Chikamoto et al., 2015), surface air temperatures (Müller et al., 2012; Xin et al., 2017; Sgubin et al., 2021) and even precipitation (i.e., Sahel rainfall, Sheen et al., 2019).

Note:- Predictability and prediction are two terms with similar meanings but are neither the same nor interchangeable. Predictability pertains to how much of a system can be predicted, theoretically. Prediction skill is the quantification of how much has been predicted (by a model). Ideally, the goal is to improve prediction skills till predictability. The skill of a prediction can be assessed by testing past cases, also called hindcasts. A model gives a hindcast (also called retrospective forecast) which is then compared to observations and the prediction skill is determined (Meehl et al., 2014).

4.2 Preprocessing of Model Output

We explore decadal prediction skills in the tropics. I analyze data from CMIP5 decadal runs as described in Section 2.1.2. We analyze the output from four models, i.e., CanCM4, MIROC5, GFDL, and BCC-CSM. All four models have multiple ensembles. Each ensemble-set was initialized every year from 1960 till 2011 and run for ten years. For example, CanCM4 has 10 ensemble members. A set of ten ensemble members is initialized in 1960 and the model is run for ten years till 1970. Another set of ten ensemble members is initialized in 1961 and run till 1971, and so on. All the model ensemble-sets are initialized similarly, from 1960-2011. Together, we have 51 ensemble members of decadal hindcasts for each model, each differing from the other in the initialization year (from 1960-2011).

Climate is a chaotic system. The errors in the initial conditions will inevitably grow as time evolves and deem the model output unusable beyond a threshold. This implies that the model uncertainties increase with each time step. Therefore, to compare each model, we average multiple ensembles with the same initialization dates. The output data from all the models are divided into 10 groups depending on the year after initialization (Fig. 4.1). Yr1, yr2, yr3... indicate 1, 2, 3 ... year(s) after initialization. Each of these groups is then compared with observations/reanalysis data to find the model prediction skills for each year after initialization.

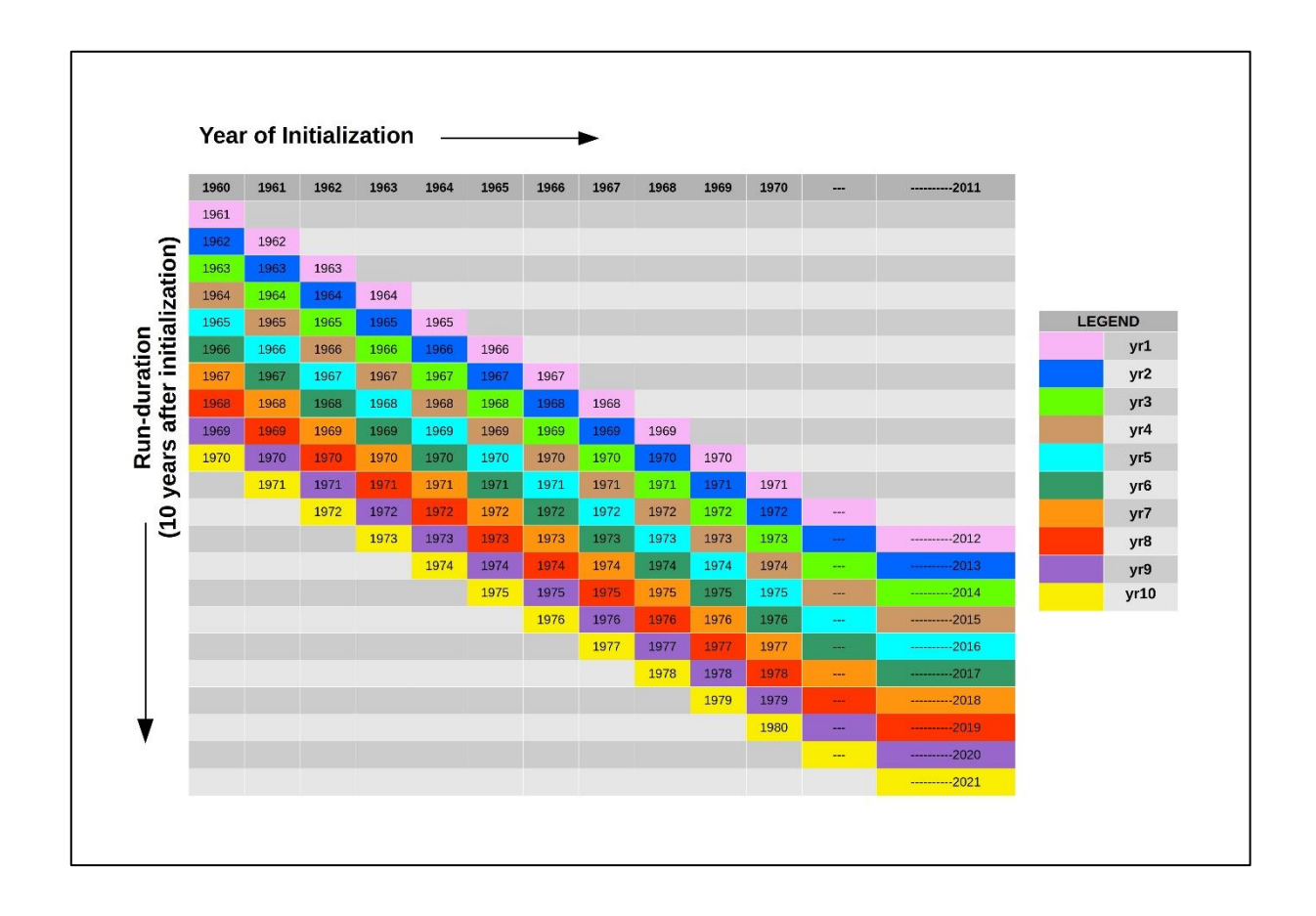


Figure 4.1: The output data from all the models, is divided into 10 groups depending on the year after initialization. Yr1, yr2, yr3... indicate 1, 2, 3 ... year(s) after initialization which is represented by individual colours.

4.3 Lead Prediction skills for ENSO

We analyze the decadal prediction skills for the El Niño Southern Oscillation (Section 1.2) by calculating the anomaly correlations between the observed NINO3 index with the corresponding hindcast NINO3 indices at different lead years for the four models. Our study shows that all the models show significant prediction skills in the first year after initialization (Figure 4.2). The skills are significant at leads up to 12-13 months. This is in agreement with earlier studies which show that ENSO can be predicted about a year ahead. Several earlier studies show that a strong ENSO event

can be predicted up to 10-12 months ahead, while a weaker ENSO has a predictability of only about 4-5 months (Latif et al., 1998; Jin et al., 2008; Sun et al., 2018). Pal et al., (2020).

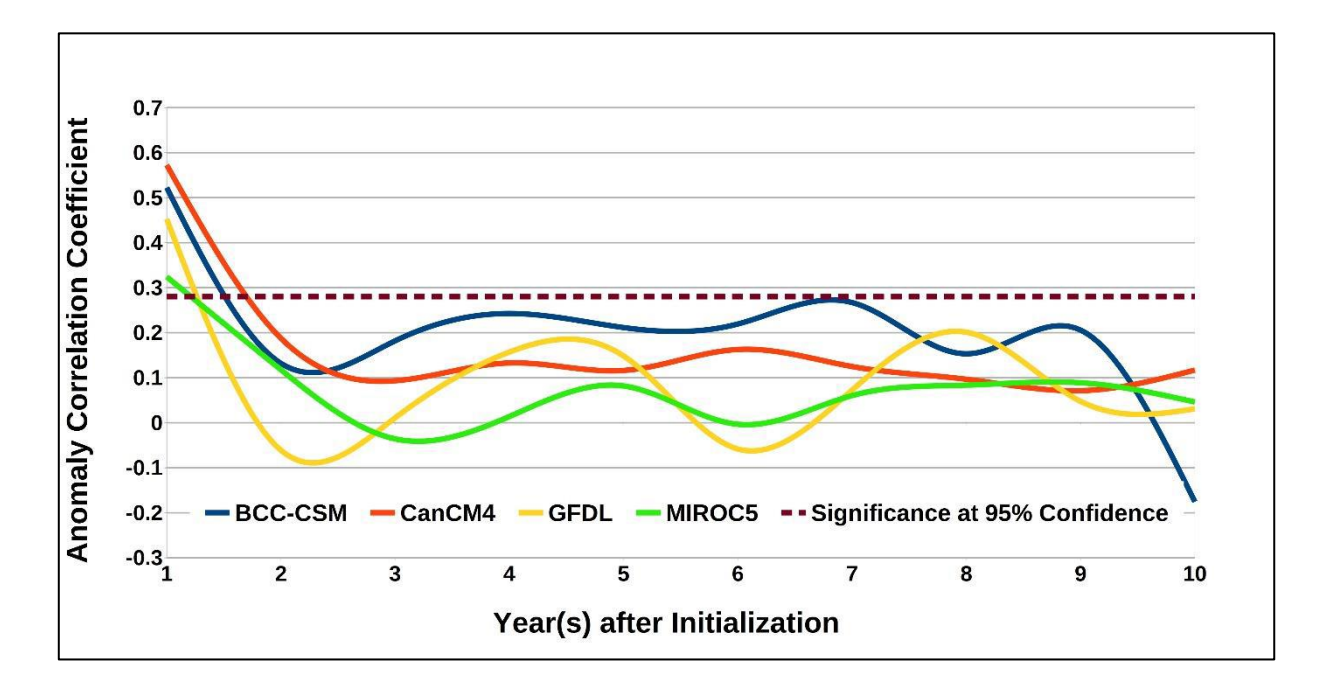


Figure 4.2: Anomaly correlations between observed NINO3 index with the corresponding predicted NINO3 index at different lead years for various models, shown in different colours. The significant correlation value at a 95% confidence level is 0.27 and is shown by the dashed line.

4.4 Lead Prediction skills for IOD

We then focus on the Indian Ocean Dipole (Section 1.4) and the skills of the four models in predicting IOD on a decadal scale. Surprisingly, the hindcasts from the MIROC5 and CanCM4 predict the IODMI during the fall season with significant lead prediction skills for at least 2-3 years (Figure 4.3). The skill levels for most of the lead times are statistically significant at the 95% confidence level from a 2-tailed Student's t-test. While the lead prediction skills of the IODMI from the CanCM4 fall below 95% confidence level at 4-5-year leads, these skill levels are still significant at a 90% confidence level. The MIROC5 also shows a weak skill for the eighth year, still significant at an 80%

confidence level. It is noteworthy that this skill is present despite the maximum lead skill of only one year for the NINO3 index in all the models. We also ascertain that the maximum lead time skill for the NINO4 is similar to those for the NINO3 index.

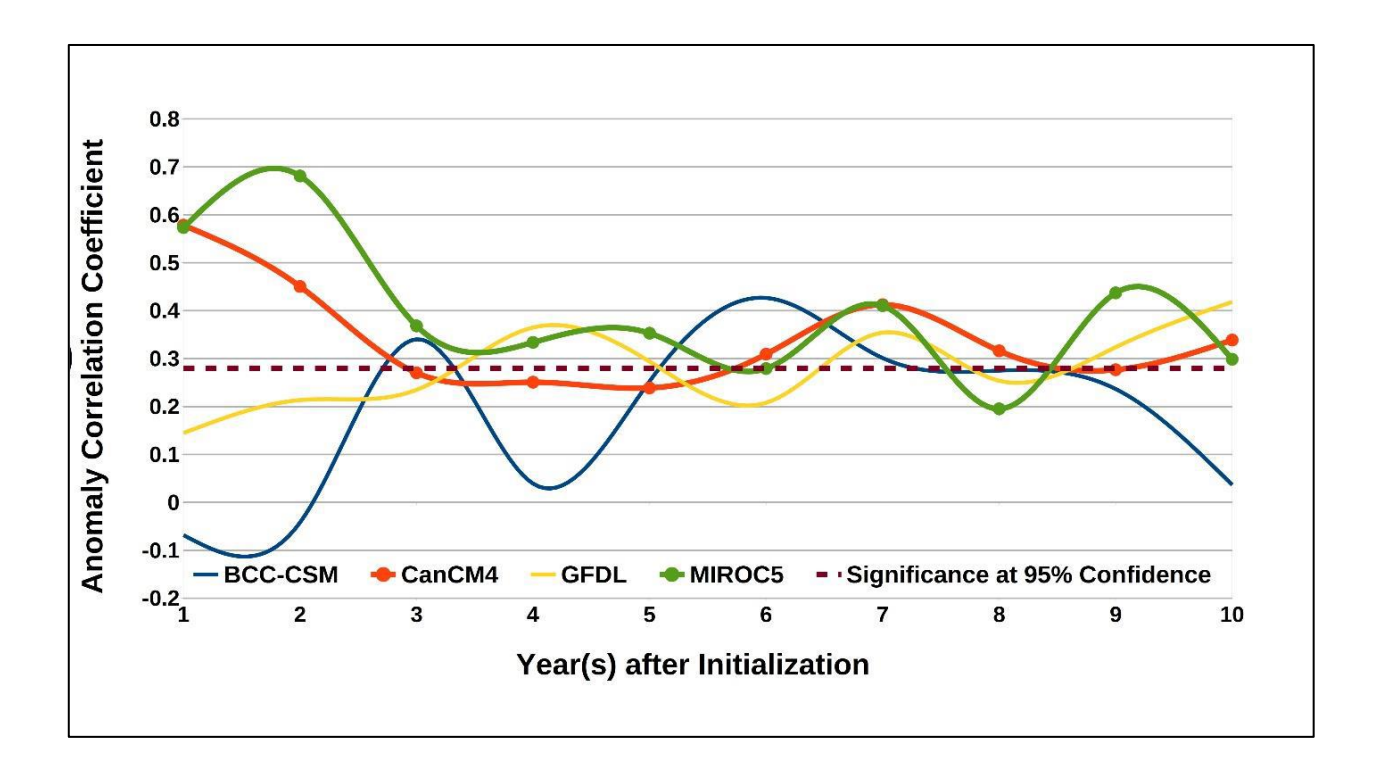


Figure 4.3: Anomaly correlations between observed IODMI with the corresponding predicted IODMI at different lead years for various models, shown in different colours. The significant correlation value at a 95% confidence level is 0.27 and is shown by the dashed line. the IODMI. The lines with circles in the figure are the two models of interest for this study.

We also compare the persistence skill of the observed IOD with the predicted IOD. Our results show that the prediction skills of the IOD for the models CanCM4 and MIROC5 are significantly better than persistence. We present a correlogram for CanCM4 and MIROC5 (Figure 4.4).

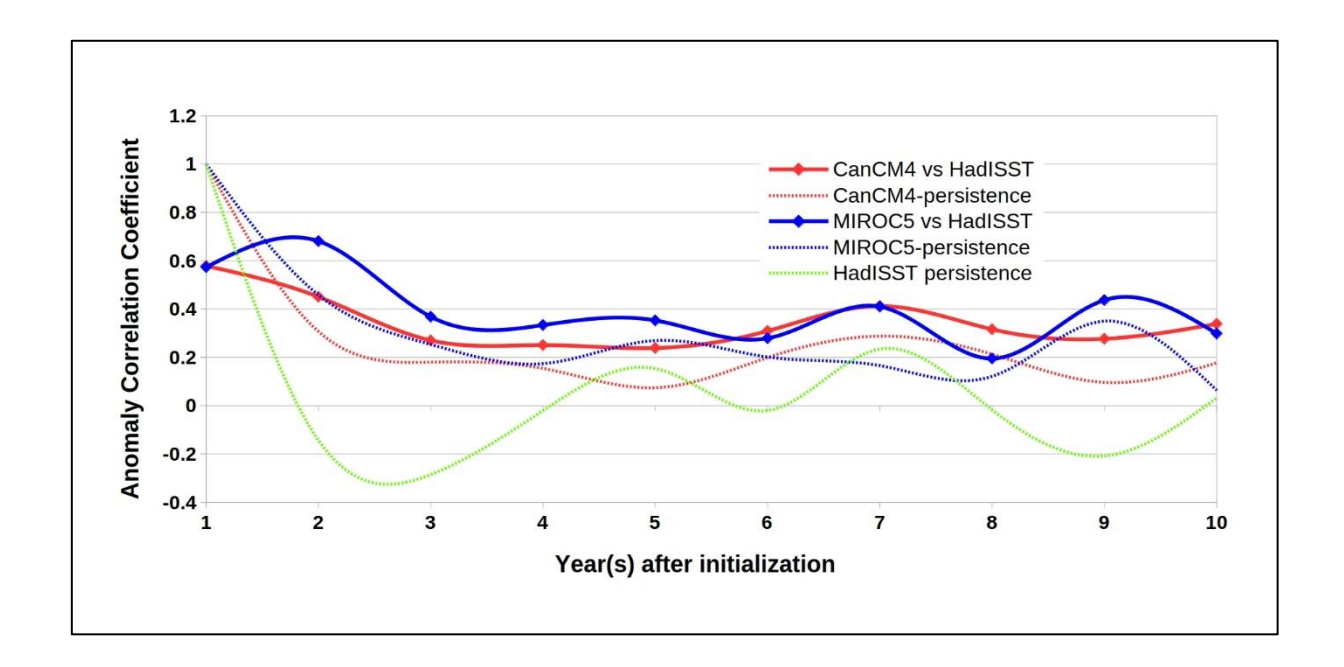


Figure 4.4: Evolution of persistence skills with respect to year1, (autocorrelation, shown in Y-axis) with years after initialization (X-axis) for the IODMI from HadISST, and that from various models. The solid lines show the autocorrelation values and the dotted lines show the correlations between observed IODMI with the corresponding predicted IODMI. The lines with circles in the figure are the two models of interest for this study.

Following standard practice in the seasonal prediction, we have used degrees of freedom 'N-2' for our correlation analysis and not the sample size 'N' for our statistical significance. (Von Storch et al., 2001; See Section 8.2). Just for better authenticity and to carefully ascertain the statistical robustness of our results we calculate the degrees of freedom using the Satterthwaite formula for a two-sample t-test using the following formula:

$$df = \frac{\left(\frac{s_1^2}{n_1} + \frac{s_2^2}{n_2}\right)^2}{\frac{1}{n_1 - 1} \left(\frac{s_1^2}{n_1}\right)^2 + \frac{1}{n_2 - 1} \left(\frac{s_2^2}{n_2}\right)^2}$$

where *s* and *n* are the standard deviation and sample size respectively. We found our results to be still valid for the predicted IODMI.

The Indian Summer Monsoon is ISM is strongly influenced by ENSO and IOD, along with other factors. Our study shows that the models show no skills in predicting the ISM, presumably due to model inadequacies in representing monsoon processes (figure not shown). Nevertheless, rainfall predictions could be improved by exploiting known statistical relationships between ENSO-ISM or IOD-ISM (Jourdain et al., 2013; Swapna et al., 2015; Dutta et al., 2018).

4.5 Fidelity of the Simulated IOD

To further ascertain whether the IODMI computed from the two hindcast datasets represents some of the observed features of the IOD (Yamagata et al., 2003), we compare the second leading simulated EOF modes of the SST from the hindcasts of MIROC5 and CanCM4 with that from the corresponding observations. Figure 4.5, derived from the EOF analysis at a one-year lead, shows that the models indeed capture the observed dominant IOD variance pattern associated with the EOF2 in terms of the location of the two centers of action. The simulated variances explained by this statistical mode from the MIROC5 is 12.2%, comparable to the corresponding observed value of 12% (Saji et al., 1999; Ashok et al., 2004). EOF2 of CanCM4 is 27.4%, which is higher than the expected value as the dipole-like structure shows more spread in the eastern Indian Ocean. The simulated EOF1, associated with the Indian Ocean Basin mode, and the corresponding variance-explained are also realistic.

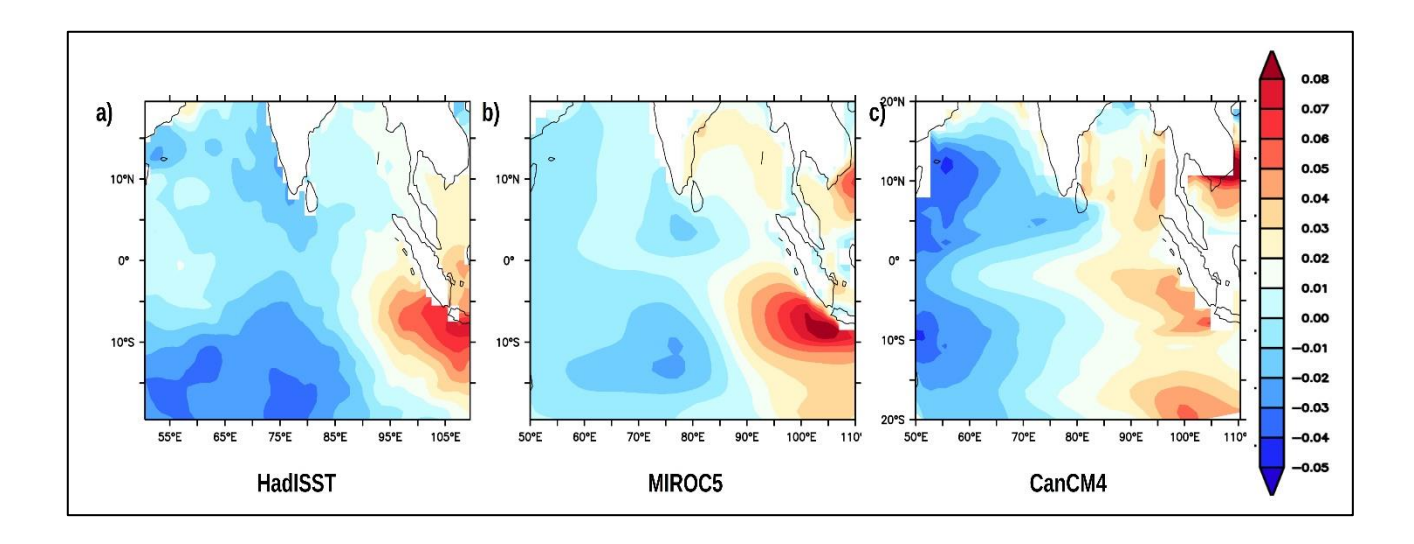


Figure 4.5: The second mode from the EOF analysis of the tropical Indian Ocean SST, from a)

HadISST (1961-2011 period). Figures b and c are the same as that of figure a but derived from

MIROC5 and CanCM4 hindcasts for the same period. The output from MIROC5 and CanCM4

exhibit the East-West anomalous temperature gradient.

We also present a direct comparison between the predicted IODMI with the observations from various models for years 1, 3, 5, and 7 in figure 4.6. The direct comparisons show that the two models are able to effectively predict the phase of an IOD.

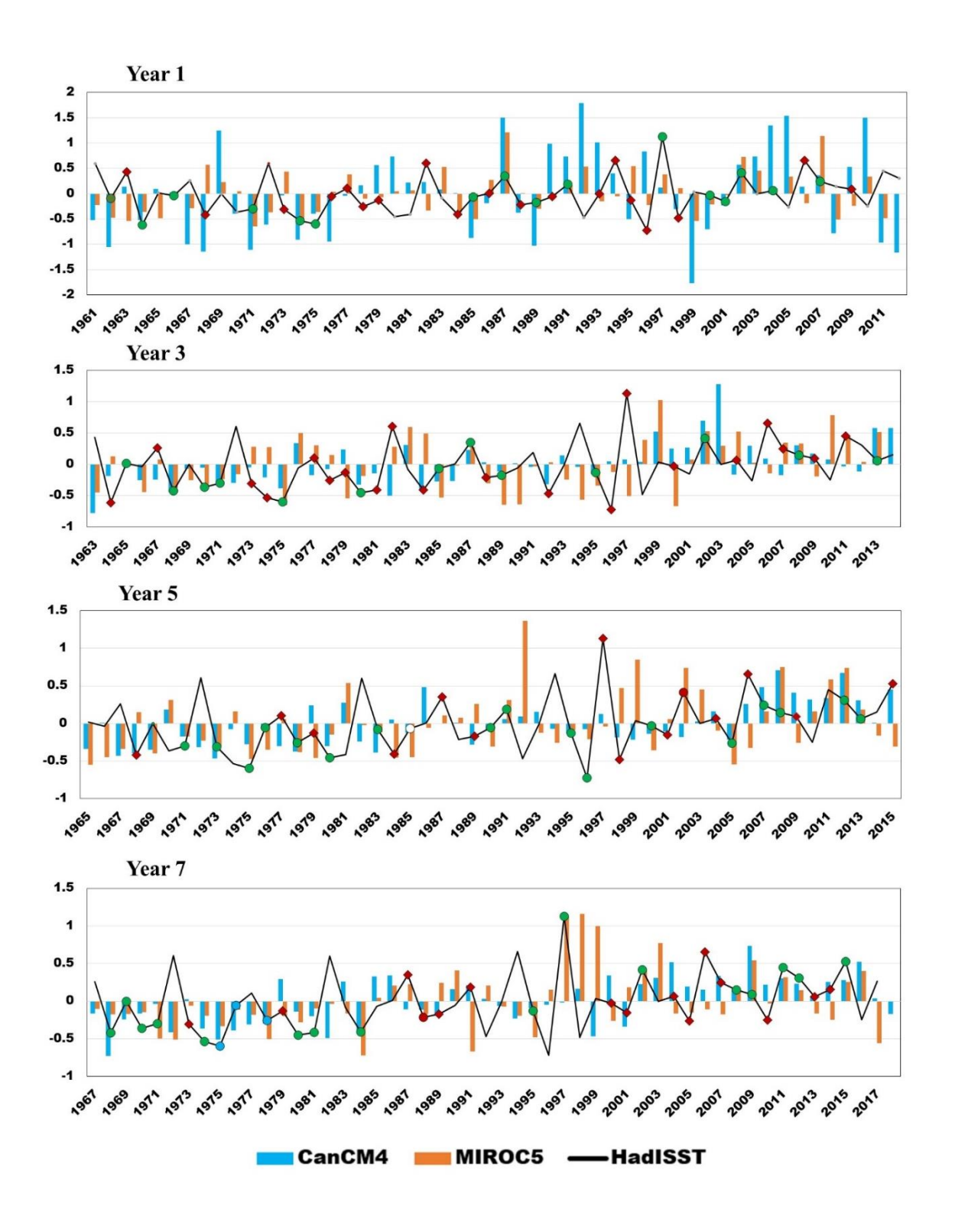


Figure 4.6: The direct comparisons of predicted IODMI with the observations from various models. The Green circles indicate the calendar years where both the models are in-phase with the observations. The Red rhombuses indicate the years where at least one model is in-phase with the observations.

4.6 Conclusion

Our analysis of the CMIP5 decadal hindcasts for the 1960-2011 period shows that two CMIP5 decadal prediction systems exhibit multi-year skill in predicting the IODMI, higher than the 17-month lead skills for the ENSO, a leading climate driver. To our knowledge, this is the first study to show decadal skill in predicting the IOD.

Skill levels for surface fields and, in particular, rainfall, are not statistically indistinguishable from zero. This is in common with long-term predictions of other climate phenomena (Scaife and Smith, 2018), and indicates the relative immaturity of this form of forecasting. It remains a challenge to both improve models and to fully exploit decadal prediction skills. Nevertheless, the potential for long-term planning in both public and private sector organizations that could be facilitated by such skillful predictions is great.

We partially conclude the third objective of the thesis by exploring the multi-year to decadal prediction skills of the tropical Indo-Pacific drivers with this chapter. In the next chapter, we find a potential source for the significant predictability of IOD on a multi-year scale.

5

Source of Decadal Predictability of The Indian Ocean Dipole

5.1 Sources of Decadal Prediction

Earlier studies have shown that decadal prediction could be skillful by understanding physical processes of climate, both internal variability and external forces along with introducing new techniques of data assimilation or model initialization ocean physical processes (Meehl et al., 2009; Moss et al., 2010). One key component of improved decadal prediction skills is understanding low-frequency modes of ocean variability (Meehl et al., 2014; Farneti et al., 2017). Meehl et al., (2009) states that low-frequency variabilities in the Pacific like Pacific decadal oscillation (PDO; Mantua et al., 1997) or the Interdecadal Pacific Oscillation (IPO; Power et al. 1999) could enhance predictive skill for the tropical Pacific and possibly for its teleconnections. Similarly in the Atlantic Ocean, low-frequency modes of variability like the Atlantic meridional overturning circulation (AMOC; Srokosz et al., 2021; Caesar et al., 2021 and the references within them) or the Atlantic Multidecadal Oscillation (AMO; Hurrell, 1995; Jones et al., 1997; Osborn, 2006; Cornes et al., 2013) could potentially increase the predictive skills on a decadal scale.

5.2 Source of the IOD Predictability on a decadal scale

We found that two models CanCM4 and MIROC5 show that the Indian Ocean Dipole (IOD) has a lead prediction skill of up to ten years. A question arises as to what processes are responsible for the IOD predictability. Earlier studies have shown that the key component of improved decadal prediction lies in ocean physical processes, which internally generated decadal climate variability (Meehl et al., 2014; Farneti et al., 2017). Thus, the memory of the upper ocean (~800m) provides improved predictability of SST variability in models on decadal timescales (Yeager et al., 2012; Wang et al., 2014). Motivated by these, we looked for a source of predictability of IOD at several levels in the subsurface temperature (every 50 meters).

We found the maximum signal in the Southern Ocean at 300m to 800m depth 7-10 years before the occurrence of the IOD event. This is evidenced by significant correlations between depth-averaged 300-800 m temperatures in the Southern Ocean, which lead the IODMI by 10 to 6 years, respectively (Figure 5.1). The significant positive correlations in the Southern Ocean indicate that a positive temperature anomaly in the Southern Ocean leads to a positive IOD event after 8-10 years, whereas a similar lead negative correlation coefficient in the Southern Ocean indicates a negative IOD event after such a time period. The signal leading the IODMI first appears in the sub-surface temperatures of the Southern Ocean just southwest of Africa between the depths of 300m to 800m, 10 years before the occurrence of the IOD event. This signal is seen to propagate towards the east along the Antarctic Circumpolar Current (ACC, or West wind drift) to about 500E to 600E about 6 years prior to the IOD event.

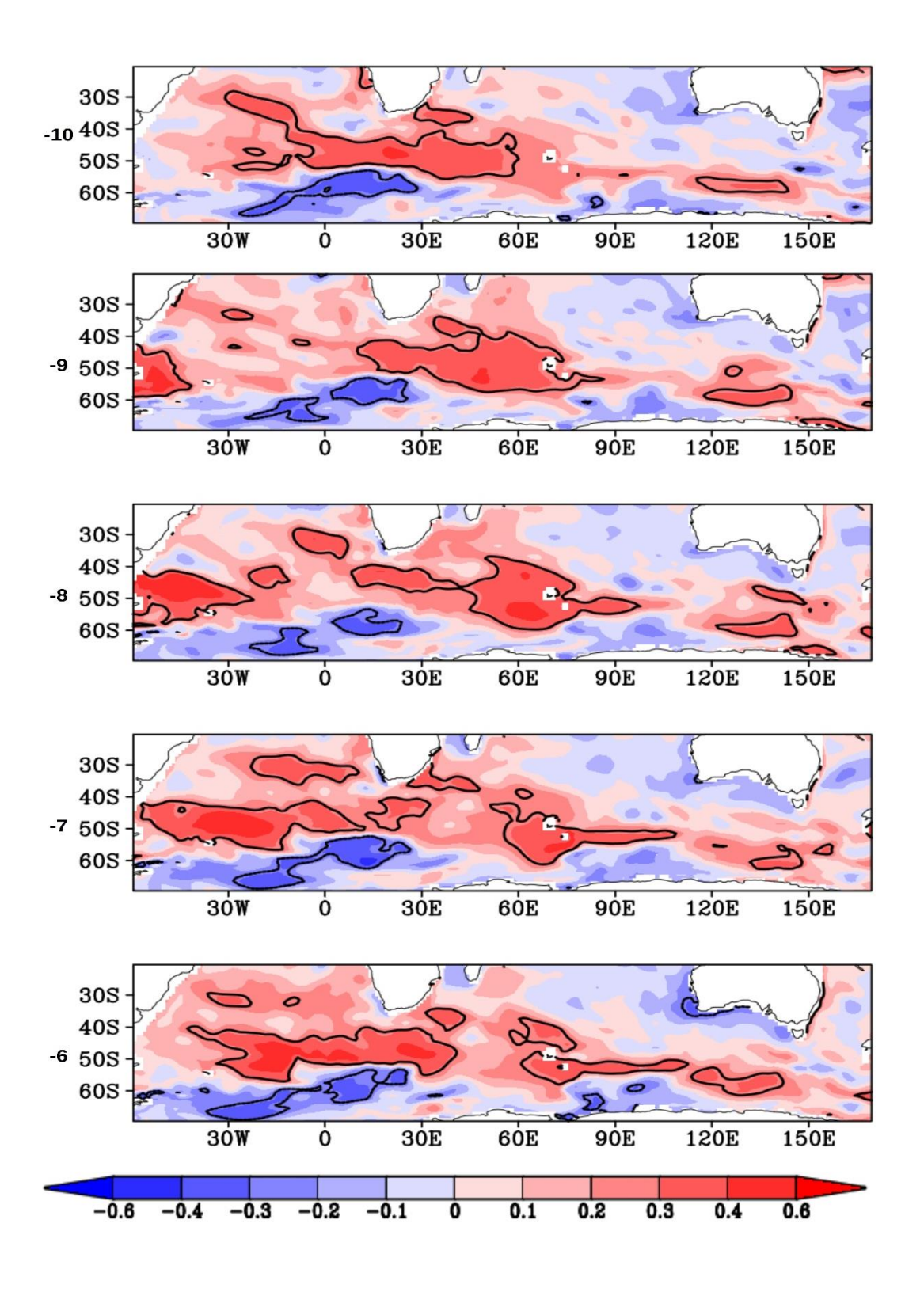


Figure 5.1: Spatial distribution of the anomaly correlation of HadISST derived IODMI with vertically averaged subsurface temperatures from ORAS4 (over 300m to 800m depth) from previous years averaged annually. The 'lag number' is the years over which the IOD lags the Southern Ocean signal. In all panels, significant correlations are at 95% confidence (contour lines - value at 0.27).

The ACC is a wind-driven current, (westerlies and hence called the West wind drift) in the Southern Ocean, encircling Antarctica. The ACC is a zonal current flowing west to east with little meridional meandering. The ACC connects the three oceans, Atlantic, Indian, and Pacific, and transports ~100Sv. The ACC speeds range from 20cm/s to 70cm/s and are mostly unidirectional (Talley et al., 2011). Because of the high speed and constant direction, the ACC is a deep current with a depth of ~1000m and can even extend till the bottom near regions of fastest flow (Eg., Drake Passage). A real-time view of the ACC can be seen at ACC view, Earth:: a global map of wind, weather, and ocean conditions (nullschool.net). The signals observed in Figure 5.1 propagate along with the ACC for 3-4 years (about 6-7 years before the occurrence of the IOD).

From here, the propagation of the signal from the deeper layers in the extra-tropics to the surface layers in the equatorial region is a pathway that is coincident with the Indian Ocean Meridional Overturning Circulation (IOMOC; Wang et al., 2014; Jayasankar et al., 2019). The time period of the propagation is in agreement with the IOMOC. The signals in the subsurface further propagate north, along the east of Madagascar, all the way to the Somali coast with the East Madagascar undercurrent (EMUC; Nauw et al., 2008) – an intermediate undercurrent at the depth of thermocline and below. The EMUC transports 2.8 ± 1.4 Sv of intermediate water from the Southern Ocean to the equatorial Indian Ocean. The signal upwells to the surface near Somalia (Somali upwelling) along with its propagation north (Figures 5.2; 5.3)

From the Somali coast, the lead heat content signal is seen to move east, reaching the central equatorial Indian Ocean 3 years before the IOD event (Figure 5.3). The signal remains in the equatorial Indian Ocean for the last 2-3 years before the occurrence of the IOD event. Furthermore, our correlation in Figure 5.3 suggests, an anomalous SST structure of opposite polarity in the equatorial Indian Ocean about a year before the occurrence of an IOD event. This is in conformation

with Saji et al. (1999), who not only note a tight coupling between the intensity of the SST dipole anomaly and zonal wind anomaly but emphasize a biennial tendency. The biennial tendency of the IOD is also noted by Meehl and Alablaster (2001), Ashok et al. (2003), etc. It is intriguing why the signal from the sub-surface at the equator does not manifest as an IOD event immediately. Several studies suggest potential drivers that can force an IOD such as the Indian summer monsoon, ENSO, and can account for the lead signals associated with the IOD with 1–2-year lead (Ashok et al., 2001; Ashok and Saji, 2007). As the current models do not show any lead skills of the Indian summer monsoon beyond a season, we can rule out that the long lead skills for the IODMI in the models come from the lead skills of monsoon, or those related to ENSO (see Fig. 2a). This might be explained by the fact that some IOD events are triggered by an atmospheric signal substantial enough to trigger the coupled evolution of the IOD (Shinoda et al., 2004; Saji et al., 2018), and hence this delay of 2-3 years.

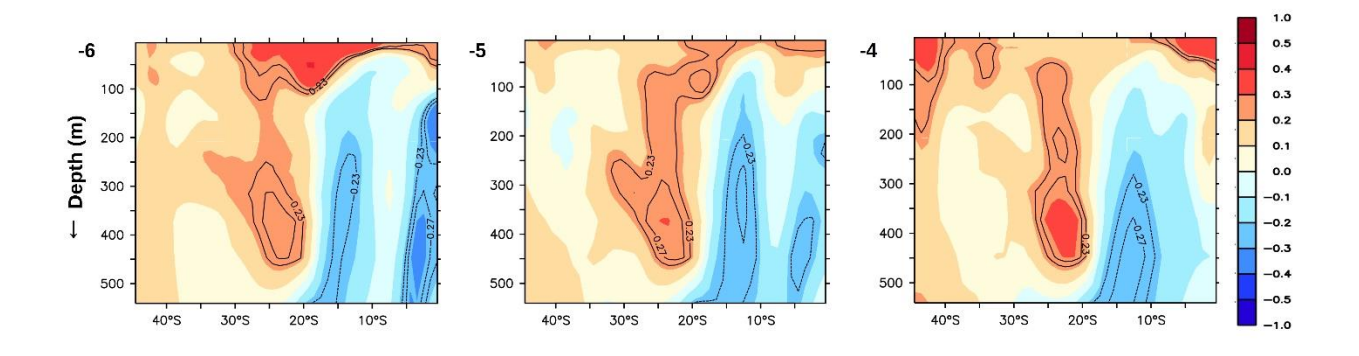


Figure 5.2: Vertical distribution of anomaly correlation of IODMI with previous years' subsurface temperatures, averaged annually over longitudes 50E to 100E. Significant correlations at 90% confidence (0.23) and at 95% confidence (0.27) are contoured.

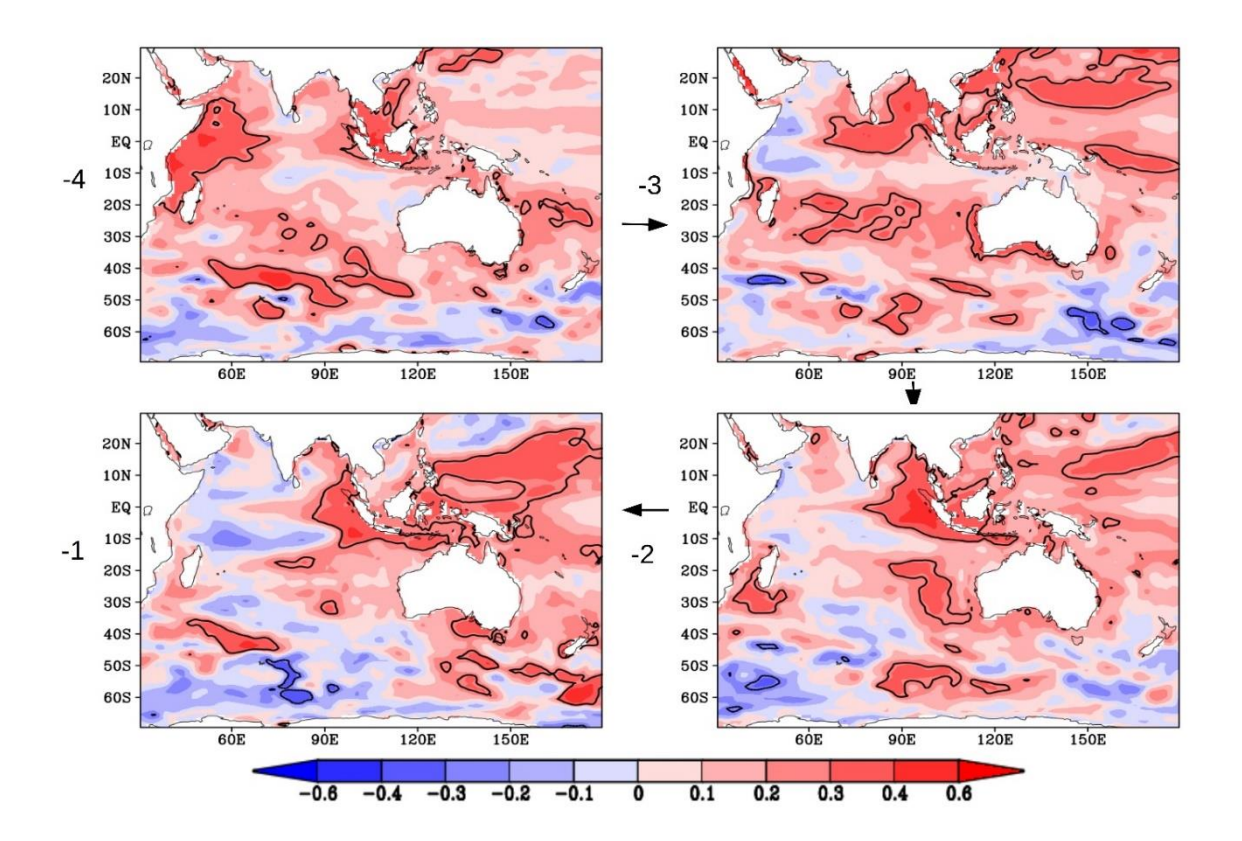


Figure 5.3: Same as Figure 5.1 but vertically averaged annually over the surface to 100m depth for the last four years leading up to an IOD event. Significant correlations at 95% confidence are shown as contour lines (value at 0.27).

A linear regression analysis carried out using HadISST and ORAS4 ocean temperature datasets (slope value=0.46) indicates that the Southern Ocean signals at decadal lead explain about 18% of the interannual variability of IOD as suggested by a goodness-of-fit measure. To put it in perspective, ENSO, known as the most prominent driver of the Indian summer monsoon interannual variability, explains about 30% of the latter.

I also present a schematic figure to show the pathway of the signal from the Southern Ocean to the equatorial Indian Ocean (Figure 5.4). The signals in deeper waters (shown in blue) propagate with ACC and then flow northward towards the equator along IODMI. The signals upwell near the Somali coast and remain in the equatorial Indian Ocean for 3-4 years before finally culminating in an IOD.

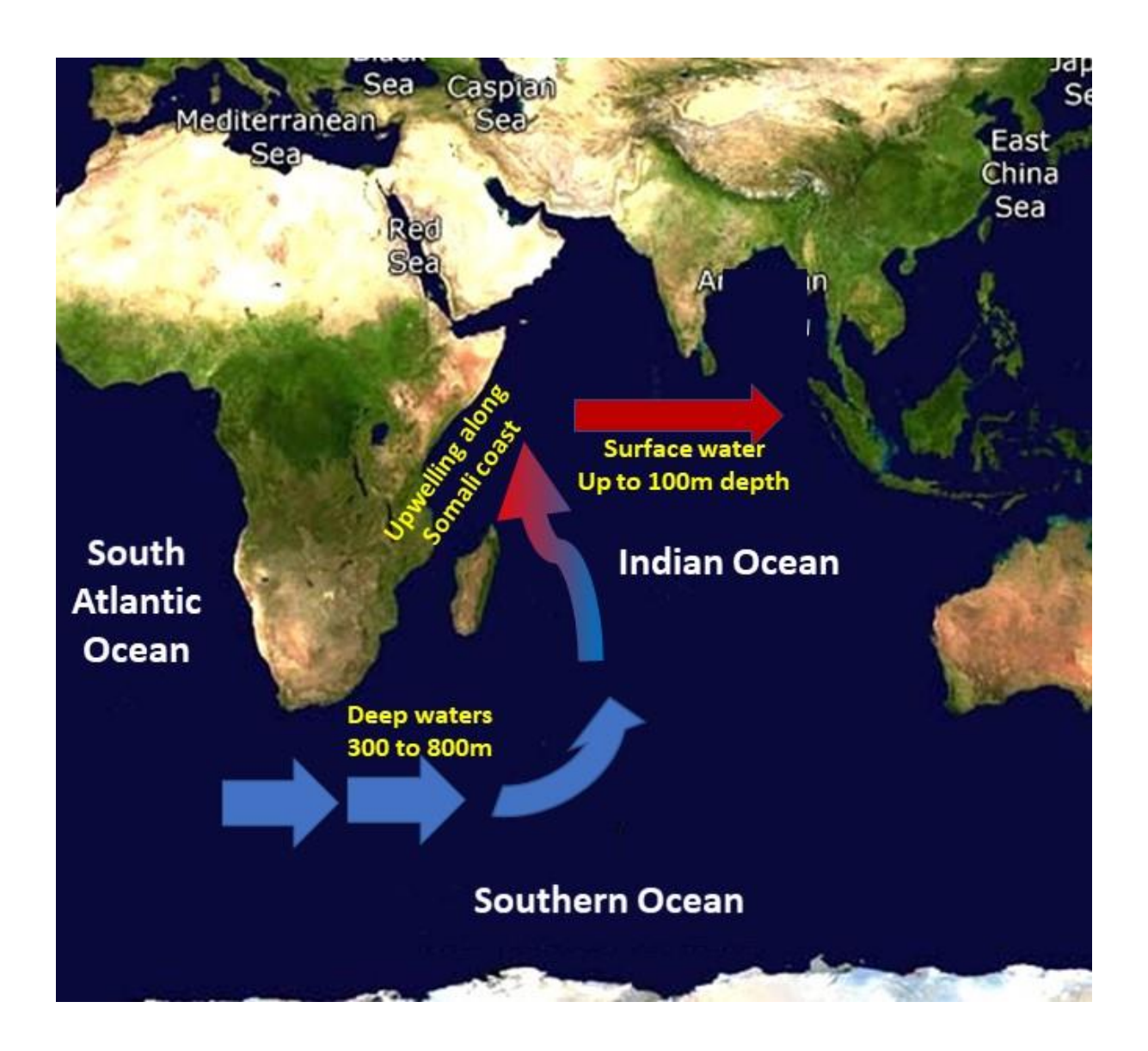


Figure 5.4: A schematic representation of the pathway of the signals from the Southern Ocean to the Equatorial Indian Ocean. The blue arrows indicate deep water (~500 to 800m) and the red indicate near-surface water (< 100m). The blue-red gradient coloured arrow shows the pathway from deeper to surface layers.

5.3 Source of IOD as predicted in the models

The source of decadal predictability for IOD in the MIROC5 and CanCM4 also apparently comes from the Southern Ocean (Figure 5.5). We find statistically significant anomaly correlations between

the depth-averaged from surface till ~800m hindcast heat content with the IODMI with the heat content leading at 10-5 years, conforming to our results from the reanalysis. The source of the signal is the Southern Ocean for both the models but the simulated signal path from here to the equatorial Indian Ocean is, however, weaker and remains unclear specifically in the MIROC5 model. But the signals re-emerge finally 2-3 years before the occurrence of the simulated IOD (Figure 5.6). The models also do not capture the biennial tendency of the IOD as in observations. Further understanding of other possible factors affecting IOD variability on decadal scales is needed.

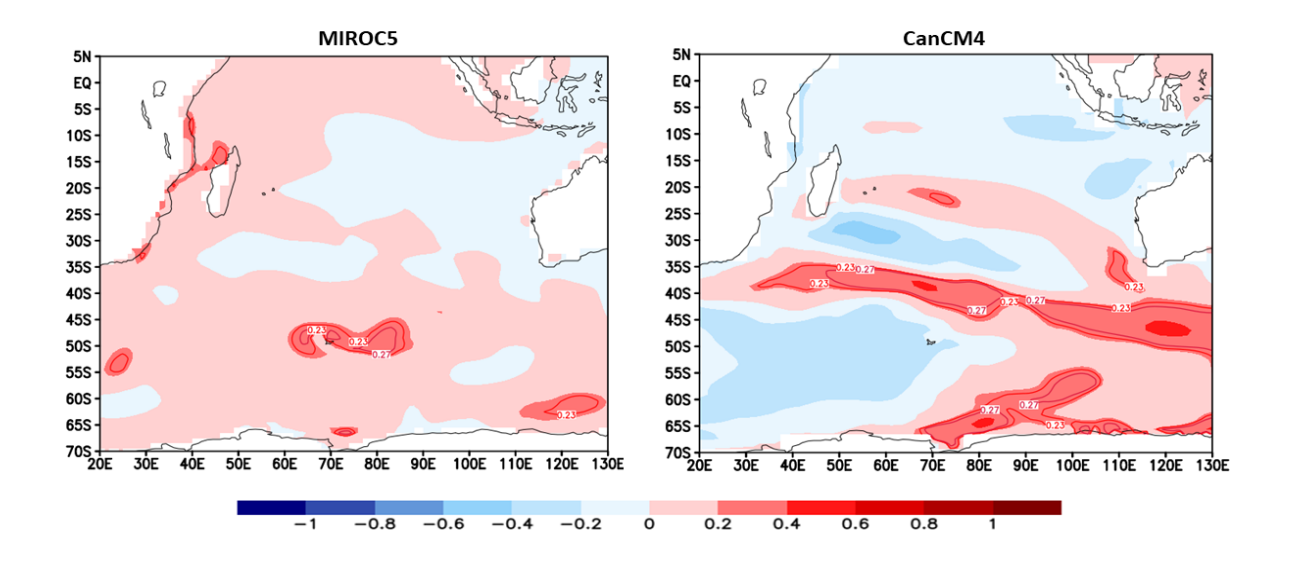


Figure 5.5: Spatial distributions of the anomaly correlation of MIROC5 and CanCM4 derived IODMI with vertically averaged subsurface temperatures annually-averaged from the same respective models from 10 years before the occurrence of the IOD event. MIROC5 is averaged from surface to 760m depth and CanCM4 from surface to 792m deep. The slight difference in bottom levels is dependent on the model levels. Significant correlations at 90% confidence (0.23) and at 95% confidence (0.27) are contoured.

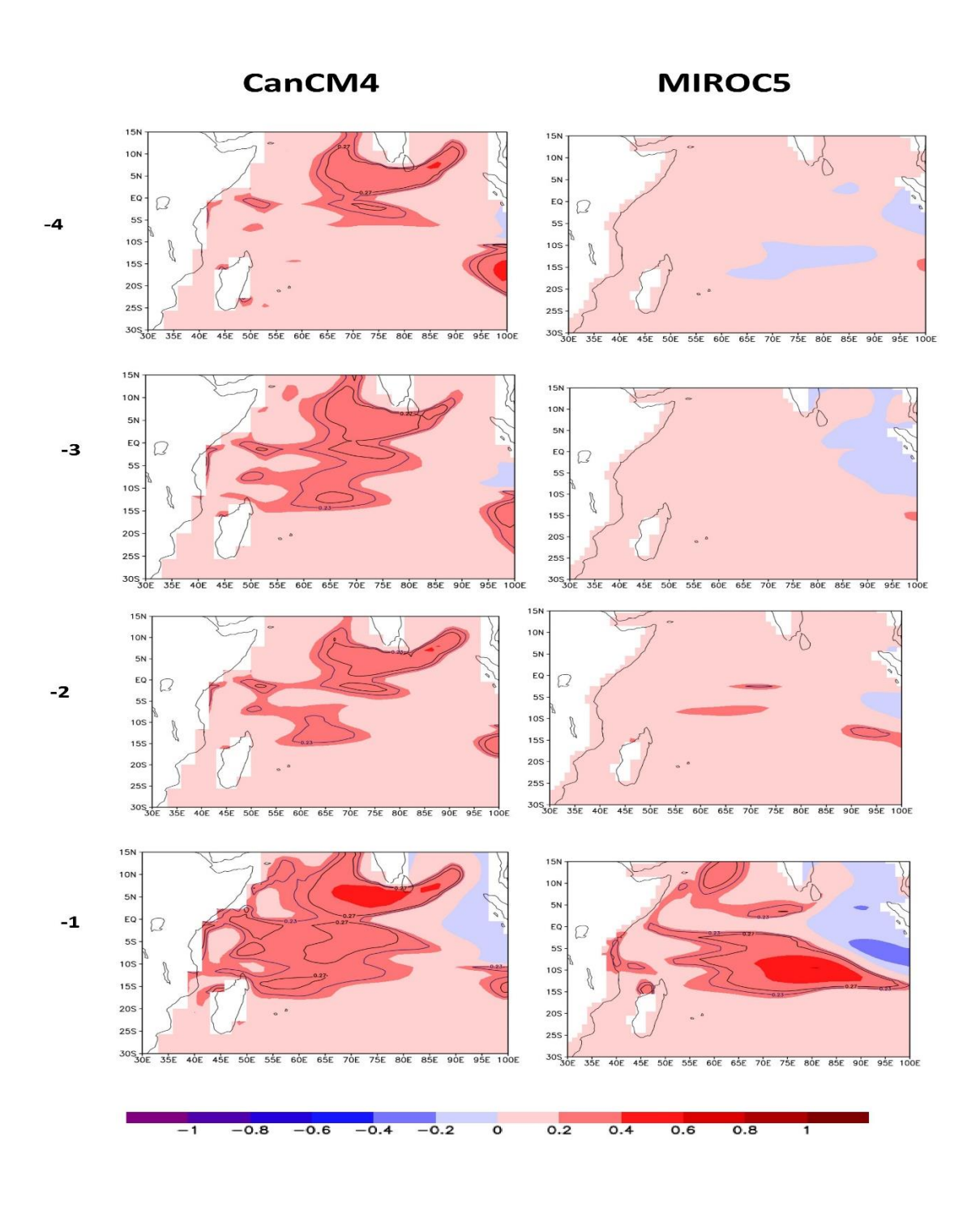


Figure 5.5: Spatial distributions of the anomaly correlation of MIROC5 and CanCM4 derived IODMI with vertically averaged subsurface temperatures annually-averaged from the same respective models from 4 years to 1 year before the occurrence of the IOD event. MIROC5 is averaged from surface to 760m depth and CanCM4 from surface to 792m deep. The slight difference in bottom levels is dependent on the model levels. Significant correlations at 90% confidence (0.23) and at 95% confidence (0.27) are contoured.

5.4 Conclusion

In this chapter, we explore the possible mechanism for decadal predictability of IOD. As, neither ISMR nor ENSO, two important phenomena that contribute to the strength of the IOD, show any significant lead prediction skills beyond a year, we explore for potential connections to the influences from the other boundary of the Indian Ocean, i.e., Southern Ocean, which can explain the lead skill of two years and beyond. We find the 'propagation of IOD skills from the extratropics to the equatorial Indian ocean. The mechanism we hypothesize is, as follows. The subsurface signals observed prior to ~ 10 years in the Southern Ocean before the occurrence of an IOD event propagate along the Antarctic Circumpolar Current (ACC). They change their direction at ~60 0 E longitude and flow towards the equator. Later, the signals shoal along with the Somali current and finally reach the equatorial region. This chapter addresses the remaining part of objective 3.

6

Conclusions and Future Scope

The Indian Summer Monsoon is the life source for over a billion people. Any attempts to expand the understanding of the Indian Summer Monsoon are of immense value. The interannual variability of the Indian Summer is mainly, though not limited to, impacted by two major climate drivers, the El Niño Southern Oscillation and the Indian Ocean Dipole. This thesis is an effort to study and understand the Indo-Pacific drivers of the Indian Summer Monsoon, their decadal variability, and their prediction on a decadal scale.

6.1 Summary

In Chapter 1, I introduce the Indian Summer Monsoon, the features of ISM, and the factors affecting the variability of ISM, i.e., ENSO and IOD. I present a detailed account of ENSO and the weakening relationships between ENSO and ISM. I also introduce IOD and its relationship with ISM. Finally, I introduce the emerging discipline of climate prediction. The mechanisms for the weakening teleconnections of ENSO- ISMR on a decadal scale are not fully understood. Also, the influence of the Indian Ocean on the links needs to be further studied. The rest of the thesis is an attempt to fill the aforementioned gaps and complete the set objectives. I restate the objectives:

- Understanding the decadal variability of Indo Pacific teleconnections to Indian Summer Monsoon
- 2. Exploring the mechanisms for the weakening of the ENSO ISM links
- 3. Exploring the multi-year to decadal prediction skills of the tropical Indo Pacific drivers and finding a potential source for any significant predictability on a multi-year scale.

In Chapter 2, all the sources of data (observations, reanalysis, and model output) are explained in detail. The models whose output has been used for this study are also clearly described. Data processing techniques carried out on the model output have also been described elaborately. All the statistical methods employed in the study are clearly defined and explained.

In Chapter 3, I begin with a brief introduction about the ENSO indices (both ocean surface and subsurface temperature indices) and how there has been a significant weakening in recent decades. We also highlight how the warm water volume of the equatorial pacific also shows a weakening despite showing a seasonal lead prediction skill. We then proceed to give a comprehensive explanation of the analysis of the surface winds over the tropical Indo-pacific region. Our analysis suggests that there is a relative intensification of the cross-equatorial flow from the southern hemisphere into the equatorial Indian Ocean associated with ISMR due to the strengthening of Mascarene High. Further, a shift in the surface wind circulation associated with monsoon over the northern pacific since the late 1970s has resulted in a strengthened cyclonic seasonal circulation south-east of Japan. These changed circulation features are a shift from the known circulation signature that efficiently teleconnect El Niño forcing to South Asia. This concludes the first and second objectives of the thesis.

In chapter 4, a short introduction of decadal prediction, building on the information given in chapter 1 is presented. We show the results of the decadal prediction analysis of ISM R, ENSO, and IOD. ISMR has no predictability in the analysed models, presumably due to model inadequacies in representing monsoon processes. We find that ENSO has a lead prediction skill for over a year for all the models. For IOD, surprisingly, two general circulation models have significant prediction skills for at least two years after initialization. We, then, focus on the significant results of skills of IOD and show the fidelity of the simulated IOD using various statistical techniques. This chapter partially concludes the third objective of the thesis.

In chapter 5, we explore the possible mechanism for decadal predictability of IOD. As, neither ISMR nor ENSO show lead prediction skills to this extent, we explore the influences from the other boundary of the Indian Ocean, i.e., the Southern Ocean. We find the propagation of IOD skills from the extratropics to the equatorial Indian ocean. We explain the mechanism where the subsurface signals observed 10 years before the prediction, propagate along the Antarctic Circumpolar Current (ACC), change direction and flow towards the equator and shoaling along with the Somali current and finally reaching the equatorial region. With this, I complete the third and final objective of the thesis.

6.2 Future Scope

No research is truly complete as each completed study raises several new questions and the cycle continues. This thesis while answering a few questions also raises several possibilities for future study.

The variability of Mascarene high highlighted in Chapter 3 could be explored. The factors affecting the variability remain unknown. Both natural variability and global warming might play a role individually or together. Model simulation experiments are necessary to understand this better. Along with the

Mascarene high, there could be other factors influencing the ISM wind circulation and thereby affecting the interplay between ENSO-ISM. This would be another interesting idea to explore.

Also, as mentioned in Chapter 4, the decadal prediction skills for ENSO could be improved upon. SThis could potentially pave way for a longer ISM prediction skill, beyond the present seasonal lead. The source of IOD prediction skills is arising from the Southern Ocean as explained in Chapter 5. There might be several factors affecting this source. Also, the reason for why and how the signals sustain in the equatorial Indian Ocean for 3-4 years before forming an IOD needs further exploration.

List of References

- Amat, H. B. and Ashok, K., 2018, "Relevance of Indian Summer Monsoon and its Tropical Indo-Pacific Climate Drivers for the Kharif Crop Production", Pure Appl. Geophys., 175, 3, p1221.
- Amat, H.B., Pradhan, M., Tejavath, C.T. et al. Value addition to forecasting: towards Kharif rice crop predictability through local climate variations associated with Indo-Pacific climate drivers. Theor Appl Climatol 144, 917–929 (2021). https://doi.org/10.1007/s00704-021-03572-6
- Ananthakrishnan R, Srinivasan V, Ramakrishna AR, Jambunathan R. 1968. Synoptic features associated with onset of southwest monsoon over Kerala. IMD Forecasting manual, Report IV–18.2.
- Annamalai, H. and Liu, P.: Response of the Asian Summer Monsoon to changes in El Niño properties, Q. J. Roy. Meteor. Soc., 131, 805–831, https://doi.org/10.1256/qj.04.08, 2005.
- Ashok K, Behera SK, Rao SA, Weng H, Yamagata T (2007) El Niño Modoki and its possible teleconnections. J Geophys Res 112:C11007. https://doi.org/10.1029/2006J C0037 98
- Ashok, K., Guan, Z., Saji, N. H. and Yamagata, T., 2004, "Individual and combined influences of the ENSO and Indian Ocean Dipole on the Indian summer monsoon", J. Climate, 17, 3141-3155.
- Ashok, K., Z. Guan, and T. Yamagata, Influence of the Indian Ocean Dipole on the Australian winter rainfall, Geophys. Res. Lett., 30(15), 1821, doi:10.1029/2003GL017926, 2003.
- Ashok, K., Guan, Z. and Yamagata, T., 2001, "Impact of the Indian Ocean Dipole on the relationship between the Indian Monsoon rainfall and ENSO", Geophys. Res. Lett., 28, 4499-4502.
- Ashok K, Nagaraju C, Sengupta A, Pai S (2014) Decadal changes in the relationship between the Indian and Australian summer monsoons. Clim Dyn 42:1043–1052. https://doi.org/10.1007/s0038 2-012-1625-4
- Ashok, K., Sabin, T. P., Swapna, P. and Murtugudde, R. G., 2012, "Is a global warming signature emerging in the tropical Pacific?", Geophysical Research Letters, 39, 2, L02701,
- Ashok, K. and Saji, N. H., 2007, "Impacts of ENSO and Indian Ocean Dipole Events on the Sub-Regional Indian Summer Monsoon Rainfall", Journal of Natural Hazards, 42, 273-285.

- Ashok, K., Shamal, M., Sahai, A. K., & Swapna, P. (2017). Nonlinearities in the evolutional distinctions between El Niño and La Niña types. Journal of Geophysical Research: Oceans, 122, 9649–9662. https://doi.org/10.1002/2017JC013129
- Ashok, K., Tam, C.-Y., Lee, W.-J., 2009a. ENSO Modoki impact on the southern hemisphere storm track activity during extended austral winter. Geophys. Res. Lett. doi:10.1029/2009 GL038847.
- Ashok, H., Yamagata, T., 2009b. Climate change: the El Niño with a difference. Nature 461, 481–484. doi:10.1038/461481a.
- Ashrit, R. G., Rupa Kumar, K. and Krishna Kumar, K., 2001, "ENSO-Monsoon relationships in a greenhouse warming scenario", Geophys. Res. Lett., 28, 1727-1730.
- Balmaseda, M. A., Mogensen, K. and Weaver, A. T. (2013), Evaluation of the ECMWF ocean reanalysis system ORAS4. Q.J.R. Meteorol. Soc., 139: 1132–1161. doi: 10.1002/qj.2063.
- Battisti, D. S. and Hirst, A. C., 1989, "Interannual variability in the tropical atmosphere-ocean model: influence of the basic state, ocean geometry and nonlinearity", J. Atmos. Sci., 45, 1687-1712.
- Behera, S. K., R. Krishnan and T. Yamagata. 1999. Unusual ocean-atmosphere conditions in the tropical Indian Ocean during 1994. Geophys. Res. Lett., 26, 3001–3004.
- Behera, S., Luo, J., and Masson, S. (2005). Paramount impact of the Indian Ocean dipole on the East African short rains: A CGCM study. Journal of Climate, pages 4514–4530.
- Behera, S. K., and T. Yamagata, 2003: Influence of the Indian Ocean Dipole on the Southern Oscillation. J. Meteor. Soc. Japan, 81, 169–177.
- Bhalme, H. N. and Jadhav, S. K., 1984, "The Southern Oscillation and its relation to the monsoon rainfall", J. Climatol., 4, 509-520.
- Bjerknes, J., 1969, "Atmospheric teleconnections from the equatorial Pacific", Mon. Weather Rev., 97, 163-172.
- Boer, G. J. et al. The Decadal Climate Prediction Project (DCPP) contribution to CMIP6. Geosci. Model Dev. 9, 3751–3777 (2016).
- Borah, P. J, V. Venugopal, J. Sukhatme, P. Muddebihal, B. N. Goswami, Indian monsoon derailed by a North

- Atlantic wavetrain, Science, 370:1335-1338, 2020.
- Borchert, L. F., Düsterhus, A., Brune, S., Müller, W. A., & Baehr, J. (2019). Forecast-oriented assessment of decadal hindcast skill for North Atlantic SST. Geophysical Research Letters, 46, 11444—11454. https://doi.org/10.1029/2019GL084758
- Borchert, L. F., Menary, M. B., Swingedouw, D., Sgubin, G., Hermanson, L., & Mignot, J. (2021). Improved decadal predictions of North Atlantic subpolar gyre SST in CMIP6. Geophysical Research Letters, 48, e2020GL091307. https://doi.org/10.1029/2020GL091307
- Borchert L F, Muller W A & Baehr J 2018 Atlantic Ocean Heat Transport Infuences Interannual-to-Decadal Surface Temperature Predictability in the North Atlantic Region Journal of Climate 31(17), 6763 [6782.
- Branstator, G., and H. Teng, 2010: Two Limits of Initial-Value Decadal Predictability in a CGCM. Journal of Climate, 23 (23), 6292–6311, doi:10.1175/2010JCLI3678.1, URL http://journals.ametsoc.org/doi/abs/10.1175/2010JCLI3678.1.
- Caesar, L., McCarthy, G.D., Thornalley, D.J.R. et al. Current Atlantic Meridional Overturning Circulation weakest in last millennium. Nat. Geosci. 14, 118–120 (2021). https://doi.org/10.1038/s41561-021-00699-z
- Cai, W., and Cowan, T. (2009), La Niña Modoki impacts Australia autumn rainfall variability, Geophys. Res. Lett., 36, L12805, doi:10.1029/2009GL037885.
- Cai, W., Santoso, A., Wang, G. et al. Increased frequency of extreme Indian Ocean Dipole events due to greenhouse warming. Nature 510, 254–258 (2014). https://doi.org/10.1038/nature13327
- Cane, M. Decadal predictions in demand. Nature Geosci 3, 231–232 (2010). https://doi.org/10.1038/ngeo823
- Cane, M. A., S. E. Zebiak, and S. C. Dolan, 1986: Experimental forecasts of El Niño. Nature, 321, 827-832.
- Carriuolo, Matthew. The Lorenz Attractor, Chaos, and Fluid Flow 2005. Web http://physics.brown.edu/physics/undergradpages/theses/matthew_carriuolo_thesis.pdf.
- Carton JA, Giese BS (2008) A reanalysis of ocean climate using simple ocean data assimilation (SODA). Mon Weather Rev 136:2999–3017. https://doi.org/10.1175/2007M WR197 8.1.
- Cash, B. A., Barimalala, R., Kinter, J. L., Altshuler, E. L., Fennessy, M. J., Manganello, J. V., Molteni, F., Towers,

- P., Vitart, F., 2017, "Sampling variability and the changing ENSO-monsoon relationship", Clim. Dyn., 48, 11-12, 4071-4079.
- Chan S, Behera S, Yamagata T, 2008: Indian Ocean dipole influence on South American rainfall. Geophys Res Lett 35(14):L14S12
- Chang, C. P., Harr, P. and Ju, J., 2001, "Possible roles of Atlantic circulation on the weakening Indian monsoon rainfall-ENSO relationship", Journal of Climate, 14, 11, 2376-2380.
- Charney J G 1969 The Inter-tropical Convergence Zone and the Hadley circulation of the atmosphere; In: Proc. WMO/IUGG Symposium on Numerical Weather Prediction, 3, 73–79, Japan Meteorol. Agency.
- Chikamoto, Y., Timmermann, A., Luo, JJ. et al. Skilful multi-year predictions of tropical trans-basin climate variability. Nat Commun 6, 6869 (2015). https://doi.org/10.1038/ncomms7869
- Collins, M (2002) Climate predictability on interannual to decadal time scales: the initial value problem, Climate Dynamics, volume 19, no. 8, pages 671-692, DOI:10.1007/s00382-002-0254-8.
- Collins, M; 2007, Ensembles and probabilities: a new era in the prediction of climate change. Phil. Trans. R. Soc. A.3651957–1970 http://doi.org/10.1098/rsta.2007.2068
- Cornes RC, Jones PD, Briffa KR, Osborn TJ (2013) Estimates of the North Atlantic Oscillation back to 1692 using a Paris–London westerly index. Int J Climatol 33:228–248
- Dai, A. and Wigley, T. M. L., 2000, "Global patterns of ENSO induced precipitation", Geophys. Res. Lett., 27, 1283-1286.
- Delworth, T.L., et al., 2006: GFDL's CM2 Global Coupled Climate Models. Part I: Formulation and Simulation Characteristics. Journal of Climate, 19(5), DOI: 10.1175/JCLI3629.1.
- DelSole T, Shukla J, 2012: Climate models produce skilful predictions of Indian summer monsoon rainfall.

 Geophys Res Lett. https://doi.org/10.1029/2012G L0512 79
- Dunstone, N. et al. Skilful predictions of the winter North Atlantic Oscillation one year ahead. Nat. Geosci. 9, 809–814 (2016)
- Dutta, R., & Maity, R. Temporal evolution of hydroclimatic teleconnection and long-lead prediction of Indian

- summer monsoon rainfall using time varying model. Scientific Reports 8:10778, https://doi.org/10.1038/s41598 (2018).
- Farneti, R., 2017: Modelling interdecadal climate variability and the role of the ocean. Wiley Interdiscip. Rev.: Climate Change, 8, e441, https://doi.org/10.1002/wcc.441.
- Findlater, J. (1969) A Major Low-Level Air Current near the Indian Ocean during the Northern Summer. Quarterly Journal of the Royal Meteorological Society, 95, 362-380. http://dx.doi.org/10.1002/qj.49709540409.
- Francis, P.A., Gadgil, S. A note on new indices for the equatorial Indian Ocean oscillation. J Earth Syst Sci 122, 1005–1011 (2013). https://doi.org/10.1007/s12040-013-0320-0
- Gadgil, S., 2018: The monsoon system: Land-sea breeze or the ITCZ? Journal of Earth System Science, 127 (1), 1.
- Gadgil Sulochana, Vinayachandran P N and Francis P A (2003) Droughts of Indian summer monsoon: Role of clouds over the Indian Ocean; Curr. Sci. 85 1713–1719.
- Gadgil, Sulochana and Vinayachandran, PN and Francis, PA and Gadgil, Siddhartha (2004) Extremes of the Indian summer monsoon rainfall, ENSO and equatorial Indian Ocean oscillation. In: Geophysical Research Letters, 31 (12). L12213-1-4.
- Gaetani, M., and E. Mohino, 2013: Decadal prediction of the Sahelian precipitation in cmip5 simulations. Journal of Climate, 49 (9-10), 7708–7719, doi:10.1175/JCLI-D-12-00635.1.
- Gershunov, A., Schneider, N. and Barnett, T., 2001, "Low-frequency modulation of the ENSO-Indian monsoon rainfall relationship: signal or noise?", J. Climate, 14, 2486-2492.
- Gill, A. E., 1980, "Some simple solutions for heat-induced tropical circulation", Quarterly Journal of Royal Meteorological Society, 106, 447-462.
- Gong D, Ho C (2002) Shift in the summer rainfall over the Yangtze River valley in the late 1970s. Geophys Res Lett 29(10):1436. https://doi.org/10.1029/2001G L0145 23
- Goswami, B., & Chakravorty, S. Dynamics of the Indian Summer Monsoon Climate. Oxford Research

 Encyclopedia of Climate Science.
 - https://oxfordre.com/climatescience/view/10.1093/acrefore/9780190228620.001.0001/acrefore-

9780190228620-e-613.

- Hrudya, P.H., Varikoden, H. & Vishnu, R. A review on the Indian summer monsoon rainfall, variability and its association with ENSO and IOD. Meteorol Atmos Phys 133, 1–14 (2021). https://doi.org/10.1007/s00703-020-00734-5
- Hu, S., Wu, B., Zhou, T. et al. A comparison of full-field and anomaly initialization for seasonal prediction of Indian Ocean basin mode. Clim Dyn 53, 6089–6104 (2019). https://doi.org/10.1007/s00382-019-04916-9
- Hu Z-Z (1997) Interdecadal variability of summer climate over East Asia and its association with 500 hPa height and global sea surface temperature. J Geophys Res 102(D16):19403–19412. https://doi.org/10.1029/97JD0 1052
- Hurrell, J.W., 1995: Decadal Trends in the North Atlantic Oscillation: Regional Temperatures and Precipitation. Science: Vol. 269, pp.676-679
- Indian Meteorological Department, 1943, "Climatological Atlas for Airmen".
- Izumo T, Lengaigne M, Vialard J, Luo JJ, Yamagata T, Madec G (2014) Influence of Indian Ocean Dipole and Pacific recharge on following year's El Niño: interdecadal robustness. Clim Dyn 42(1–2):291–310
- Jadhav J et al (2015) On the possible cause of distinct El Niño types in the recent decades. Sci Rep 5:17009. https://doi.org/10.1038/srep1 7009
- Jayasankar, T., Murtugudde, R., & Eldho, T. I. (2019). The Indian Ocean deep meridional overturning circulation in three ocean reanalysis products. Geophysical Research Letters, 46, 12146— 12155. https://doi.org/10.1029/2019GL084244
- Jin, E.K., Kinter, J.L., Wang, B. et al. Current status of ENSO prediction skill in coupled ocean–atmosphere models. Clim Dyn 31, 647–664 (2008). https://doi.org/10.1007/s00382-008-0397-3
- Jin, F.-F., 1997a: An equatorial ocean recharge paradigm for ENSO. Part I: Conceptual model. J. Atmos. Sci., 54, 811-829.
- Jin, F.-F., 1997b: An equatorial ocean recharge paradigm for ENSO. Part II: A stripped-down coupled model. J. Atmos. Sci., 54, 830-847.

- Jones PD, Jonsson T, Wheeler D (1997) Extension to the North Atlantic oscillation using early instrumental pressure observations from Gibraltar and south-west Iceland. Int J Climatol 17:1433–1450
- Joseph PV, Eishcheid JK, Pyle RJ. 1994. Interannual variability of the onset of the Indian summer monsoon and its association with atmospheric features, El Nino and sea surface temperature anomalies. ~ Journal of Climate 7: 81–105.
- Jourdain, N.C., Sen Gupta, A., Taschetto, A.S., Ummenhofer, C.C., Moise, A.F. and Ashok, K. (2013) The Indo-Australian monsoon and its relationship to ENSO and IOD in reanalysis data and the CMIP3/CMIP5 simulations. Climate Dynamics, 41, 3073–3102.
- Ju, J. and Slingo, J., 1995, "The Asian summer monsoon and ENSO", Q. J. R. Meteorol. Soc., 121, 525, 1133-1168.
- Kalnay, E., Kanamitsu, M., Kistler, R., Collins, W., Deaven, D., Gandin, L., et al., 1996. The NCEP/
 NCAR 40-year reanalysis project. B. Am. Meteorol. Soc. 77, 437–471. doi:10.1175/15200477(1996)077<0437:TNYRP>2.0.CO;2.
- Kaplan, A., Y. Kushnir, M. A. Cane, and M. B. Blumenthal (1997), Reduced space optimal analysis for historical data sets: 136 years of Atlantic Sea surface temperatures, J. Geophys. Res., 102(D13), 27,835–27,860.
- Kao, H. Y. and Yu, J. Y., 2009, "Contrasting Eastern-Pacific and Central-Pacific Types of ENSO", J. Climate, 22, 615-632.
- Kawamura, R., 1998, "A possible mechanism of the Asian summer monsoon-ENSO coupling", J. Meteorol. Soc. Japan, 76, 1009-1027.
- Keenlyside, N., Latif, M., Jungclaus, J. et al. Advancing decadal-scale climate prediction in the North Atlantic sector. Nature 453, 84–88 (2008). https://doi.org/10.1038/nature06921
- Keshavamurthy, R. N., 1982, "Response of the atmosphere to sea surface temperature anomalies over the equatorial Pacific and teleconnections of the Southern Oscillation", J. Atmos. Sci., 39, 1241-1259.
- Koteswaram, P., 1958, "Easterly jet streams in the tropics", Tellus, 10, 43-57.
- Kothawale, D., and M. Rajeevan, 2017: Monthly, seasonal and annual rainfall time series for all-India,

- homogeneous regions and meteorological subdivisions: 1871-2016. IITM Research Report No. RR-138.
- Krishnamurti, T. N., and H. Bhalme, 1976: Oscillations of a monsoon system. part i. observational aspects. Journal of the Atmospheric Sciences, 33 (10), 1937–1954.
- Krishnamurthy, Lakshmi, and V Krishnamurthy, May 2014: Influence of PDO on South Asian summer monsoon and monsoon–ENSO relation. Climate Dynamics, 42(9-10), DOI:10.1007/s00382-013-1856-z.
- Krishnamurthy L, Krishnamurthy V (2017) Indian monsoon's relation with the decadal part of PDO in observations and NCAR CCSM4. Int J Climatol 37:1824–1833. https://doi.org/10.1002/joc.4815
- Krishnaswamy, Jagdish & Vaidyanathan, Srinivas & Rajagopalan, Balaji & Bonell, Mike & Sankaran, Mahesh & Bhalla, Ravinder & Badiger, Shrinivas. (2014). Non-stationary and non-linear influence of ENSO and Indian Ocean Dipole on the variability of Indian monsoon rainfall and extreme rain events. Climate Dynamics. 45. 1-10. 10.1007/s00382-014-2288-0.
- Kucharski, F., A. Bracco, J. Yoo, and F. Molteni, 2007: Low-frequency variability of the Indian monsoon–enso relationship and the tropical atlantic: The weakening of the 1980s and 1990s. Journal of Climate, 20 (16), 4255–4266.
- Kucharski, F., A. Bracco, J. Yoo, and F. Molteni, 2008: Atlantic forced component of the Indian monsoon interannual variability. Geophysical Research Letters, 35 (4).
- Kug, J. S., Jin, F. F. and An, S. I., 2009, "Two-types of El Niño events: Cold Tongue El Niño and Warm Pool El Niño", J. Climate, 22, 1499-1515.
- Kug J-S, Kang I-S (2006) Interactive feedback between the Indian Ocean and ENSO. J Clim 19:1784–1801.
- Kumar KK, Rajagopalan B, Cane MA (1999) On the weakening relationship between the Indian Monsoon and ENSO. Science 284(5423):2156–2159. https://doi.org/10.1126/science.284.5423.2156
- Kumar KK, Rajagopalan B, Hoerling M, Bates G, Cane M (2006) Unraveling the Mystery of Indian Monsoon Failure During El Niño. Science 314:115–119. https://doi.org/10.1126/science.11311 52
- Kushnir, Y., Scaife, A.A., Arritt, R. et al. Towards operational predictions of the near-term climate. Nature Clim Change 9, 94–101 (2019). https://doi.org/10.1038/s41558-018-0359-7

- Lai, Ying-Cheng & Grebogi, Celso & Kurths, Juergen. (1999). Modeling of deterministic chaotic systems. Phys. Rev. E. 59. 10.1103/PhysRevE.59.2907.
- Larkin, N. K. and Harrison, D. E., 2005, "Global seasonal temperature and precipitation anomalies during El Niño autumn and winter", Geophys. Res. Lett., 32, L16705, doi:10.1029/2005GL022860.
- Latif, M. (1998). Dynamics of Interdecadal Variability in Coupled Ocean–Atmosphere Models, Journal of Climate, 11(4), 602-624.
- Lau, N. C. and Nath, M. J., 2000, "Impact of ENSO on the variability of the Asian-Australian monsoons as simulated in GCM experiments", J. Climate, 13, 4287-4309.
- Lindzen, R. S. and Nigam, S., 1987, "On the role of sea surface temperature gradients in forcing low-level winds and convergence in the Tropics", J. Atmos. Sci., 44, 2418-2436.
- Lorenz, Edward N., 1963: Deterministic Nonperiodic Flow. Journal of the Atmospheric Sciences, 20, 130-141, doi:0.1175/1520-0469(1963)020<0130:DNF>2.0.CO;2
- Mantua, N. J., S. R. Hare, Y. Zhang, J. M. Wallace, and R. C. Francis, 1997: A Pacific Interdecadal Climate Oscillation with Impacts on Salmon Production. Bull. Amer. Meteor. Soc, 78, 1069–1079.
- Marathe, Shamal & Ashok, Karumuri. (2021). Chapter- The El Niño Modoki. In book: Tropical and Extratropical Air-Sea Interactions (pp.93-114). 10.1016/B978-0-12-818156-0.00009-5.
- Marathe, S., Ashok, K., Panickal, S. and Sabin, T. P., 2015, "Revisiting El Niño Modokis", Climate Dynamics, 45, 11-12, 3527-3545.
- Marathe, Shamal & Terray, Pascal & Ashok, Karumuri. (2021). Tropical Indian Ocean and ENSO relationships in a changed climate. Climate Dynamics. 56. 10.1007/s00382-021-05641-y.
- Masumoto, Y. and Yamagata, T., 1991, "Response of the western tropical Pacific to the Asian winter monsoon: the generation of the Mindanao Dome", Journal of Physical Oceanography, 21, 1386-1398.
- Matsuno, T., 1966, "Quasi-geostrophic motions in the equatorial area", J. Meteor. Soc. Japan, 44, 25-43.
- Meehl, Gerald & Arblaster, Julie. (2001). The Tropospheric Biennial Oscillation and Indian Monsoon Rainfall.

 Geophysical Research Letters Geophys Res Lett. 28. 1731-1734. 10.1029/2000GL012283.

- Meehl, G. A., Goddard, L., Boer, G., Burgman, R., Branstator, G., Cassou, C., Corti, S., Danabasoglu, G., Doblas-Reyes, F., Hawkins, E., Karspeck, A., Kimoto, M., Kumar, A., Matei, D., Mignot, J., Msadek, R., Navarra, A., Pohlmann, H., Rienecker, M., Rosati, T., Schneider, E., Smith, D., Sutton, R., Teng, H., van Oldenborgh, G. J., Vecchi, G., & Yeager, S. (2014). Decadal Climate Prediction: An Update from the Trenches, Bulletin of the American Meteorological Society, 95(2), 243-267.
- Meehl, G. A., Goddard, L., Murphy, J., Stouffer, R. J., Boer, G., Danabasoglu, G., Dixon, K., Giorgetta, M. A., Greene, A. M., Hawkins, E., Hegerl, G., Karoly, D., Keenlyside, N., Kimoto, M., Kirtman, B., Navarra, A., Pulwarty, R., Smith, D., Stammer, D., & Stockdale, T. (2009). Decadal Prediction, Bulletin of the American Meteorological Society, 90(10), 1467-1486.
- Meinen CS, McPhaden MJ (2000) Observations of warm water volume changes in the equatorial Pacific and their relationship to El Niño and La Niña. J Clim 13:3551–3559
- Merryfield, W. J., Lee, W., Boer, G. J., Kharin, V. V., Scinocca, J. F., Flato, G. M., Ajayamohan, R. S., Fyfe, J. C., Tang, Y., & Polavarapu, S. (2013). The Canadian Seasonal to Interannual Prediction System. Part I: Models and Initialization, Monthly Weather Review, 141(8), 2910-2945.
- Mohanty, U. C., Nayak, H. P., Sinha, P., Osuri, K. K., & Niyogi, D. (2019). Land surface processes over Indian summer monsoon region: a review. Mausam, (July) 70, 551–560.
- Moss, R. H., Edmonds, J. A., Hibbard, K. A., Manning, M. R., Rose, S. K., van Vuuren, D. P., ... Wilbanks, T. J. (2010). The next generation of scenarios for climate change research and assessment. Nature, 463(7282), 747–756. doi:10.1038/nature08823
- Mujumdar M, Preethi B, Sabin TP, Ashok K, Sajjad S, Pai DS, Krishnan R (2012) The Asian summer monsoon response to the La Niña event of 2010. Meteorol Appl 19:216–225. https://doi.org/10.1002/met.1301
- Müller, W. A., Baehr, J., Haak, H., Jungclaus, J. H., Kröger, J., Matei, D., Notz, D., Pohlmann, H., von Storch, J. S., and Marotzke, J. (2012), Forecast skill of multi-year seasonal means in the decadal prediction system of the Max Planck Institute for Meteorology, Geophys. Res. Lett., 39, L22707, doi:10.1029/2012GL053326.
- Murakami, T, 1987.: Effects of the Tibetan Plateau. In Monsoon Meteorology, edited by C. P. Chang and T. N. Krishnamurti, Oxford University Press, New York, 235–270.

- Murtugudde, R., J. P. McCreary, and A. J. Busalacchi, 2000: Oceanic processes associated with anomalous events in the Indian Ocean with relevance to 1997–98. J. Geophys. Res., 105, 3295–3306.
- Nauw, J. J., van Aken, H. M., Webb, A., Lutjeharms, J. R. E., and de Ruijter, W. P. M. (2008). Observations of the southern East Madagascar Current and undercurrent and counter current system. J. Geophys. Res. 113:C08006. doi: 10.1029/2007JC004639
- Navarra, A., Ward, M. N. and Miyakoda, K., 1999, "Tropical-wide teleconnection and oscillation I: Teleconnection indices and type I/type II states", Quart. J. Roy. Meteor. Soc., 125, 2909-2935.
- Nigam, S., 1994, "On the dynamical basis for the Asian summer monsoon rainfall-El Niño relationship", J. Climate, 7, 1750-1771.
- Osborn TJ (2006) Recent variations in winter North Atlantic Oscillation. Weather 61:353–355
- Pai DS, Bandgar A, Devi S, Musale M, Badwaik MR, Kundale AP, Gadgil S, Mohapatra M, Rajeevan M. 2020.

 New normal dates of onset/progress and withdrawal of southwest monsoon over India. Mausam Vol. 71

 No. 4 (2020); Pages 553-570.
- Pal, M., Maity, R., Ratnam, J.V., Nonaka, M., & Behera, S. K. Long-lead Prediction of ENSO Modoki Index using Machine Learning algorithms, Scientific Reports 10:365, DOI:10.1038/s41598-019-57183-3 (2020).
- Palmer, T. N., Brankovic, C., Viterbo P. and Miller, M. J., 1992, "Modeling interanual variations of summer monsoons", J. Climate, 5, 399-417.
- Palmer & R. Hagedorn (Eds.), Predictability of Weather and Climate (pp. 1-29). Cambridge: Cambridge University Press. doi:10.1017/CBO9780511617652.002
- Pant, G. B., and K. R. Kumar, 1997: Climates of south Asia. Wiley-Blackwell.
- Pant, G.B., Parthasarathy, S.B. Some aspects of an association between the southern oscillation and Indian summer monsoon. Arch. Met. Geoph. Biocl., Ser. B 29, 245–252 (1981). https://doi.org/10.1007/BF02263246
- Parthasarathy, B., A. Munot, and D. Kothawale, 1994: All-India monthly and seasonal rainfall series: 1871–1993.

 Theoretical and Applied Climatology, 49 (4), 217–224.
- Philander, S., J. R. Holton, and R. Dmowska, 1989: El Niño, La Niña, and the southern oscillation, Vol. 46.

- Academic press.
- Pokhrel, S., Chaudhari, H.S., Saha, S.K. et al. ENSO, IOD and Indian Summer Monsoon in NCEP climate forecast system. Clim Dyn 39, 2143–2165 (2012). https://doi.org/10.1007/s00382-012-1349-5
- Pottapinjara, V., Girishkumar, M.S., Sivareddy, S., Ravichandran, M. and Murtugudde, R. (2016), Relation between the upper ocean heat content in the equatorial Atlantic during boreal spring and the Indian monsoon rainfall during June–September. Int. J. Climatol., 36: 2469-2480. https://doi.org/10.1002/joc.4506
- Power, S., Casey, T., Folland, C. et al. Inter-decadal modulation of the impact of ENSO on Australia. Climate Dynamics 15, 319–324 (1999). https://doi.org/10.1007/s003820050284
- Preethi B, Mujumdar M, Kripalani RH, Prabhu A Krishnan R (2016) Recent trends and tele-connections among South and East Asian summer monsoons in a warming environment. Clim Dyn https://doi.org/10.1007/s0038 2-016-3218-0
- Rajeevan M, McPhaden MJ (2004) Tropical Pacific upper ocean heat content variations and Indian summer monsoon rainfall. Geophys Res Lett 31(18): L18203. https://doi.org/10.1029/2004G L0206 31
- Ramage, C., 1971: [Monsoon Meteorology]. Academic Press.
- Rao, Y., 1976: Southwest monsoon (meteorological monograph, synoptic meteorology no. 1). Indian Meteorological Department, New Delhi, 367pp.
- Rao, S. A., S. K. Behera, Y. Masumoto, and T. Yamagata, Interannual variability in the subsurface tropical Indian Ocean with a special emphasis on the Indian Ocean Dipole, Deep-Sea Res. II, 49, 1549–1572, 2002
- Rasmusson, E. M. and Carpenter, T. H., 1983, "The relationship between the eastern Pacific Sea surface temperature and rainfall over India and Sri Lanka", Mon. Weather. Rev., 111, 517-528.
- Ratna, S. B., Cherchi, A., Osborn, T. J., Joshi, M., & Uppara, U. (2021). The extreme positive Indian Ocean dipole of 2019 and associated Indian summer monsoon rainfall response. Geophysical Research Letters, 48, e2020GL091497. https://doi.org/10.1029/2020GL091497
- Rawlinson, H. G. (1916). Intercourse between India and the Western World. Cambridge University Press.
- Rayner, N., D. E. Parker, E. Horton, C. K. Folland, L. V. Alexander, D. Rowell, E. Kent, and A. Kaplan, 2003:

- Global analyses of sea surface temperature, sea ice, and night marine air temperature since the late nineteenth century. Journal of Geophysical Research: Atmospheres, 108 (D14).
- Riehl, Herbert., 1954: Tropical Meteorology. New York: McGraw-Hill Book Co.
- Robson, J., R. Sutton, and D. Smith, 2013: Predictable Climate Impacts of the Decadal Changes in the Ocean in the 1990s. Journal of Climate, 26 (17), 6329–6339, doi:10.1175/JCLI-D-12-00827.1, URL http://journals.ametsoc.org/doi/abs/10.1175/JCLI-D-12-00827.1.
- Ropelewski, C. F. and Halpert, M. S., 1987, "Global and regional scale precipitation patterns associated with the El Niño Southern Oscillation", Mon. Wea. Rev., 115, 1606-1626.
- Ross SM (2020) Introduction to probability and statistics for engineers and scientists. Academic Press, Cambridge
- Saji N. Hameed. The Indian Ocean Dipole, in Oxford Research Encyclopaedia of Climate Science (ed. Hans von Storch) (Oxford University Press, Oxford, 2018)
- Saji, N. H., B. N. Goswami, P. N. Vinayachandran, and T. Yamagata,1999: A dipole mode in the tropical Indian Ocean. Nature, 401, 360–363.
- Saji NH, Yamagata T (2003) Possible impacts 209 of Indian Ocean dipole mode events on global climate. Clim Res 25:151–169. doi:10.3354/cr025151.
- Sarachik, Edward S and Cane, Mark A. The El Niño-Southern Oscillation Phenomenon. Cambridge University

 Press
- Schott, F. A., Xie, S.-P., and McCreary, J. P. (2009), Indian Ocean circulation and climate variability, Rev. Geophys., 47, RG1002, doi:10.1029/2007RG000245.
- Scientific Committee on Oceanic research (SCOR) 1983: Prediction of El Niño. Proceedings No. 19 Paris. Annex VI, SCOR WG 55 47-51.
- Sgubin, G., Swingedouw, D., Borchert, L.F. et al. (2021) Systematic investigation of skill opportunities in decadal prediction of air temperature over Europe. Clim Dyn. https://doi.org/10.1007/s00382-021-05863-0
- Sheen, K. et al. Skilful prediction of Sahel summer rainfall on inter-annual and multi-year timescales. Nat. Commun. 8, 14966 (2017).

- Shepard. Donald, 1968. A two-dimensional interpolation function for irregularly-spaced data. In Proceedings of the 1968 23rd ACM national conference (ACM '68). Association for Computing Machinery, New York, NY, USA, 517–524. DOI:https://doi.org/10.1145/800186.810616
- Shukla, J. and J. M. Wallace, 1983, "Numerical simulation of the atmospheric response to equatorial sea surface temperature anomalies", J. Atmos. Sci., 40, 1613-1630.
- Shukla, J. and Paolino, D. A., 1983, "The southern oscillation and long-range forecasting of the summer monsoon rainfall over India", Mon. Weather Rev., 111, 1830-1837, doi: 10.1175/1520-0493.
- Sikka, D., 1980: Some aspects of the large-scale fluctuations of summer monsoon rainfall over India in relation to fluctuations in the planetary and regional scale circulation parameters. Proceedings of the Indian Academy of Sciences-Earth and Planetary Sciences, 89 (2), 179–195.
- Sikka, D. R., and Sulochana Gadgil, 1980: On the maximum cloud zone and the ITCZ over India longitude during the southwest monsoon. Mon. Weather Rev., 108, 1840-1853.
- Slingo, J. M. and Annamalai, H., 2000, "1997: The El Niño of the century and the response of the Indian summer monsoon", Mon. Weather Rev., 128, 1778-1797.
- Smith DM, Cusack S, Colman AW, Folland CK, Harris GR, Murphy JM. Improved surface temperature prediction for the coming decade from a global climate model. Science. 2007 Aug 10;317(5839):796-9. doi: 10.1126/science.1139540. PMID: 17690292.
- Smith DM, Eade R, Pohlmann H (2013) A comparison of full-field and anomaly initialization for seasonal to decadal climate prediction. Clim Dyn 41(11–12):3325–3338. https://doi.org/10.1007/BF02967433
- Smith, D.M., Eade, R., Scaife, A.A. et al. Robust skill of decadal climate predictions. npj Clim Atmos Sci 2, 13 (2019). https://doi.org/10.1038/s41612-019-0071-y
- Soman, M. K. and Slingo, J., 1997, "Sensitivity of the Asian summer monsoon to aspects of sea-surface-temperature anomalies in the tropical Pacific Ocean", Q. J. R. Meteor. Soc., 123, 309-336.
- Sreejith, O. P., Panickal, S., Pai, S. and Rajeevan, M., 2015, "An Indian Ocean precursor for Indian summer monsoon rainfall variability", Geophys. Res. Lett., 42, 9345-9354.
- Srokosz, M., Danabasoglu, G., & Patterson, M. (2021). Atlantic meridional overturning circulation: Reviews of

- observational and modeling advances—An introduction. Journal of Geophysical Research: Oceans, 126, e2020JC016745. https://doi.org/10.1029/2020JC016745
- Suarez, M. J. and Schopf, P. S., 1988, "A delayed action oscillator for ENSO", J. Atmos. Sci., 45, 3283-3287.
- Sun, Q., Bo, W. U., Zhou, T. J. & Yan, Z. X. ENSO hindcast skill of the IAP-DecPreS near term climate prediction system: comparison of full field and anomaly initialization. Atmospheric and Oceanic Science Letters 11(1), 54–62, https://doi.org/10.1080/167428 (2018).
- Swapna, P., Roxy, M. K., Aparna, K., Kulkarni, K., Prajeesh, A. G., Ashok, K., Krishnan, R., Moorthi, S., Kumar, A. and Goswami, B. N, 2015, "The IITM earth system model: Transformation of a seasonal prediction model to a long-term climate model", Bulletin of the American Meteorological Society, 96, 1351-1368, https://doi.org/10.1175/BAMS-D-13-00276.1.
- Talley L., Pickard G., Emery W. And Swift J., 2011 Descriptive Physical Oceanography: an Introduction. Sixth Edition. Elsevier, Boston, MA.
- Taylor, K. E., Stouffer, R. J., & Meehl, G. A. (2012). An Overview of CMIP5 and the Experiment Design, Bulletin of the American Meteorological Society, 93(4), 485-498.
- Tejavath CT, Ashok K, Chakraborty S, Ramesh R (2018) The ENSO teleconnections to the Indian summer monsoon climate through the Last Millennium as simulated by the PMIP3. Clim Past Discuss. https://doi.org/10.5194/cp-2018-7
- Tozuka, T., J. J. Luo, S. Masson, and T. Yamagata, 2007: Decadal modulations of the Indian Ocean Dipole in the SINTEX-F1coupled GCM.J. Climate, 20,2881–2894
- Tyagi, A., Asnani, P. G., De, U. S., Hatwar, H. R. and Mazumdar, A. B. 2012. The Monsoon Monograph, Vols. 1 and 2. Indian Meteorological Department.
- Von Storch, H., and F. W. Zwiers, 1999: Statistical analysis in climate research. Cambridge university press.
- Walker, G. T., 1923, "Correlation in Seasonal Variations of Weather, VIII: A Preliminary Study of World Weather", Mem. India Meteorol. Dep., 24, 75-131.
- Walker, G. T., 1924, "Correlation in seasonal variations of weather, IX: A further study of world weather", Memoirs of the India Meteorological Department, 24, 9, 275-333.

- Walker, G. T., 1928, "World weather", Q. J. R. Meteor. Soc, 54, 79-87.
- Wang, C., 2000, "On the atmospheric responses to tropical Pacific heating during the mature phase of El Niño", J. Atmos. Sci., 57, 3767-3781.
- Wang, C., Weisberg, R. H. and Virmani, J. I., 1999, "Western Pacific interannual variability associated with the El Niño-Southern Oscillation", J. Geophys. Res., 104, 5131-5149.
- Wang, W., Zhu, X., Wang, C., & Köhl, A. (2014). Deep meridional overturning circulation in the Indian Ocean and its relation to Indian Ocean Dipole. Journal of Climate, 27(12), 4508–4520. https://doi.org/10.1175/JCLID1300472.1.
- Warner, T. (2010). Model initialization. In Numerical Weather and Climate Prediction (pp. 198-293). Cambridge: Cambridge University Press. doi:10.1017/CBO9780511763243.007
- Watanabe, M., Suzuki, T., O'ishi, R., Komuro, Y., Watanabe, S., Emori, S., Takemura, T., Chikira, M., Ogura, T., Sekiguchi, M., Takata, K., Yamazaki, D., Yokohata, T., Nozawa, T., Hasumi, H., Tatebe, H., & Kimoto, M. (2010). Improved Climate Simulation by MIROC5: Mean States, Variability, and Climate Sensitivity, Journal of Climate, 23(23), 6312-6335.
- Webster, P. J., V. O. Magana, T. Palmer, J. Shukla, R. Tomas, M. Yanai, and T. Yasunari, 1998: Monsoons: Processes, predictability, and the prospects for prediction. Journal of Geophysical Research: Oceans, 103 (C7), 14 451–14 510.
- Webster, P. J, A. Moore, J. Loschnigg, and M. Leban, 1999: Coupled dynamics in the Indian Ocean during 1997–1998. Nature, 401, 356–360.
- Webster, P. J. and Yang, S., 1992, "Monsoon and ENSO: Selectively Interactive Systems", Quart. J. Roy. Meteor. Soc., 118, 877-926.
- Weisberg, R. H. and Wang, C., 1997, "A western Pacific oscillator paradigm for the El Niño-Southern Oscillation", Geophy. Res. Lett., 24, 779-782.
- Weng, H., Ashok, K., Behera, S., Rao, S.A., Yamagata, T., 2007. Impacts of recent El Niño Modoki on dry/wet conditions in the Pacific rim during boreal summer. Clim. Dyn. 29, 113–129.

- doi:10.1007/s00382-007-0234-0.
- Wu T., et al., 2013: Global carbon budgets simulated by the Beijing climate center climate system model for the last century. J. Geophys. Res. Atmos., 118.
- Wu R, Li C, Lin J (2017) Enhanced winter warming in the Eastern China coastal waters and its relationship with ENSO. Atmos Sci Lett 18:11–18. https://doi.org/10.1002/asl.718
- Wu, Y., Tang, Y. Seasonal predictability of the tropical Indian Ocean SST in the North American multimodel ensemble. Clim Dyn 53, 3361–3372 (2019). https://doi.org/10.1007/s00382-019-04709-0
- Wyrtki, K., 1985: Water displacements in the Pacific and the genesis of El Niño cycles. J. Geophys. Res., 90, 7129-7132.
- Xin, X., Gao, F., Wei, M., Wu, T., Fang, Y. and Zhang, J. (2018), Decadal prediction skill of BCC-CSM1.1 climate model in East Asia. Int. J. Climatol, 38: 584-592. https://doi.org/10.1002/joc.5195
- Yadav, R. K., G. Srinivas, and J. S. Chowdary, 2018: Atlantic Niño modulation of the Indian summer monsoon through Asian jet. Npj Climate and Atmospheric Science, 1 (1), 23.
- Yamagata, T., S. K. Behera, J.-J. Luo, S. Masson, M. Jury, and S. A. Rao 2004: Coupled ocean-atmosphere variability in the tropical Indian Ocean. In Earth Climate: The Ocean-Atmosphere Interaction, C. Wang, S.-P. Xie and J.A. Carton (eds.), Geophys. Monogr., 147, AGU, Washington D.C., 189-212.
- Yamagata, Toshio & Behera, Swadhin & Rao, Suryachandra & Guan, ZY & Ashok, Karumuri & Hameed, Saji. (2003). Comments on "Dipoles, Temperature Gradients, and Tropical Climate Anomalies" [4]. Bulletin of the American Meteorological Society. 84. 10.1175/BAMS-84-10-1418.
- Yang, S., 1996, "ENSO-snow-monsoon associations and seasonal interannual predictions", International Journal of Climatology, 16, 2, 125-134, https://doi.org/10.1002.
- Yeager, S., A. Karspeck, G. Danabasoglu, J. Tribbia, and H. Teng, 2012: A Decadal Prediction Case Study: Late Twentieth-Century North Atlantic Ocean Heat Content. Journal of Climate, 25 (15), 5173–5189, doi:10.1175/JCLI-D-11-00595.1, http://journals.ametsoc.org/doi/abs/10.1175/JCLI-D-11-00595.1.
- Yeh S-W, Kug J-S, An S-I (2014) Recent progress on two types of El Niño: Observations, dynamics, and future changes, Asia-Pac. J Atmos Sci 50:69–81

- Yeh, S.-W., Kug, J., Dewitte, B., Kwon, M.-H., Kirtman, P., Jin, F.F., 2009. El Niño in a changing climate. Nature 461, 511–514.
- Zebiak, S. E. and Cane, M. A., 1987, "A model El Niño-Southern Oscillation", Monthly Weather Review, 115, 2262-2278.
- Zhang, S., M.J. Harrison. A. Rosati, and A.T. Wittenberg, 2007: System Design and Evaluation of Coupled Ensemble Data Assimilation for Global Oceanic Climate Studies. Monthly Weather Review, 135(10), DOI:10.1175/MWR3466.1.
- Zhang, Y., Wallace, J. M. and Iwasaka, N., 1996, "Is climate variability over the North Pacific a linear response to ENSO?", Journal of Climate, 9, 1468-1478.
- Zhang, J., and R. Zhang, 2015: On the evolution of Atlantic Meridional Overturning Circulation Fingerprint and implications for decadal predictability in the North Atlantic. Geophysical Research Letters, 42 (13), 5419–5426, doi:10.1002/2015GL064596, http://doi.wilev.com/10.1002/2015GL064596.
- Zhao, S., Stuecker, M. F., Jin, F., Feng, J., Ren, H., Zhang, W., & Li, J. (2020). Improved Predictability of the Indian Ocean Dipole Using a Stochastic Dynamical Model Compared to the North American Multimodel Ensemble Forecast, Weather and Forecasting, 35(2), 379-399.
- Zhou L et al (2009) Spatial patterns of diurnal temperature range trends on precipitation from 1950 to 2004. Clim

 Dynam 32:429–440

The Indo-Pacific drivers of the Indian Summer Monsoon – Decadal Variability and Prediction

by Feba Francis

Submission date: 16-Nov-2021 04:45PM (UTC+0530)

Submission ID: 1704480476

File name: Feba_Francis.pdf (5.7M)

Word count: 15698 Character count: 81975 frami Ahr

Prof. KARUMURI ASHOK

Centre for Earth, Ocean & Atmospheric Sciences

University of Hyderabad

Hyderabad-500 046, INDIA.

The Indo-Pacific drivers of the Indian Summer Monsoon – Decadal Variability and Prediction

	LITY REPORT	bility and Predict	.1011		
3 SIMILA	5% RITY INDEX	31% INTERNET SOURCES	33% PUBLICATIONS	5% STUDENT PA	APERS
PRIMARY	/ SOURCES			on the	8
1	link.spr	nger.com	Polaris bords	Time (14%
2	www.fro	ontiersin.org	Weirs / Lo	mi AMD (13%
3	Submitte Hydera Student Pape		of Hyderabac	1 ,	2%
4	journals Internet Sou	s.ametsoc.org			1%
5	WWW.SC	ience.gov			1%
6		ng. "The Asian M and Business M			<1%
7	Satish F Predicti Frontie	Karumuri Asho R. Shetye. "Emer on of the Indian rs in Climate, 20	ging Skill in M Ocean Dipole	ulti-Year	<1%

Prof. KARUMURI ASHOK

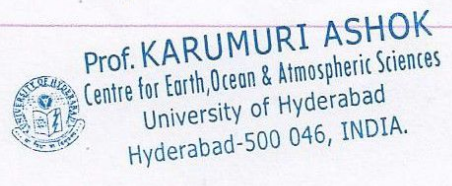
8	"Earth's Climate", Wiley, 2004 Publication	<1%
9	worldwidescience.org Internet Source	<1%
10	www.climatechange2013.org	<1%
11	Gershunov, Alexander, Niklas Schneider, and Tim Barnett. "Low-Frequency Modulation of the ENSO-Indian Monsoon Rainfall Relationship: Signal or Noise?", Journal of Climate, 2001.	<1%
12	assets.researchsquare.com Internet Source	<1%
13	Meinen, Christopher S., and Michael J. McPhaden. "Observations of Warm Water Volume Changes in the Equatorial Pacific and Their Relationship to El Niño and La Niña", Journal of Climate, 2000. Publication	<1%
14	Fang Zou, Robert Tenzer, Hok Sum Fok, Guojie Meng, Qian Zhao. "The sea level changes in Hong Kong from tide-gauge records and remote sensing observations over the last seven decades", IEEE Journal of Selected	<1%

Prof. KARUMURI ASHOK
Prof. KARUMURI ASHOK
(entre for Earth, Ocean & Atmospheric Sciences
University of Hyderabad
University of Hyderabad
Hyderabad-500 046, INDIA.

Topics in Applied Earth Observations and Remote Sensing, 2021

Publication

15	www.weathergraphics.com Internet Source	<1%
16	Submitted to University of Durham Student Paper	<1%
17	"Regional Climate Studies of China", Springer Science and Business Media LLC, 2008 Publication	<1%
18	Guohong Fang. "Trends and interannual variability of the South China Sea surface winds, surface height, and surface temperature in the recent decade", Journal of Geophysical Research, 10/31/2006 Publication	<1%
19	LiJuan Li, Bin Wang, TianJun Zhou. "Impacts of external forcing on the 20th century global warming", Chinese Science Bulletin, 2007	<1%
20	Samir Pokhrel, H. S. Chaudhari, Subodh K. Saha, Ashish Dhakate, R. K. Yadav, Kiran Salunke, S. Mahapatra, Suryachandra A. Rao. "ENSO, IOD and Indian Summer Monsoon in NCEP climate forecast system", Climate Dynamics, 2012 Publication	<1%
	WARLIMIRI ASHOR	



21	acp.copernicus.org	<1%
22	Submitted to University of Reading Student Paper	<1%
23	Hemadri Bhusan Amat, Maheswar Pradhan, C. T. Tejavath, Avijit Dey, Suryachandra A. Rao, A. K. Sahai, Karumuri Ashok. "Value Addition to Forecasting: Towards Kharif Rice Crop Predictability Through Local Climate Variations Associated With Indo-Pacific Climate Drivers.", Research Square, 2021	<1%
24	P. Chang, T. Yamagata, P. Schopf, S. K. Behera, J. Carton, W. S. Kessler, G. Meyers, T. Qu, F. Schott, S. Shetye, SP. Xie. "Climate Fluctuations of Tropical Coupled Systems— The Role of Ocean Dynamics", Journal of Climate, 2006 Publication	<1%
25	P. H. Hrudya, Hamza Varikoden, R. Vishnu. "A review on the Indian summer monsoon rainfall, variability and its association with ENSO and IOD", Meteorology and Atmospheric Physics, 2020 Publication	<1%
26	F. Feba, K. Ashok, M. Ravichandran. "Role of changed Indo-Pacific atmospheric circulation	<1%

Prof. KARUMURI ASHOK

Prof. KARUMURI ASHOK

Prof. KARUMURI ASHOK

Prof. KARUMURI ASHOK

Atmospheric Sciences

Centre for Earth, Diean & Atmospheric Sciences

University of Hyderabad

University of Hyderabad

Hyderabad-500 046, INDIA.

Hyderabad-500 046, INDIA.

in the recent disconnect between the Indian summer monsoon and ENSO", Climate Dynamics, 2018

Publication

Hong-Li Ren, Fei-Fei Jin. "Recharge Oscillator Mechanisms in Two Types of ENSO", Journal of Climate, 2013 Publication	<1%
Shamal Marathe, Karumuri Ashok, P. Swapna, T. P. Sabin. "Revisiting El Niño Modokis", Climate Dynamics, 2015 Publication	<1%
Zhibiao Wang, Renguang Wu. "Land surface signal of the Indochina Peninsular precipitation variability during the early rainy season", International Journal of Climatology, 2020 Publication	<1%
science.nature.nps.gov Internet Source	<1%
Submitted to Heriot-Watt University Student Paper	<1%
Sulochana Gadgil. "The Indian Monsoon and Its Variability", Annual Review of Earth and Planetary Sciences, 2003	<1%
	Mechanisms in Two Types of ENSO", Journal of Climate, 2013 Publication Shamal Marathe, Karumuri Ashok, P. Swapna, T. P. Sabin. "Revisiting El Niño Modokis", Climate Dynamics, 2015 Publication Zhibiao Wang, Renguang Wu. "Land surface signal of the Indochina Peninsular precipitation variability during the early rainy season", International Journal of Climatology, 2020 Publication science.nature.nps.gov Internet Source Submitted to Heriot-Watt University Student Paper Sulochana Gadgil. "The Indian Monsoon and Its Variability", Annual Review of Earth and Planetary Sciences, 2003

33 Submitted to Syracuse University

Prof. KARUMURI ASHOK
Prof. KARUMURI ASHOK
Centre for Earth, Ocean & Atmospheric Sciences
University of Hyderabad
University of Hyderabad
Hyderabad-500 046, INDIA.

Student Paper

- 34
- Submitted to Universiti Teknologi MARA
 Student Paper

<1%

- 35
- Submitted to University of Sussex

<1%

- 36
- "Observed Climate Variability and Change over the Indian Region", Springer Science and Business Media LLC, 2017

< 1 %

- Jose Eric Ruiz, Ian Cordery, Ashish Sharma.
 "Integrating Ocean Subsurface Temperatures in Statistical ENSO Forecasts", Journal of Climate, 2005

<1%

- Publication
- 38

advances.sciencemag.org

Internet Source

<1%

Exclude quotes

On

Exclude bibliography On

Exclude matches

< 14 words

Prof. KARUMURI ASHOK



Role of changed Indo-Pacific atmospheric circulation in the recent disconnect between the Indian summer monsoon and ENSO

F. Feba¹ · K. Ashok¹ · M. Ravichandran²

Received: 5 July 2017 / Accepted: 6 April 2018 © Springer-Verlag GmbH Germany, part of Springer Nature 2018

Abstract

We explore the decadal variability of teleconnection from tropical Pacific to the Indian summer monsoon rainfall (ISMR) using various observational and Reanalysis datasets for the period 1958–2008. In confirmation with the earlier findings, we find that the interannual correlations between the various SST indices of ENSO and ISMR have continued to weaken. Interestingly, we find that even the robust lead correlations of the tropical pacific warm-water-volume with ISMR have weakened since late 1970s. Our analysis suggests that there is a relative intensification of the cross-equatorial flow from the southern hemisphere into the equatorial Indian Ocean associated with ISMR due to strengthening of Mascarene High. Further, a shift in the surface wind circulation associated with monsoon over the northern pacific since late 1970s has resulted in a strengthened cyclonic seasonal circulation south-east of Japan. These changed circulation features are a shift from the known circulation-signatures that efficiently teleconnect El Niño forcing to South Asia. These recent changes effectively weakened the teleconnection of the El Niño to ISMR.

 $\textbf{Keywords} \ \ ENSO \cdot Indian \ summer \ monsoon \cdot Pacific \ surface \ winds \cdot Decadal \ variability \cdot Warm \ water \ volume \cdot Wind \ circulation$

1 Introduction

No other tidings in the field of tropical climate science have caused as much commotion as the variability of ENSO-Monsoon Teleconnections did in the recent periods. ENSO is one of the strongest drivers of the Indian summer monsoons. The ENSO teleconnections to ISMR have been extensively studied (e.g. Walker and Bliss 1932; Sikka 1980; Keshavamurthy 1982; Rasmusson and Carpenter 1983; Kripalani and Kulkarni 1997a, b; Navarra et al. 1999; Lau and Nath 2000; Ashok et al. 2001, 2004; Ashok and Saji 2007) in parallel to those that addressed its existence, evolution, and variability,

Electronic supplementary material The online version of this article (https://doi.org/10.1007/s00382-018-4207-2) contains supplementary material, which is available to authorized users.

F. Feba feba.cookie@gmail.com

Published online: 20 April 2018

- Centre for Earth and Space Sciences, University of Hyderabad, Hyderabad, India
- National Centre for Antarctic and Ocean Research, Goa, India

etc. (Zebiak and Cane 1987; Torrence and Webster 1999; Saravanan and Chang 2000; Krishnamurthy and Kirtman 2003; McPhaden et al. 2006; Ashok et al. 2007; Annamalai et al. 2007; Kripalani et al. 2007; Choi et al. 2012; Marathe et al. 2015). In addition to the well-known southern oscillation index, other ENSO indices derived from the Sea surface temperature (SST), based such as the NINO3 index have been used as a major predictor in the statistical forecast of the ISMR. Other indices like warm water volume (WWV) over entire Pacific basin are also available (Rajeevan and McPhaden 2004); the WWV has the highest (3–4 month) lead predictive skill.

Notably, the observed ENSO-ISMR link has weakened in the late twentieth century (Kumar et al.1999; Chang et al. 2001; Krishnamurthy and Kirtman 2003; Kawamura et al. 2005; Horii et al. 2012). Ashok et al. (2001, 2004), and Ashok and Saji (2007) suggest that this weakening is owing to the increased positive IOD events. Another study by Chang et al. (2001) suggests that the strengthening and pole ward shift of the jet stream over the North Atlantic might be the cause of this weakening. Sreejith et al. (2015) argue that the air-sea coupled interaction over tropical Indian ocean is the reason for weakening of the ENSO-ISMR links.



Interestingly, the interannual manifestations of the tropical Pacific variability are also undergoing through significant changes over the recent period. Specifically, we see more and more of El Nino Modoki events, with anomalous warming along the central Pacific with anomalous cooling on both sides (Kug and Kang 2006; Ashok et al. 2007; Yeh et al. 2014) since late 1970s. On the other hand, the frequency of the canonical El Nino events, typified by anomalous warming (cooling) in the eastern (western) tropical has reduced substantially since then. The tropical Pacific also witnessed the hitherto unforeseen anomalous basin wide warming from May 2009 through April 2010 and then in 2014 (Ashok et al. 2012; Jadhav et al. 2015).

These conditions make it interesting to take a relook at the decadal variability of the teleconnections of the Pacific basin to the ISMR. It will be particularly worthwhile to see if there are any recent internal changes in the pacific atmosphere, which have a bearing for the monsoon teleconnections. This forms the main objective of this paper.

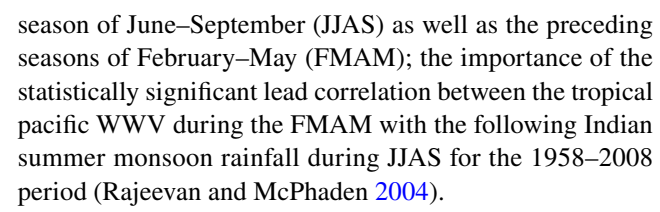
The remaining portion of the current manuscript is divided as follows. In the Sect. 2, we briefly discuss the Datasets and Methodology used in this study, followed by our results in Sect. 3. We provide our conclusions in Sect. 4.

2 Data and methodology

In the current study, we use the monthly-mean Indian summer monsoon rainfall data sets for homogenised area-averaged rainfall sets (Parthasarathy et al. 1994). We use the atmospheric circulation data and sea level pressure (SLP) from Derived National Centers for Environmental Prediction (NCEP) Reanalysis data, provided by the NOAA/OAR/ESRL PSD, Boulder, Colorado, USA (Kalnay et al. 1996), and those from the first atmospheric reanalysis, (ERA-20C) from European Centre for Medium-Range Weather Forecasts (ECMWF).

We also use the Met Office Hadley Centre Sea Ice and Sea Surface Temperature dataset (HadISST) (Rayner et al. 2003) for the same period, along with the Simple Ocean Data Assimilation (SODA) Reanalysis 2.1.6 dataset (Carton and Giese 2008) for the 1958–2008 period for calculation of the WWV. Following Meinen and McPhaden (2000), we define the tropical pacific warm water volume, henceforth referred to as the WWV, as the integrated volume of water above the 20 °C isotherm between 5N–5S, 120E and 80W.

All the datasets have been de-trended for the 1958–2008 period in order to remove the linear trends and to emphasize only the interannual variability. Correlations have been calculated between ISMR and the SST indices, and those between ISMR and WWV, for three partially overlapping 30-year periods starting from 1958, specifically, 1958–1987, 1968–1997 and 1978–2007 for the monsoon



Further, we also compute various correlations between tropical 1000 hPa winds and ISMR for the broad period of 1958–2008 and its various portions i.e., the periods 1958–1987, 1968–1997 and 1978–2007, in order to tease out any decadal variability. We also carry out a complementary regression analysis to attribute the relevance of any circulation changes in the pacific region for the changes in the tropical pacific teleconnections to the ISMR.

The significance of the correlation is calculated using the Student's two tailed test. The degrees of freedom have been ascertained as N-2, where N is the number of samples. As we take the interannual boreal summer values that are largely independent from 1 year to the other, this is a reasonable supposition. Therefore, the threshold of the significant correlation stands at 0.36 (0.28) for 30 (51) years at 95% confidence level.

Further, we have ascertained the significance of the correlations between the ISMR and two NINO indices by a boot-strapping test (1000 simulations). For this, we used the bootstrapping subroutine "bootstrap_correl", from the NCAR Command Language (NCL) package. This routine takes, as inputs, two input timeseries for which the correlations need to be obtained (the ISMR and NINO3 SST, for example, in our case). Based on these input series, it generates 1000 time-series pairs randomly, and computes correlations between each pair. After that, the correlations are ordered as per magnitude. Once this is done, the 50th highest correlation among the 1000 correlations computed, for example, gives us the 0.05 significance level (i.e., 95% confidence level) for the correlations. In case of correlation differences between two time-series, the differences of correlations are ordered as per magnitude to identify the significant threshold values.

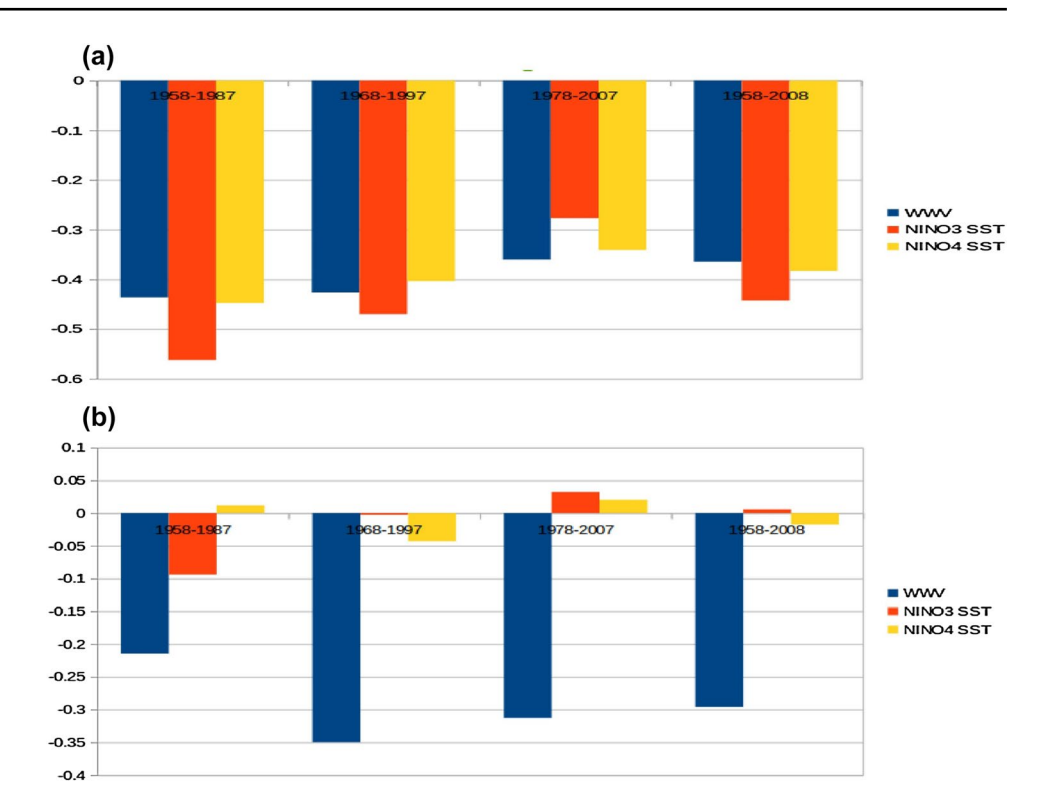
The results from the above bootstrapping test show that the correlations for recent period (1978–2008) differ from the total period (1958–2008) at 90% confidence level.

3 Results

Figure 1a shows the simultaneous correlations of the ISMR with the various ENSO indices, i.e., WWV, NINO3 and NINO4, for JJAS season for each 30-year overlapping periods (1958–1987, 1968–1997, 1978–2007) and total period (1958–2008). In accordance with the earlier findings (Kumar et al. 1999; Ashok et al. 2001; Rajeevan and McPhaden 2004), the results for this season show gradually weakening



Fig. 1 Correlation of Pacific Indices with ISMR during **a** JJAS and **b** FMAM



correlations of the ISMR with various Pacific SST indices over the time. The correlations with Nino3 index particularly show a very rapid decrease, with the correlations becoming insignificant during the recent period, i.e., 1978–2007. The Nino4 index, more relevant to the Indian summer monsoon rainfall owing to its relative proximity to the sub-continent (Kumar et al. 2006; Ashok et al. 2007), also shows gradually weakening association with the ISMR over the period, though the correlations are still significant at 95% confidence level even through the late 2000s. The multi-decadal correlation coefficient between the WWV and ISMR, also decreased from a high -0.44 in 1958–1987 to -0.36 in 1978–2007, though the recent correlations are still statistically significant at 95% confidence level.

Following Rajeevan and McPhaden (2004), we present the lead correlations of the various Pacific indices during the pre-monsoon season (FMAM) with the subsequent ISMR over different overlapping periods (Fig. 1b). Our results are in conformation with earlier findings in the sense that the lead correlations of the pre-monsoon WWV with the ISMR have been, all the while significant at 95% confidence level. However, just as the weakening simultaneous correlations, the magnitude of the lead correlation of the WWV with the ISMR has also steadily decreased. We also find that the lead correlation during FMAM has significant lead predictive skill, though it has weakened further and is insignificant for the recent period, 1978–2007.

For the 1958–2008 period as a whole, the seasonal correlations of ISMR with WWV show that these are maximum

when computed simultaneously, just as that in case of the ISMR correlations with any simultaneous tropical pacific SST index. For ascertaining our results, we also use the WWV dataset from Tropical Atmosphere Ocean (TAO) project, (Auxiliary Figure 1).

Thus our analysis shows that weakening of ENSO-Monsoon correlation in the recent period can be attributed to changes associated with ENSO characteristics, or PDO. Having said that, one should be aware of the fact that such a weakening of correlation for the 1978-2008 period as compared to 1958–2008 period is potentially due to internal modulations in monsoon, and not necessarily related to any discernible external cause (E.g. Gershunov et al. 2001; Ashok et al. 2014; Wu et al. 2017), or in other words, just an issue of sampling (Delsole and Shukla 2012; Cash et al. 2017). From this context, it is pertinent to mention about our recent analysis of PMIP3 simulations for the last millenium (Tejavath et al. 2018), which show that, four of seven models simulate a statistically significantly weakened intra-annual ENSO-Monsoon correlations from Medieval Warm Period (1000–1199 AD) to Little Ice Age (1550–1749 AD) apparently during changes in ENSO characteristics.

3.1 Analysis of the surface winds over tropical Indo-pacific

We analyse the JJAS surface winds over the tropical Indian and Pacific Oceans. During the 51 year period, 1958–2008, the winds over the Tropical Indian Ocean (TIO) show a



weakening correlation with ISMR (Figs. 2, 3). By intercomparing these correlations over various sub-periods (Figs. 2a-c, 3a-c), we find that, the surface winds during JJAS over tropical Indo-Pacific basin show the strongest links over the Pacific basin during 1958–1977 and over

Indian subcontinent than anywhere else in the tropical region. Specifically the eastern tropical Pacific circulation exhibits rather weak links to ISMR during the recent period. Looking at the circulation patterns, the correlations show a shift in the circulation pattern during the recent period.

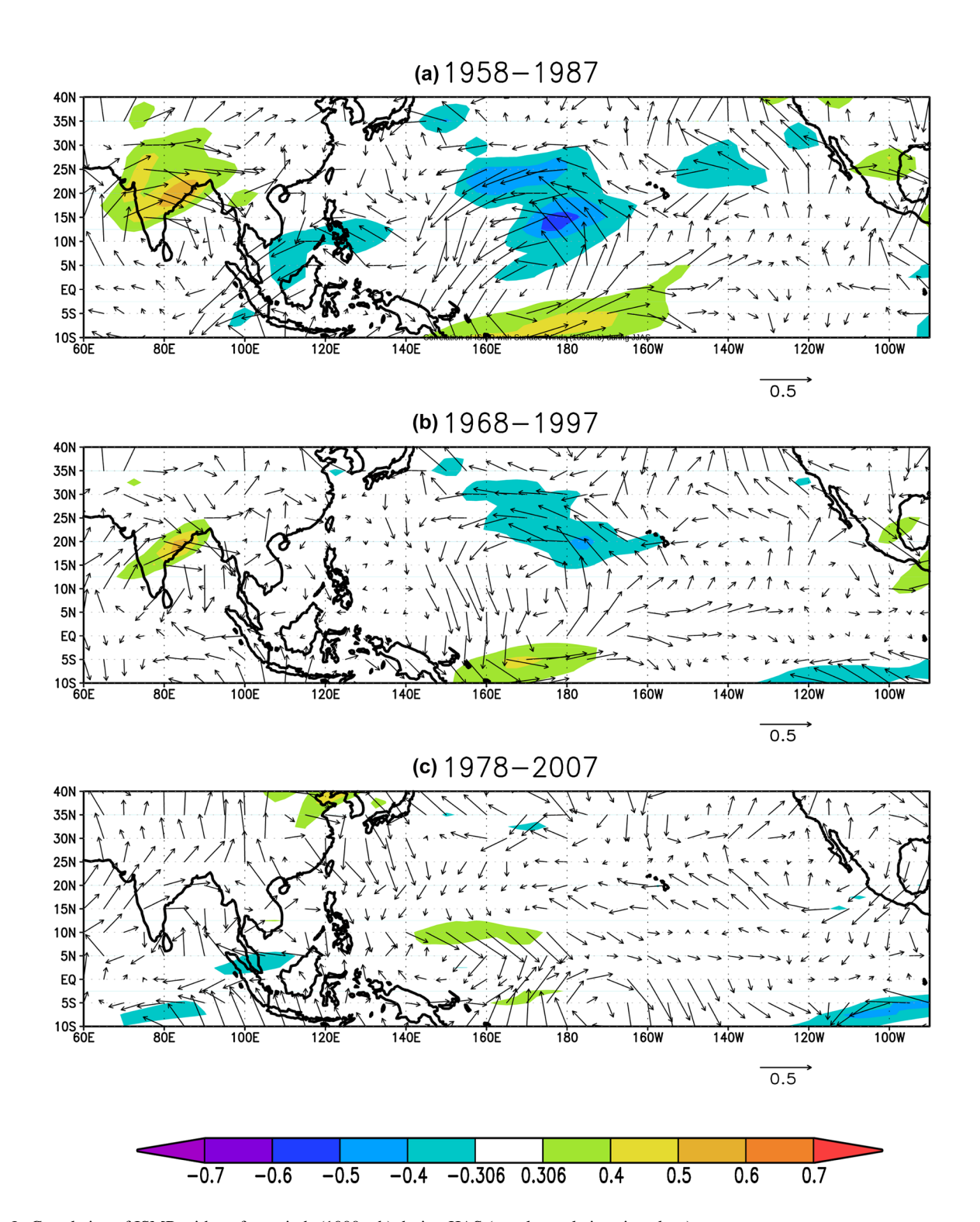


Fig. 2 Correlation of ISMR with surface winds (1000 mb) during JJAS (zonal correlations in colour)



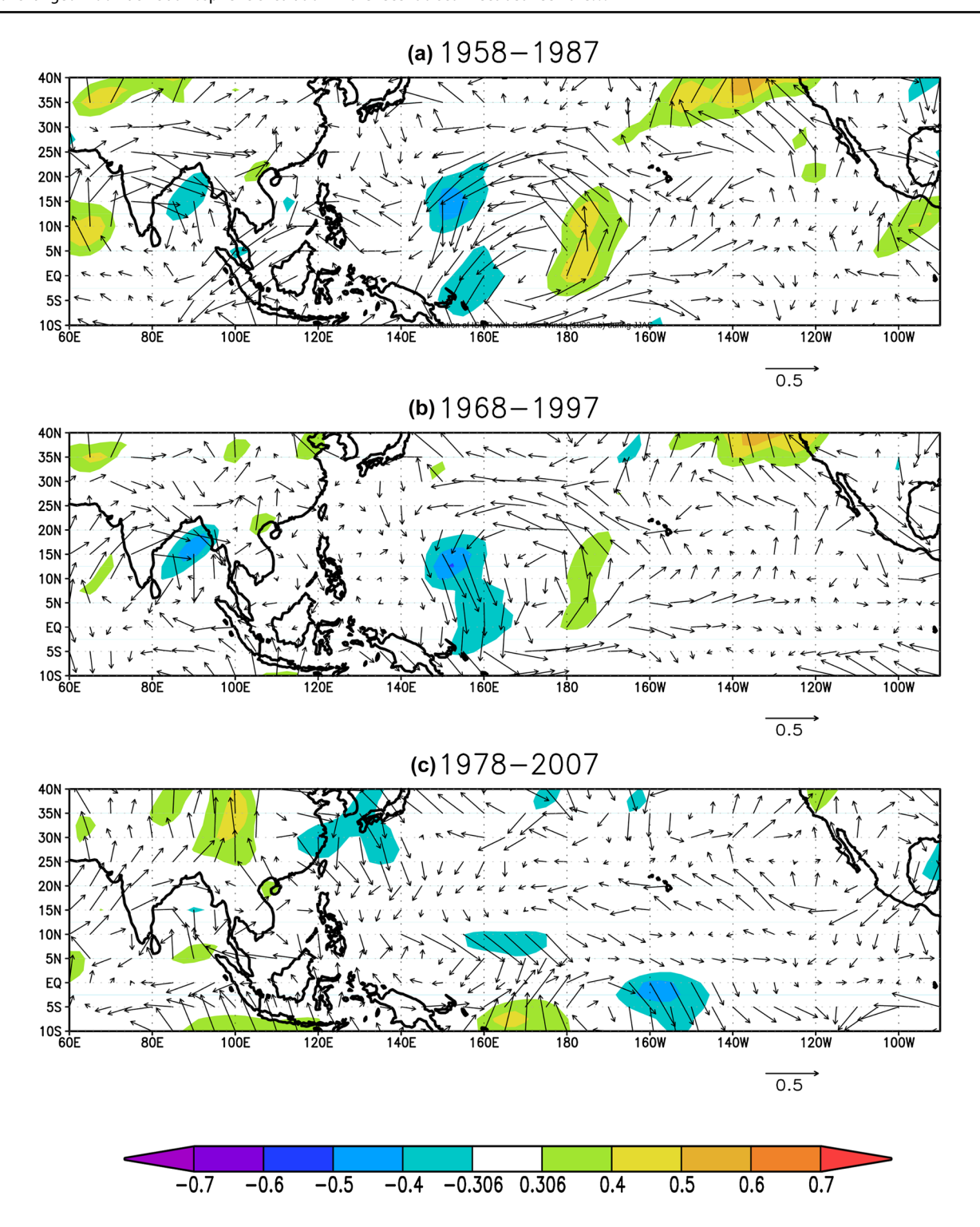


Fig. 3 Correlation of ISMR with surface winds (1000 mb) during JJAS (meridional correlations in colour)

There is a prominent weakening of the cyclonic circulation (observed in Figs. 2a, b, 3a, b) associated with ISMR over the tropical Pacific during the recent period (Figs. 2c, 3c). The corresponding correlations for the 1978–2007 period indicate a 'disconnect' in correlation vectors between the tropical Pacific and TIO. We believe that this is mainly due

to a decadal change in the mean circulation over Indo-Pacific region.

A linear regression analysis (Figs. 4, 5) has been carried out to estimate and understand the apparent shift of dependence of ISMR. With the local zonal and meridional winds as independent variables and ISMR as the



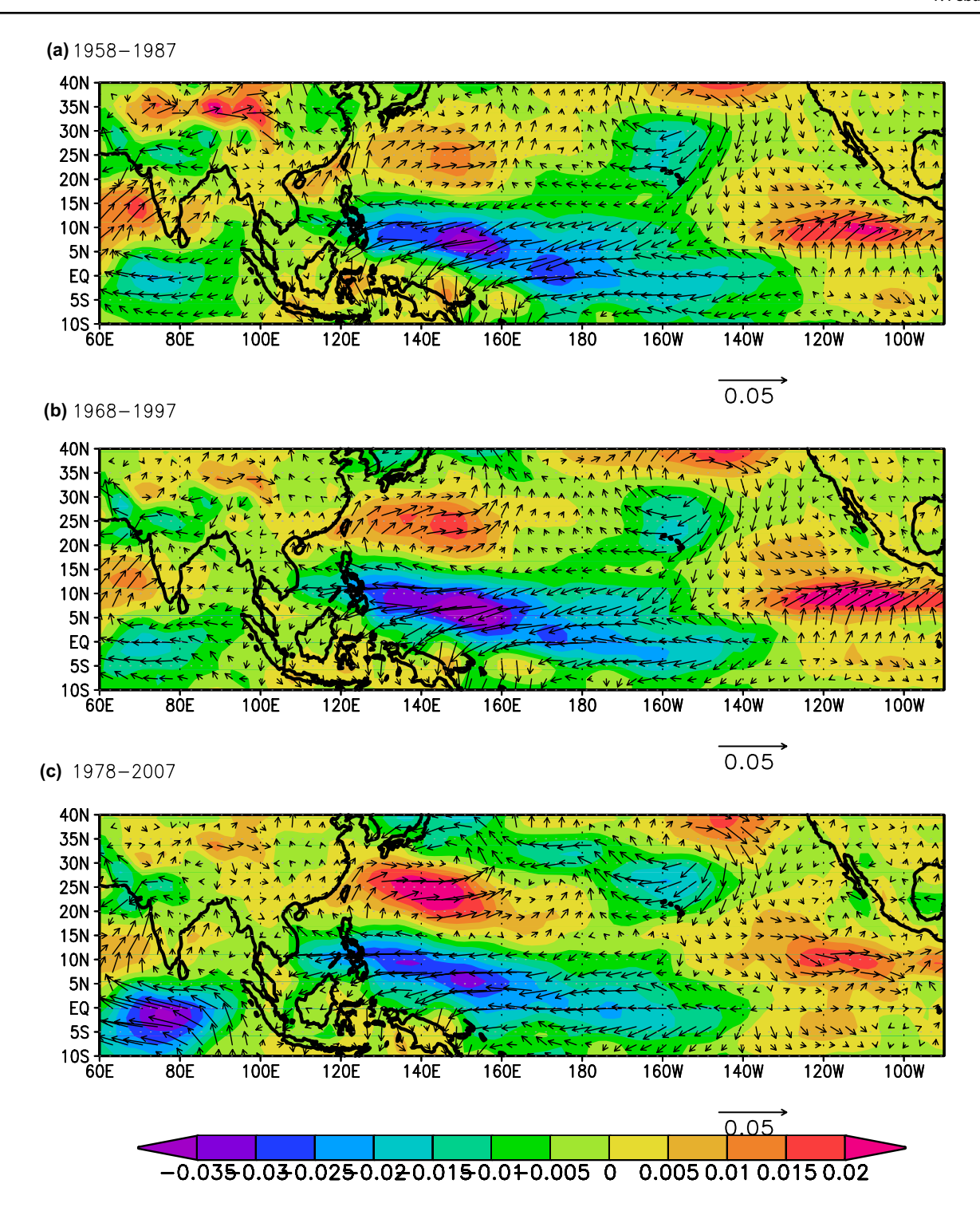


Fig. 4 Regression of ISMR with surface winds (1000 mb) during JJAS (zonal regression in colour)

dependent variable, the regression analysis show similar patterns, we find that this link over the whole period is mainly being contributed only from the early period. We notice a sudden increase of an apparent relevance of the circulation in TIO during 1978–2007 (Fig. 5c).

We also find strong regression vectors in western Pacific at 25°N (Figs. 4c, 5c) (Krishnamurthy and Krishnamurthy 2017). Some studies show that there is a westward shift of subtropical high (Hu 1997; Gong and Ho 2002; Zhou et al. 2009; Mujumdar et al. 2012; Preethi et al. 2016), we believe



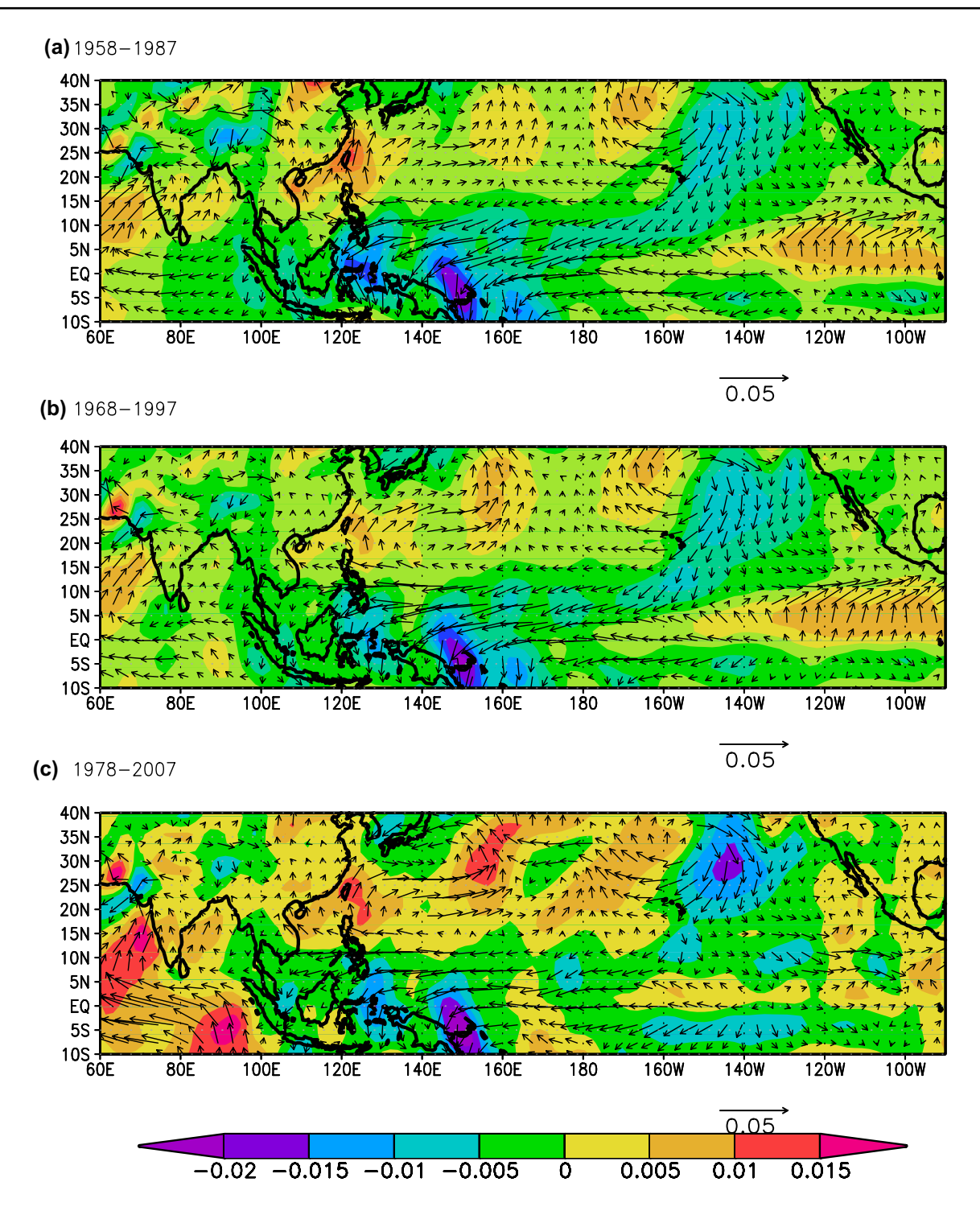


Fig. 5 Regression of ISMR with surface winds (1000 mb) during JJAS (meridional correlations in colour)

this shift might be arising mainly due to this westward intensification of subtropical high. This suggests a paramount relevance of the changes in the circulation over the western Pacific region for the weakening of the ENSO teleconnections to the ISMR. Indeed, a difference plot (Fig. 6) obtained by subtracting the regressions for the 1958–2008 from the

recent decades of 1978–2008 indicate a strenghtening in the cyclonic correlation/regression vectors associated with ISMR south-east of Japan in the recent period. In this context, it is pertinent to recall the Figs. 7 and 8 of a seminal study by Lau and Nath (2000) figure which shows an anticyclone southeast of Japan and an anomalous cyclone



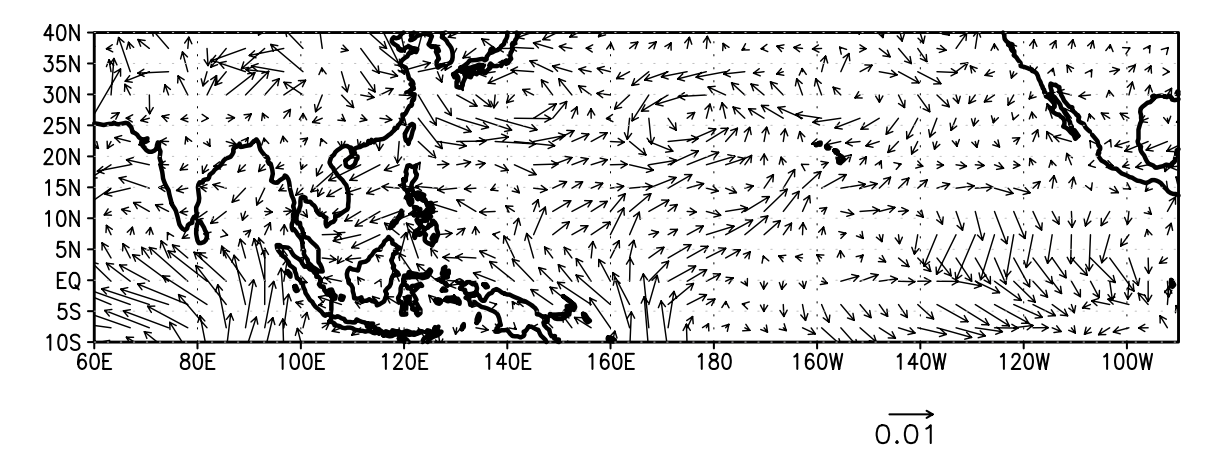


Fig. 6 Difference of regression of ISMR with surface winds (1000 mb) during 1978–2008 from 1958–2008 (51 years)

over the Bay of Bengal and the Indian region during boreal summer months in El Nino years. Evidently, the weakening of this anticyclonic circulation (or rather strengthening of the cyclonic circulation) associated with ISMR effectively weakened the ENSO-ISMR links.

Interestingly, the correlations shown in Figs. 2, 3, 4 and 5 also suggest a low level cross-equatorial strenghtening of the regression vectors over TIO. cross-equatorial circulation over the TIO and Bay of Bengal regions during 1978–2007 period as compared to the previous decades, along with the correspondingly strengthened cyclonic circulation southeast of Japan. The winds over TIO seem to have a north easterly directional shift post 1970s. The cross-equatorial flow which was limited to the west of the TIO has broadened eastwards, basin wide, along TIO. A further investigation into this shows that the variability of Mascarene High is relatively more relevant to the ISMR variability in the recent decades. The standard deviation of an SLP-based Mascarene high index (25°S:35°S; 40°E:90°E) for the 1978-2008 is 6.68% higher than that for the 1951–2008 period, suggesting that there is a decadal change in the Mascarene High strength, and consequently the associated circulation (Auxilliary Figs. 2 and 3). We believe that this has resulted in the observed relatively stronger association of monsoon rainfall with the cross-equatorial low level circulation in TIO in the recent decades. While further examination of this aspect is beyond the scope of the current study, it will be worth investigating a mechanism for this apparent decadal variability of Mascarene High.

4 Conclusion and discussion

Irrespective of the choice of the indices, the teleconnections of Pacific and ISMR seem to weaken, though WWV still has significance. WWV has a lead prediction skill

during pre-monsoon season and the highest correlation was found to be during FMAM.

Our study shows that there is a shift in the mean state of winds in the recent period of 1978-2007 (Fig. 5). Particularly, the winds over north western Pacific show an cyclonic intensification during the same period. There is a weakening of an anticyclonic circulation correlation vectors south-east of Japan which connected ENSO to ISMR. A simultaneous strengthening of an cross-equatorial circulation in TIO as compared to the pre-1977 periods is also observed. An increased relevance of the cross-equatorial flow due to the decadal variability of Mascarene High. This is opposite to the circulation over Eastern TIO associating El Nino with ISMR. Such a change in the background state apparently disrupts the teleconnections of the ENSO impact which results in weakening of the ENSO connections. We have verified these apparent decadal changes by analysing the ERA-20C circulation datasets (figures not shown).

All this suggests that a shift in the ISMR associated surface wind circulation in recent decades over the Indo-Pacific region which weakens the El Niño transfer mechanism in recent decades. We also plan to reconfirm the results reported in the current work through analysis of various CMIP5 model outputs and by conducting some dynamical simulations.

Acknowledgements We express our sincere gratitude to Profs. In-Sik Kang and Raghu Murtugudde for their valuable suggestions and Dr. Michael McPhaden for his suggestions in improving this manuscript, at the CLIVAR-2016 conference. We also thank three unknown reviewers for their comments on an earlier version of the manuscript. Figures in this study were generated using the GrADs software from IGES/COLA, USA. For data manupulation, we used CDO of Max Planck Institute for Meteorology and NCL. We also acknowledge Council of Scientific and Industrial Research (CSIR) for the Junior Research Fellowship.



References

- Annamalai H, Hamilton K, Sperber KR (2007) The South Asian summer monsoon and its relationship with ENSO in the IPCC AR4 simulations. J Clim 20(6):1071–1092. https://doi.org/10.1175/JCLI4035.1
- Ashok K, Saji NH (2007) On the impacts of ENSO and Indian Ocean dipole events on sub-regional Indian summer monsoon rainfall. Nat Hazards 42(2):273–285. https://doi.org/10.1007/s11069-006-9091-0
- Ashok K, Guan Z, Yamagata T (2001) Impact of the Indian Ocean dipole on the relationship between the Indian monsoon rainfall and ENSO. Geophys Res Lett 28(23):4499–4502. https://doi.org/10.1029/2001GL013294
- Ashok K, Chan W-L, Motoi T, Yamagata T (2004) Decadal variability of the Indian Ocean dipole. Geophys Res Lett 31:L24207. https://doi.org/10.1029/2004GL021345
- Ashok K, Behera SK, Rao SA, Weng H, Yamagata T (2007) El Niño Modoki and its possible teleconnections. J Geophys Res 112:C11007. https://doi.org/10.1029/2006JC003798
- Ashok K, Sabin TP, Swapna P, Murtugudde RG (2012) Is a global warming signature emerging in the tropical Pacific? Geophys Res Lett 39:L02701. https://doi.org/10.1029/2011GL050232
- Ashok K, Nagaraju C, Sengupta A, Pai S (2014) Decadal changes in the relationship between the Indian and Australian summer monsoons. Clim Dyn 42:1043–1052. https://doi.org/10.1007/s00382-012-1625-4
- Carton JA, Giese BS (2008) A reanalysis of ocean climate using simple ocean data assimilation (SODA). Mon Weather Rev 136:2999–3017. https://doi.org/10.1175/2007MWR1978.1.
- Cash BA, Barimalala R, Kinter JL, Altshuler EL, Fennessy MJ, Manganello JV et al. (2017) Sampling variability and the changing ENSO-monsoon relationship. Clim Dyn 48(11–12):4071–4079. https://doi.org/10.1007/s00382-016-3320-3
- Chang CP, PHarr, J Ju (2001) Possible roles of atlantic circulation on the weakening Indian monsoon rainfall-ENSO relationship. J Clim 14(11):2376–2380. https://doi.org/10.1175/1520-0442(2001)014<2376:PROACO>2.0.CO;2
- Choi J, Il An S, Yeh SW (2012) Decadal amplitude modulation of two types of ENSO and its relationship with the mean state. Clim Dyn 38(11–12):2631–2644. https://doi.org/10.1007/s00382-011-1186-y
- DelSole T, Shukla J, 2012: Climate models produce skillful predictions of Indian summer monsoon rainfall. Geophys Res Lett. https://doi.org/10.1029/2012GL051279
- Gershunov A, Schneider N, Barnett T (2001) Low-frequency modulation of the ENSO-Indian monsoon rainfall relationship: signal or noise?. J Climate 14:2486-2492. https://doi.org/10.1175/1520-0442(2001)014<2486:LFMOTE>2.0.CO;2
- Gong D, Ho C (2002) Shift in the summer rainfall over the Yangtze River valley in the late 1970s. Geophys Res Lett 29(10):1436. https://doi.org/10.1029/2001GL014523
- Horii T, Ueki I, Hanawa K (2012) Breakdown of ENSO predictors in the 2000s: decadal changes of recharge/discharge-SST phase relation and atmospheric intraseasonal forcing. Geophys Res Lett 39(10):2–6. https://doi.org/10.1029/2012GL051740
- Hu Z-Z (1997) Interdecadal variability of summer climate over East Asia and its association with 500 hPa height and global sea surface temperature. J Geophys Res 102(D16):19403–19412. https://doi.org/10.1029/97JD01052
- Jadhav J et al (2015) On the possible cause of distinct El Niño types in the recent decades. Sci Rep 5:17009. https://doi.org/10.1038/ srep17009
- Kalnay E et al (1996) The NCEP/NCAR 40-year reanalysis project

- Kawamura R, Uemura K, Suppiah R (2005) On the recent change of the Indian summer monsoon-ENSO relationship. SOLA 1:201–204. https://doi.org/10.2151/sola.2005-052
- Keshavamurthy RN (1982) Response of the atmosphere to sea surface temperature anomalies over the equatorial Pacific and the teleconnections of the Southern Oscillation. J Atmos Sci 39:1241–1259
- Kripalani RH, Kulkarni A (1997a) Climatic impact of El Nino/ La Nina on the Indian monsoon: a new perspective. Weather 52:39–46. https://doi.org/10.1002/j.1477-8696.1997.tb06267.x
- Kripalani RH, Kulkarni A (1997b) Rainfall variability over South–East Asia—connections with Indian monsoon and ENSO extremes: new perspectives. Int J Climatol 17(11):1155–1168. https://doi.org/10.1002/(SICI)1097-0088(199709)17:11<1155::AID-JOC188>3.0.CO:2-B
- Kripalani RH, Oh JH, Kulkarni A, Sabade SS, Chaudhari HS (2007) South Asian summer monsoon precipitation variability: coupled climate model simulations and projections under IPCC AR4. Theor Appl Climatol 90(3–4):133–159. https://doi.org/10.1007/ s00704-006-0282-0
- Krishnamurthy V, Kirtman BP (2003) Variability of the Indian Ocean: relation to monsoon and ENSO. Q J R Meteorol Soc 129(590):1623–1646. https://doi.org/10.1256/qj.01.166
- Krishnamurthy L, Krishnamurthy V (2017) Indian monsoon's relation with the decadal part of PDO in observations and NCAR CCSM4. Int J Climatol 37:1824–1833. https://doi.org/10.1002/joc.4815
- Kug J-S, Kang I-S (2006) Interactive feedback between the Indian Ocean and ENSO. J Clim 19:1784–1801
- Kumar KK, Rajagopalan B, Cane MA (1999) On the weakening relationship between the Indian Monsoon and ENSO. Science 284(5423):2156–2159. https://doi.org/10.1126/science.284.5423.2156
- Kumar KK, Rajagopalan B, Hoerling M, Bates G, Cane M (2006) Unraveling the Mystery of Indian Monsoon Failure During El Niño. Science 314:115–119. https://doi.org/10.1126/science.1131152
- Lau NC, Nath MJ (2000) Impact of ENSO on the variability of the Asian-Australian monsoons as simulated in GCM experiments. J Clim 13:4287–4309. https://doi.org/10.1175/1520-0442(2000)013<4287:IOEOTV>2.0.CO;2
- Marathe S, Ashok K, Swapna P, Sabin TP (2015) Revisiting El Niño Modokis. Clim Dyn. https://doi.org/10.1007/s00382-015-2555-8
- McPhaden MJ, Zebiak SE, Glantz MH (2006) ENSO as an integrating concept in earth science. Science 314(5806):1740–1745. https://doi.org/10.1126/science.1132588
- Meinen CS, McPhaden MJ (2000) Observations of warm water volume changes in the equatorial Pacific and their relationship to El Niño and La Niña. J Clim 13:3551–3559
- Mujumdar M, Preethi B, Sabin TP, Ashok K, Sajjad S, Pai DS, Krishnan R (2012) The Asian summer monsoon response to the La Niña event of 2010. Meteorol Appl 19:216–225. https://doi.org/10.1002/met.1301
- Navarra A, Ward MN, Miyakoda K (1999) Tropical-wide teleconnection and oscillation. I: teleconnection indices and type I/type II states. Quart J Roy Meteor Soc 125:2909–2935
- Parthasarathy B, Munot AA, Kothawale DR (1994) All-India monthly and seasonal rainfall series: 1871–1993. Theor Appl Climatol 49:217–224
- Preethi B, Mujumdar M, Kripalani RH, Prabhu A Krishnan R (2016) Recent trends and tele-connections among South and East Asian summer monsoons in a warming environment. Clim Dyn https:// doi.org/10.1007/s00382-016-3218-0
- Rajeevan M, McPhaden MJ (2004) Tropical Pacific upper ocean heat content variations and Indian summer monsoon rainfall. Geophys Res Lett 31(18):L18203. https://doi.org/10.1029/2004GL020631



- Rasmusson EM, Carpenter TH (1983) The relationship between eastern equatorial Pacific sea surface temperature and rainfall over India and Sri Lanka. Mon Weather Rev 111:517–528
- Rayner NA, Parker DE, Horton EB, Folland CK, Alexander LV, Rowell DP, Kent EC, Kaplan A (2003) Global analyses of sea surface temperature, sea ice, and night marine air temperature since the late nineteenth century. J Geophys Res 108(D14):4407. https://doi.org/10.1029/2002JD002670
- Saravanan R, Chang P (2000) Interaction between tropical atlantic variability and El Niño—southern oscillation. J Clim 13(13):2177–2194. https://doi.org/10.1175/1520-0442(2000)013<2177:IBTAV A>2.0.CO:2
- Sikka DR (1980) Some aspects of the large scale fluctuations of summer monsoon rainfall over India in relation to fluctuations in the planetary and regional scale circulation parameters. Proc Indian Acad Sci Earth Planet Sci 89:179–195
- Sreejith OP, Panickal S, Pai S, Rajeevan M (2015) An Indian Ocean precursor for Indian summer monsoon rainfall variability. Geophys Res Lett 42:9345–9354. https://doi.org/10.1002/2015G L065950
- Tejavath CT, Ashok K, Chakraborty S, Ramesh R (2018) The ENSO teleconnections to the Indian summer monsoon climate through

- the Last Millennium as simulated by the PMIP3. Clim Past Discuss. https://doi.org/10.5194/cp-2018-7 (in review)
- The NCARC (2017) Language (Version 6.4.0) [Software]. UCAR/NCAR/CISL/TDD, Boulder. https://doi.org/10.5065/D6WD3XH5
- Torrence C, Webster PJ (1999) Interdecadal changes in the ENSOmonsoon system. J Clim 12(8 PART 2):2679–2690. https://doi. org/10.1175/1520-0442(1999)012<2679:ICITEM>2.0.CO;2
- Walker GT, Bliss EW (1932) World weather V. Mem R Meteorol Soc 4:53–84
- Wu R, Li C, Lin J (2017) Enhanced winter warming in the Eastern China coastal waters and its relationship with ENSO. Atmos Sci Lett 18:11–18. https://doi.org/10.1002/asl.718
- Yeh S-W, Kug J-S, An S-I (2014) Recent progress on two types of El Niño: Observations, dynamics, and future changes, Asia-Pac. J Atmos Sci 50:69–81
- Zebiak S, Cane M (1987) A model EI Nino-southern oscillation. Mon Weather Rev 115(1985):2262–2278
- Zhou L et al (2009) Spatial patterns of diurnal temperature range trends on precipitation from 1950 to 2004. Clim Dynam 32:429–440



The Indian summer monsoon rainfall and ENSO

KARUMURI ASHOK, F. FEBA and CHARAN TEJA TEJAVATH

Centre for Earth, Ocean and Atmospheric Sciences, University of Hyderabad, Hyderabad – 500 046, India

e mail: ashokkarumuri@uohyd.ac.in

सार – एल नीनो-दिक्षिणी दोलन (ENSO) को भारतीय ग्रीष्मकालीन मॉनसून परिवर्तनशीलता का सबसे महत्वपूर्ण चालक माना जाता है। इस पत्र में हमने भारतीय ग्रीष्मकालीन मानसून पर ENSO के प्रभावों पर अब तक के शोध और विभिन्न तंत्र जो उष्णकिटबंधीय प्रशांत से मॉनसून क्षेत्र में टेली-कनेक्शन को समझाने के लिए प्रस्तावित किए गए हैं, उनका दस्तावेजीकरण करने का प्रयास किया गया है। यहाँ हमने मोडोकी और कैनोनिकल एल नीनो के प्रभावों के बारे में भी संक्षेप में चर्चा की हैं। हमारा मानना है कि मॉनसून पर हाल में एन्सो (ENSO) के आंशिक रूप से कमजोर पड़ने से जो प्रभाव पड़ा वह कई अंतर-वार्षिक से दशकों की प्रक्रियाओं के कारण हो सकता है, जैसा 2015 के दौरान कमजोर मॉनसून की स्थिति और चरम एल-नीनो के एक साथ होने के परिणामस्वरूप हुआ।

ABSTRACT. The El Niño-Southern Oscillation (ENSO) is deemed as the most important driver of the Indian summer monsoon variability. In this paper we make an effort to document the research so far on the impacts of ENSO on the Indian summer monsoon and the various mechanisms that have been proposed to explain the tele-connection from the tropical Pacific to the monsoon region. We also briefly discuss about the distinctions between impacts of canonical El Niño and El Niño Modoki. We believe that the recent apparent weakening of the ENSO impact on the monsoon may simply be due to a combination of several inter-annual to decadal processes, as evidence by the deficit monsoon conditions during 2015 which co-occurred with an extreme El Niño.

Key words – Indian Summer Monsoon, El Niño, ENSO, El Nino Modoki.

1. Introduction

The Indian Summer Monsoon (ISM) has been the focus of considerable fascination for a long time. Agriculturists have revered and seafaring traders and sailors have depended on the ISM since centuries. The scientific allure of ISM probably might have started with Henry Blandford and Sir Gilbert Walker with their early attempts at ISM observations and prediction (Blandford, 1884, 1886; Walker, 1923, 1924, 1928). The Indian Meteorological Department (IMD) has been studying and predicting ISM for over 100 years now. Importantly, Walker's attempts to find lead predictions skills for the Indian summer monsoon rainfall have resulted in the discovery of what has been later known as the Southern Oscillation, the atmospheric component of the El Niño-Southern Oscillation (ENSO). Incidentally, ENSO is known as the strongest driver of the Indian summer monsoon rainfall variability.

The present manuscript is divided into five sections. Sections 2 and 3 provide brief introductions to ISM and ENSO. Section 4 describes the relationship between ISM-ENSO, followed by a discussion is in Section 5.

For the few figures presented in this general review note, IMD gridded rainfall data for Indian regional/sub-divisional Monthly Rainfall are used (Rajeevan *et al.*, 2006). We also use the Met Office Hadley Centre Sea Ice and Sea Surface Temperature dataset (HadISST; Rayner *et al.*, 2003).

2. Indian summer monsoon

Monsoon is an Arabic term, which, it is believed, to have been derived from the Arabic/Persian word 'Mausam', alluding to a seasonal reversal of winds. Therefore, it is not surprising that Ramage, in the year 1971, defined a few characteristics of monsoonal regions, mainly based on the kinematic consideration of the winds (Ramage, 1971). Summed up, the four criteria talk about seasonal reversal, persistence, sufficient strength. Having said this, a critical component that is missing from the definition is the rainfall, which is not only important for societal purposes, but plays a major role in monsoonal dynamics and variability (Rao, 1976). The onset of ISM is in the first week of June over Kerala coast associated with northward shift of the Sub Tropical Jet (Yin, 1949). The onset is also dependent on other factors, like warming of Eurasian region by diabatic

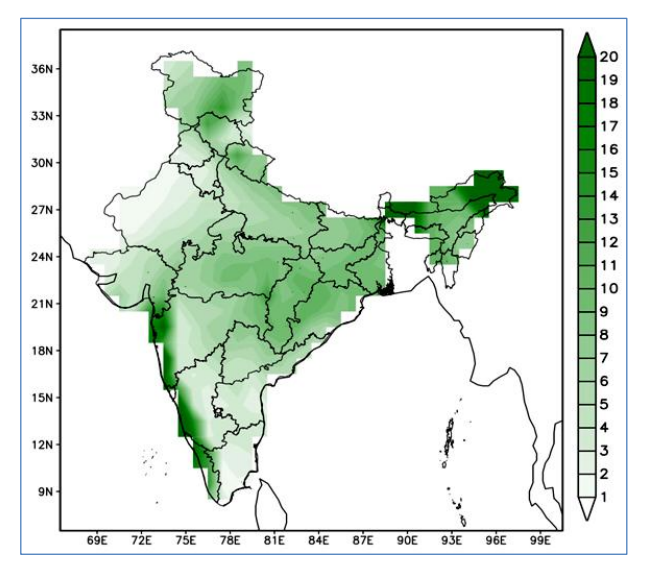


Fig. 1. Climatological distribution of the Mean summer monsoon (JJAS) rainfall (mm/day) during the 1901-2009 period

heating (Murakami and Ding, 1982) or the dynamical influences of Tibetan Plateau (Yanai et al., 1992; Yanai et al., 2006). From June to September, ISM remains over India as a stationary wave (Goswami and Shukla, 1984). ISM rainfall shows great spatial variability (Fig. 1) with highest rainfall along the western coast of India, due to the orographic effects and over the head of Bay of Bengal with a northwest-ward stretch along the monsoon trough. This northwestward stretching region is called the Monsoon Zone (Sikka and Gadgil, 1980). There are several publications and reports that have characterized the mean monsoonal features and variability. Rao (1976), Pant and Kumar (1997) and the Monsoon Monograph series (Tyagi et al., 2012) provide excellent summaries of all these aspects.

The interannual variability of an area-averaged ISM rainfall index is shown in Fig. 2. It has a 10% standard deviation (Gadgil, 2003). Contributions from various Sea Surface Temperature (SST) anomalies, particularly the tropical pacific, affect the ISM resulting in a prominent interannual variability (Fig. 3). The interannual variability of ISM shows about 10% standard deviation from the mean (Gadgil, 2003). ENSO is one of the primary drivers of ISM, accounting for about 40% of its interannual variability (Sikka, 1980; Keshavamurty, 1982; Shukla and Paolina, 1983; Rasmussen and Carpenter, 1983). Along with ENSO, drivers from other tropical oceans, such as strong Indian Ocean Dipole (IOD; Webster et al., 1999; Saji et al., 1999; Murtugudde et al., 2000) events also affect ISM interannual variability. Strong IOD events modulate the effects of any co-occurring ENSO on ISM (Ashok et al., 2001; Ashok and Saji, 2007). Furthermore, Atlantic is also receiving attention as a driver of the Indian

summer monsoon rainfall Kucharski *et al.*, 2008; Pottapinjara *et al.*, 2015; Yadav, 2017). Of all these, ISM-ENSO relationship naturally demands a weighty attention.

3. The El Nino - Southern Oscillation

Due to various reasons beyond the scope of the current manuscript, in some years, we find a large-scale anomalous warming in the tropical eastern Pacific Ocean, associated with anomalous cooling in the tropical western pacific, causing widespread ramifications globally. This anomalous condition, normally seasonally phase locked from boreal spring through ensuing boreal winter when it peaks, is referred to as an El Niño. As mentioned earlier, this oceanic signature of the ENSO is strongly coupled to the anomalous changes in the associated see-saw of sea level pressure between the equatorial eastern and western Pacific Ocean, referred to as the Southern Oscillation (Bjerkenes, 1969). A positive SST anomaly in the equatorial eastern Pacific reduces the east-west thermal gradient, weakening the trade winds and thereby the Walker circulation (Gill, 1980; Lindzen and Nigam, 1987). The weaker trades further enhance the warming and this form a positive ocean-atmosphere feedback causing a very warm state - The El Niño. Conversely, a cold phase, with cooler than normal SST anomalies in the equatorial eastern pacific strengthens the trade winds and the Walker circulation - The La Niña (Philander, 1985, 1990).

ENSO, to a significant extent, can be deemed as a self-sustaining positive ocean-atmosphere feedback. The delayed oscillator theory explains that the Rossby waves generated in the eastern Pacific propagate west and reflect from the western boundary returning as Kelvin waves and reverse ENSO effect (Zebiak and Cane, 1987; Suarez and Schopf, 1988; Battisti and Hirst, 1989). From another perspective, the divergence by Sverdrup transport discharges the equatorial heat content which gets recharged by climatological upwelling. This is known as the recharge-discharge oscillator theory (Jin, 1997a). Another hypothesis is that off-equatorial SST anomalies induce equatorial easterly wind anomalies (off-equatorial anomalous anticyclones), causing upwelling and subsequent cooling. This mechanism is called the western Pacific oscillator mechanism (Weisberg and Wang, 1997; Wang et al., 1999). In addition, external land heating and interaction with the previous coupled anomalies play a role (Masumoto and Yamagata, 1991).

In addition to the well-known canonical El Niño, a new type of El Niño with anomalous warming in the central tropical pacific straddled by cooling of SST anomalies on its both flanks, have been occurring with increased frequency since mid-1970s (Ashok *et al.*, 2007;

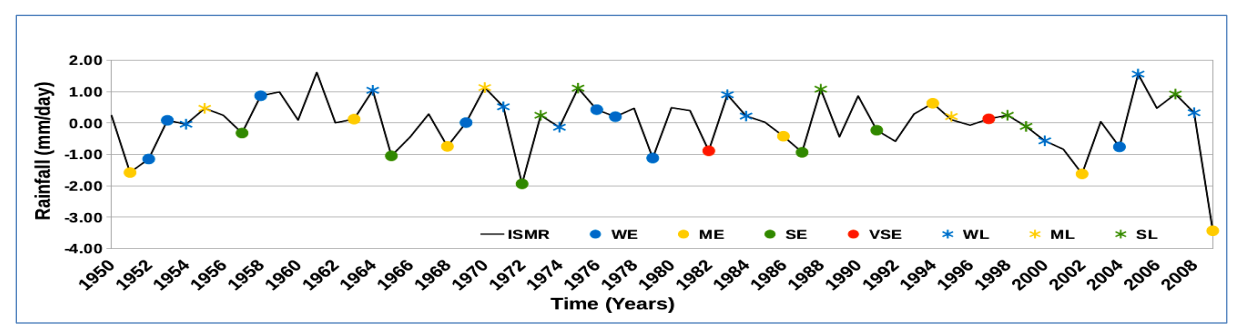


Fig. 2. The interannual variability of the Indian summer rainfall area-averaged over the Indian land region (66.5° E-101.5° E; 6.5° N-39.5° N) during the 1951-2009 period. Here WE, ME, SE and VSE stand for weak, moderate, strong and very strong El Niños, respectively; WL, ML and SL stand for Weak, Moderate and Strong La Ninas, respectively, as per https://ggweather.com/enso/oni.htm

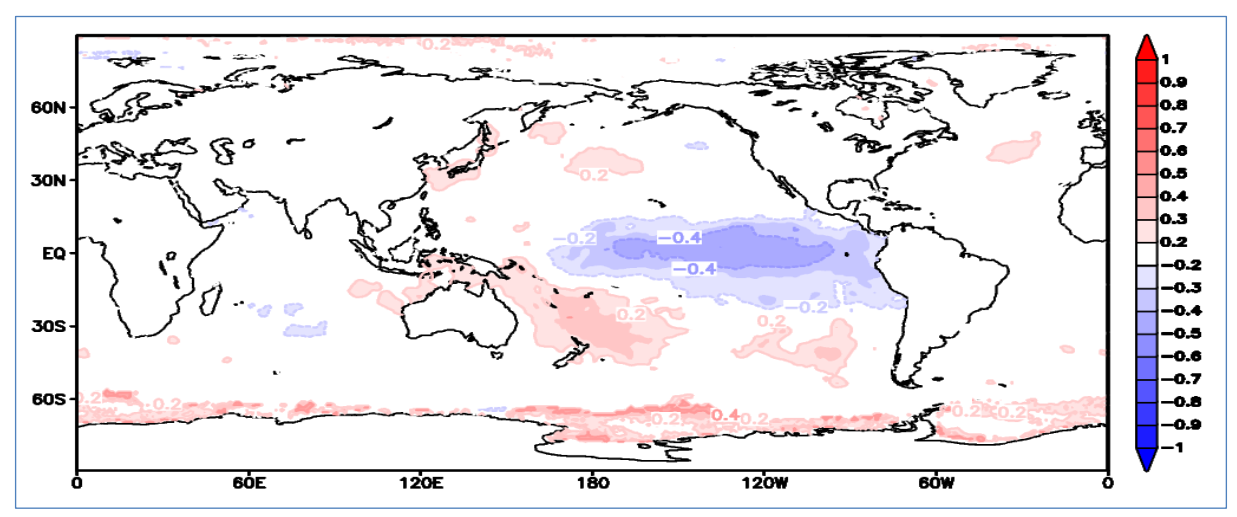


Fig. 3. Simultaneous linear correlation between the Indian summer monsoon rainfall index with the JJAS SST for the 1901-2009 period. Only significant correlation values have been plotted (±0.20 is the 0.05 significance level from a 2-tailed Student's *t*-test)

Kao and Yu, 2009; Kug et al., 2009; Marathe et al., 2015). These events, which occurred recently are seasonally phase-locked from boreal summer through ensuing winter and are named as the El Niño Modoki. Furthermore, the location of the heat source has relevance on the domain of its impacts (Matsuno, 1966; Gill, 1980; Keshavamurty, 1982; Soman and Slingo, 1987; Larkin and Harrison, 2005; Annamalai and Liu, 2005). This is particularly applicable to the ISM as well, as would be discussed later. Therefore, a study of ISM-ENSO dynamics and its variability is incomplete without considering El Niño Modoki.

3.1. ENSO impacts on the Indian summer monsoon and mechanisms

Most of severe summer monsoon droughts over India are associated with the El Niño events. However, as Rajeevan (Monsoon Monographs, Ed. Tyagi *et al.*, 2012) mentions, there is no one-to-one relationship between them. On the simplest terms, El Niño events show a

propensity to be associated with a weaker than normal summer monsoon rainfall over India, while the La Niña events with a greater than normal rainfall, as indicated by several studies. The relationship between ISM and ENSO, has been studied extensively for the past few decades (Sikka, 1980; Keshavamurty, 1982; Shukla and Paolina, 1983; Rasmussen and Carpenter, 1983; Ropelewski and Halpert, 1987; Webster and Yang, 1992; Nigam, 1994; Ju and Slingo, 1995; Yang, 1996; Zhang et al., 1996; Kawamura, 1998; Navarra et al., 1999; Slingo and Annamalai, 2000; Lau and Nath, 2000; Wang, 2000; Ashok et al., 2004; Ashok and Saji, 2007). Fig. 4 shows the simultaneous linear correlations between the NINO3.4 index¹ and local rainfall anomalies over India during June-September (JJAS), the summer monsoon season. It is seen that most of the correlations are negative, implying that the anomalously warm conditions during boreal summer

 $^{^1}$ NINO3.4 Index: defined as the area-averaged SST anomaly over the region bounded by 170° W-120° W; 5° S-5° N, which is used to represent the ENSO variability.

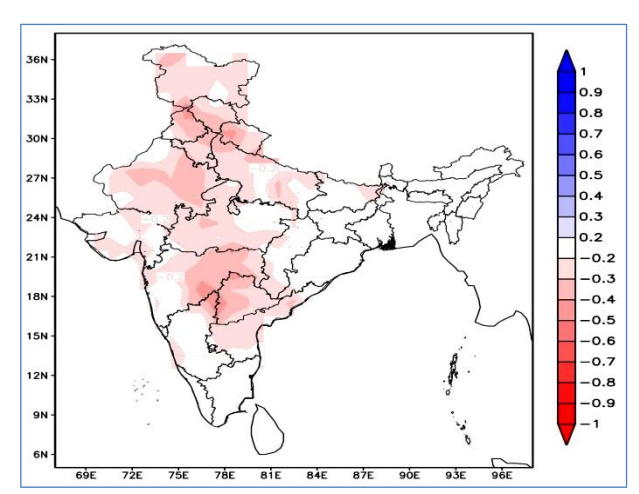


Fig. 4. Simultaneous linear correlations between Niño3.4 index with the JJAS rainfall for the period of CE1901-2009. Only significant correlation values have been plotted (±0.20 is value for 0.05 significance level from a 2-tailed Student's *t*-test)

over the eastern tropical pacific can result in anomalously deficit rainfall over India during summer monsoon season. However, Kumar et al. (2006) suggest that the El Niño Modoki events reduce the ISM rainfall more effectively than the conventional El Niño. From linear considerations, there is an apparent propensity for the canonical El Niños to be associated with negative rainfall anomalies along the monsoon trough, while the Modoki El Niños cause anomalously deficit rainfall more in the peninsular India (Figs. 5 & 6 from Ashok et al., 2007; Amat and Ashok, 2018). The composite rainfall anomalies shown in Fig. 5 indeed give a qualitative indication that Modoki El Ninos are not associated with negative rainfall anomalies along the monsoon trough. This conforms to results from various AGCM experiments (Ashok et al., 2009; Chen and Tam, 2010) etc.

Further, for the first time, a hitherto unnoticed anomalous basin wide warming across the tropical pacific has occurred in the tropical pacific during JJAS season of 2009, which collapsed the Walker circulation across the basin (Ashok *et al.*, 2012). AGCM experiments suggest that the severe drought observed over India that season was associated with this warming (Ratnam *et al.*, 2010; Ashok *et al.*, 2012). The year 2014 also experienced similar conditions in the tropical pacific and at least partially responsible for the anomalous dry conditions during summer monsoon season (Jadhav *et al.*, 2015).

Several mechanisms have been proposed to explain the ENSO impact on the ISM. This section revisits some of the mechanisms and attempts to introduce some outstanding issues. The suggested mechanisms to explain the ENSO teleconnections could be broadly classified into two groups.

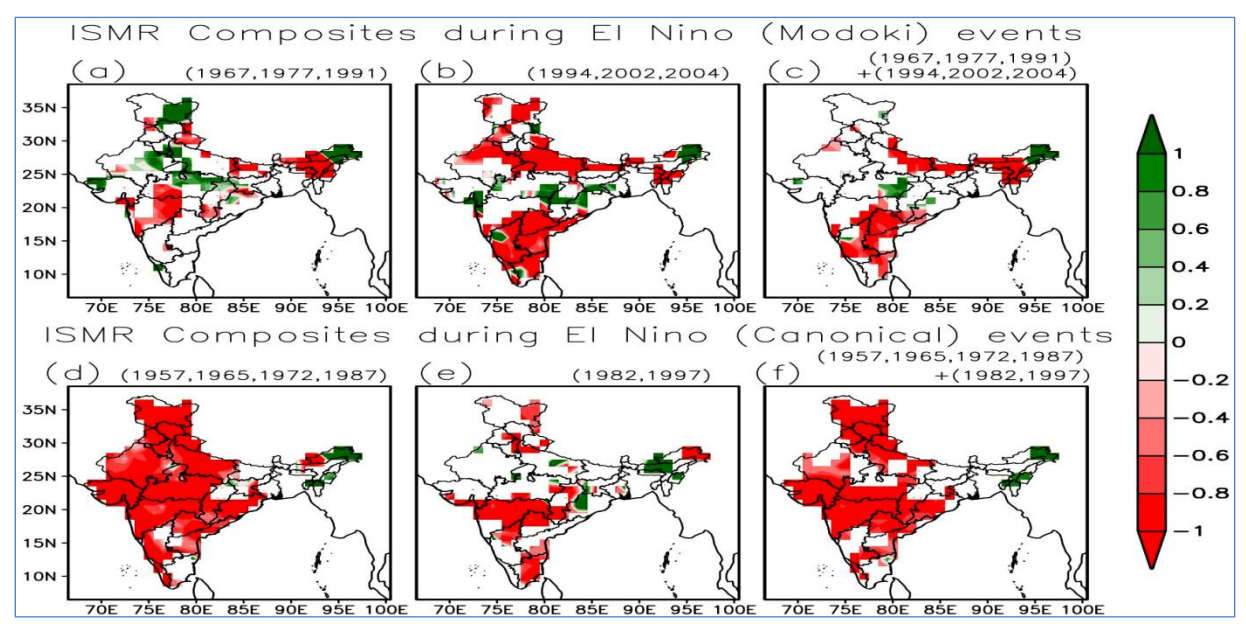
3.1.1. The Walker and Hadley cell connections

Given the intimate connection between the tropical pacific SST with the Walker circulation/southern oscillation, it is reasonable to consider that a mechanism of how the SST changes in the eastern tropical pacific transmit into the Indian summer monsoon region involves through a Walker circulation changes. Bhalme and Jadhav (1984), analyzing Indian rainfall datasets for the 1875-1980 period, reported a drier Indian Ocean and large monsoon rainfall deficiency occurring concurrently with weak Walker circulations. Shukla and Paolino (1983), through an analysis of Indian summer monsoon rainfall of and the Darwin pressure associated intimately with ENSO datasets for the 1901-1950, suggested that an anomalously high (low) Darwin pressure coincides with anomalously low (high) monsoon rainfall. Pant and Parthasarathy (1981 also have documented the relevance of the southern oscillation changes for the Indian summer monsoon.

Webster *et al.* (1998) indicated that boundary anomalies, such produced by ENSO, produce a temporally persistence and spatially large-scale descent over the Indian monsoon region, reducing rainfall either by producing a displacement of the seasonal mean rainfall patterns. All these studies imply that changes in the Walker Circulation with ENSO are considered to affect the ISM.

Atmospheric GCM experiments by Keshavamurty (1982); Palmer et al. (1992); Shukla and Wallace (1983); Navarra et al. (1999); Ju and Slingo (1995); Soman and Slingo (1997); Dai and Wigley, 2000; Ashok et al. (2004), etc. demonstrate that the tropical pacific SST anomalies associated with ENSO indeed influence the Indian summer monsoon through modulation of zonal circulation cells. Broadly, these studies suggest that large scale circulation changes due to eastward (westward) shift of Walker Circulation and decreased (increased) equatorial divergence over the tropical Indian Ocean during El Niño (La Niña) years. The anomalous convergence in the tropical Indian Ocean results in the modulation of the cross-equatorial meridional circulation, which causes an anomalous divergence over the Indian region and thereby a drier (wetter) than normal ISM. Indeed, this type of signals can be seen in the Indian region and the Indian Ocean to its south, in years such as 1987 (Ashok et al., 2001) when the El Niño event does not co-occur with any other tropical oceanic climate driver such as the strong IOD - which can interfere with the anomalous signal of ENSO.

Among these studies, Keshavamurty (1982) and several others explore the relative importance of anomalous signals in the western, central and eastern



Figs. 5(a-f). Composited anomaly correlations of the rainfall during (a) Moderate El Niño Modokis (b) strong El Niño Modokis (c) all El Niño Modokis. Figs. (d-f) are similar to Figs. (a-c) respectively, except that these are all for canonical El Niño events. The events have been selected based on the classification of the El Niño types by Marathe *et al.* (2015). Only statistically significant values have been plotted. For panels (a), (b), (d), (e) significance level is fixed at 0.2 and for (c), (f) significance level is fixed at 0.1 from a one-tailed Student's t-test

tropical pacific for the Indian summer monsoon variability. Further, local coupled air-sea feedback in the Indian Ocean is suggested to condition the ENSO impacts on the ISM (Wu and Kirtman, 2004).

3.1.2. ISM-ENSO: Impacts through extratropics and upper atmosphere

Suggesting a different mechanism, Ju and Slingo (1995) noted that weak ISM years are associated with an increased upper-level westerlies. This is associated with the latitudinal shift in the position of the subtropical westerly jet over northern India influenced by Pacific SST anomalies. AGCM studies by Krishnan et al. (1998) indicate that, in addition to the Walker circulation changes introduced by ENSO and ensuing and Hadley cell modulations, the anomalous ENSO divergent forcing over the tropical Pacific Ocean can act as a potential source for Rossby wave dispersion. Furthermore, Krishnan et al. (2009) suggest that meridionally propagating Rossby waves, which emanate from the El Niño forcing region, interact with the subtropical westerlies and generate quasistationary anomalous highs and lows in the subtropics and extratropics over west Asia, Pakistan and northwest India during drought years co-occurring with El Niños.

According to Wang *et al.* (2000), during El Niño years, as a Rossby response to the SST anomalies in the western tropical pacific, an anomalous anti-cyclonic

pattern appears from the Philippine Sea through the core Indian summer monsoon region, teleconnections.

As far as the El Niño Modoki is concerned, AGCM experiments (Ashok *et al.*, 2009) suggest that during the, an anomalous convergence zone is seen in the Philippines Sea region associated with these events as a Rossby response to the anomalous warming in the neighboring central tropical pacific (Chen and Tam, 2010); this not only exacerbates the local typhoon frequency (Chen and Tam, 2010; Pradhan *et al.*, 2011), but also facilitates an east-west out-of-phase precipitation variability over the NW Pacific and the Indian summer monsoon region (Mujumdar *et al.*, 2007) and thereby a drought-like condition in El Niño Modoki years such as 2002 and 2004 in the peninsular India.

Goswami and Xavier (2005) argue that ENSO affects the meridional tropospheric temperature gradient over the Indian region thereby effectively modulating the strength and duration of the monsoon. Shaman and Tziperman (2007) claim that ENSOs affect the upper tropospheric meridional temperature gradient during ISM through the subtropical jet.

Interestingly, (Rajeevan and McPhaden, 2004) suggest that warm water volume over the entire tropical pacific 3-4 months earlier to the monsoon has the highest lead predictive skill for the Indian summer monsoon

rainfall. The decaying ENSO may also be relevant to the following ISM (Choudary *et al.*, 2015; Chakraborty *et al.*, 2018)

3.2. ISM & ENSO - Weakening links or a slow variability?

Kripalani and Kulkarni (1997) suggest a natural decadal variability of the Monsoon and therefore, that the ENSO impacts may not be as strongly perceived in the strong monsoonal epochs as could be in the weaker monsoonal epochs. The ISM-canonical ENSO links have shown a weakening in the recent decades (Kumar et al., 1999; Kawamura et al., 2005) argue that the recent weakening of the ISM-ENSO is in fact, a change in dominance of the spatial correlation pattern, from northwest to northeast after the late 1970s. Background and circulation changes associated with global warming have been proposed as a potential reason for the weakening by Kumar et al. (1999) and Ashrit et al. (2001). Kumar et al. (1999) attribute, through a running correlation analysis, that the weakening observed in late 1990s due to a shift in background circulation associated with global warming. On the other hand, Gershunov et al. (2001) suggest that the monsoon-ENSO relationship is less variable on decadal scales. In other words, even though many physical processes may be partially responsible for the modulation of the interannual correlation, it is not possible to distinguish their effects from stochastic noise in running correlation analyses and therefore, it could just be an issue of sampling (Cash et al., 2017). Having said this, from a predictability point of view, it will indeed be useful to understand if a random interaction with impacts on the monsoon from any other events could be playing a role in such weakening of an interannual variability beyond a few years. Chang et al. (2001) attribute this weakening to the strengthening and simultaneous poleward shift of the jet stream over the North Atlantic region. Ashok et al. (2001, 2004, 2007) indicate that that the apparent ENSO-Monsoon weakening during the late 20th century is due to increased frequency of positive IOD events of 1994 and 1997. This is attributed to the anomalous convergence in the Head Bay of Bengal and neighboring monsoonal trough (Behera et al., 1999; Guan et al., 2003; Rao et al., 2004) induced by the subsidence from the eastern colder-than-normal pole of the positive IOD and that in the northwest portion of the monsoonal trough (Ashok et al., 2004) associated with the modulated meridional circulation owing to the anomalous warm conditions in the western box of the IOD region, this zone of anomalous convergence associated with strong positive IOD events in years such as 1997 results in anomalous surplus rainfall along the monsoon trough and reduces the ENSO influence. On a related note, EQUINOO (Equatorial Indian Ocean Oscillation), an

atmospheric index associated with the IOD, along with an ENSO index, seems to account for most of the interannual variability of the ISM rainfall (Francis and Gadgil, 2013). In addition, as mentioned earlier, the El Niño Modoki events, which have occurred in years such as 1986, 1990, 1991, 1994, 2002 and 2004 summers are also associated anomalously dry conditions over India.

Some studies have also observed the impact of Pacific Decadal Oscillation (PDO) on ISM-ENSO relations (Krishnamurthy and Goswami, 2000; Krishnan and Sugi, 2003; Krishnamurthy and Krishnamurthy, 2014). Krishnamurthy and Goswami (2000) show that during the eastern Pacific warm (cold) phase of the interdecadal SST variation, the regional Hadley circulation associated with El Niño (La Niña) strengthens the prevailing anomalous interdecadal Hadley circulation while that associated with La Niña (El Niño) opposes the prevailing interdecadal Hadley circulation. Therefore, during the warm (cold) phase of the interdecadal oscillation, El Niño (La Niña) events are expected to be strongly related to monsoon droughts while La Niña (El Niño) events may not have a significant relation. Krishnamurthy and Krishnamurthy (2014) propose that the PDO modulates ISM-ENSO relationship by enhancing (counteracting) ENSO effects when in (out of) phase. Sreejith et al. (2015) claim that the reason for the recent monsoon-ENSO weakening is the change in air-sea coupled interactions over the tropical Indian Ocean. A shift in the mean ISM winds, with a cyclone-like intensification over northwestern Pacific is seen in the recent decades (Mujumdar et al., 2012; Feba et al., 2017). Feba et al. (2018) suggest that this decadal cyclonic intensification opposes the anomalous anticyclonic signature associated with the canonical El Niños (Lau and Nath, 2000) and therefore 'disconnects' the impact of the El Niño through this pathway. Interestingly, Feba et al. (2018) also find a simultaneous strengthening of cross equatorial winds over the equatorial Indian Ocean in recent decades in association with the weakening of ISM-ENSO links.

The last millennium climate is supposed to be the nearest to the current day climate, at least prior to 1970s when the anthropogenic warming is dominant. Climate simulations of the PMIP3 vintage are a valuable source to understand the long term variations of the ISM-ENSO links. Tejavath *et al.* (2019), through an analysis of model outputs from nine models, find a multi-decadal through centennial fluctuations in the correlation between an ENSO index with the area-averaged Indian summer monsoon rainfall. Their results show that the simulated interannual ISM-ENSO negative correlations are statistically significant in the two dominant epochs of the last millennium, known as the 'Medieval Warm Period' (CE 950-1350), roughly followed by a relatively cooler

period, the Little Ice Age (CE 1500-1850). Importantly, these correlations are significantly modulated by slow background changes (a multi-centennial modulation), which modulate the anomalous east-west zonal circulation and the meridional circulation in the Indian Ocean-Indian region. Such changes are associated with slow changes in summer monsoon rainfall in various sub-regions of the subcontinent and not necessarily the whole India. This indicates a strong influence in the interplay of various temporal scales, which have implications for impacts at regional level.

4. Discussions

As a community, we can now ascertain that Indian summer monsoon is indeed significantly influenced by the ENSO types on interannual timescales. This relationship is of course subject to impacts from other interannual climate drivers as well as decadal processes and phenomena, which can result in an apparent weakening of the ISM-ENSO links. The important outcome of the studies such as Tejavath (2019) and Kawamura et al. (2005) is that any change in the association may be owing to interannual through centennial processes external to the ENSO-monsoon system. It may be that the apparent weakening is due to a shift in the impacted region, which may not be clear when a rainfall index area-averaged over the whole region is considered. The inherent decadal variability either in the monsoons and/or ENSO can also result in a stochastic weakening of the monsoon-ENSO relationship. This conclusion of course points out to a need to explore if there are mechanisms other than those proposed so far to explain the ENSO impact on monsoons. Importantly, the severe weak monsoon condition in India during 2015 was associated with one of the most extreme El Niño events. This suggests that strong El Niños indeed affect the ISM rainfall. Further, it is not just the occurrence of the ENSO that needs to be predicted with a lead time, but its intensity and, to some extent, its type.

There are studies indicating that the ENSO events can influence the intraseasonal processes of the ISM. For example, as per Joseph (2014), during a co-occurring El Niño year, the low level Jet stream can be modulated to extend eastwards up to the date line creating an area of shallow ocean mixed layer there, which in turn is proposed to lengthen the active-break cycle to two months in an El Niño year. Webster *et al.* (1998) summed up that seasonally persistent ENSO-induced boundary anomalies and spatially large-scale descent over the Indian monsoon region, reduce rainfall either by reducing the intensity and life cycle of the monsoon disturbances or by producing a displacement of the seasonal mean rainfall patterns. Discussing these scale interactions and time scales higher

than interannual teleconnections is beyond the scope of the current note.

There are several other topics relevant to the association of the ENSO with the Indian monsoons, such as the impact of the Indian summer monsoon on the ENSO (Krishnamurthy and Goswami, 2000; Kirtman and Shukla, 2006), which have not been discussed in this note. For example, the tropical pacific SST indices exhibit a positive correlation with the northeastern monsoon rainfall over the southeastern peninsular India (Raj et al., 2004 and Boyaj et al., 2017 for more details, including the references on earlier works). This is owing to the fact that, unlike the summer monsoon period, the seasonal climatological winds are northeasterlies, which are enhanced by the ENSO-induced anomalous easterlies. This is a situation analogous to that in Australia where the ENSO impact is stronger during austral spring rather than austral summer (Hendon et al., 2007).

Recent studies even suggest that aerosol loadings can influence the Indian summer monsoon (Ramanathan *et al.*, 2005; Lau *et al.*, 2006; Krishnamurti *et al.*, 2013; Sarangi *et al.*, 2018) and these can have implications for the ENSO impacts on monsoon (Fadnavis *et al.*, 2017). Needless to say, we need more observations and better models to understand the monsoon-ENSO relationship and extraneous factors that influence the relationship.

Acknowledgement

The contents and views expressed in this research paper are the views of the authors and do not necessarily reflect the views of their organizations.

References

- Amat, H. B. and Ashok, K., 2018, "Relevance of Indian Summer Monsoon and its Tropical Indo-Pacific Climate Drivers for the Kharif Crop Production", Pure Appl. Geophys., 175, 3, p1221,
- Annamalai, H. and Liu, P., 2005, "Response of Asian summer monsoon to changes in El Nino properties", *Quarterly Journal of the Royal Meteorological Society*, **131**, 805-831,
- Ashok, K. and Saji, N. H., 2007, "Impacts of ENSO and Indian Ocean Dipole Events on the Sub-Regional Indian Summer Monsoon Rainfall", *Journal of Natural Hazards*, **42**, 273-285.
- Ashok, K., Behera, S. K., Rao, S. A., Weng, H. and Yamagata, T., 2007, "El Niño Modoki and its possible teleconnection", *J. Geophys. Res.*, **112**, C11007, doi:10.1029/2006JC00379.
- Ashok, K., Guan, Z. and Yamagata, T., 2001, "Impact of the Indian Ocean Dipole on the relationship between the Indian Monsoon rainfall and ENSO", *Geophys. Res. Lett.*, **28**, 4499-4502.
- Ashok, K., Guan, Z., Saji, N. H. and Yamagata, T., 2004, "Individual and combined influences of the ENSO and Indian Ocean Dipole on the Indian summer monsoon", J. Climate, 17, 3141-3155.

- Ashok, K., Iizuka, S., Rao, S. A., Saji, N. H. and Lee, W. J., 2009, "Processes and boreal summer impacts of the 2004 El Niño Modoki: An AGCM study", Geophys. Res. Lett., 36, L04703.
- Ashok, K., Sabin, T. P., Swapna, P. and Murtugudde, R. G., 2012, "Is a global warming signature emerging in the tropical Pacific?", Geophysical Research Letters, 39, 2, L02701,
- Ashrit, R. G., Rupa Kumar, K. and Krishna Kumar, K., 2001, "ENSO-Monsoon relationships in a greenhouse warming scenario", Geophys. Res. Lett., 28, 1727-1730.
- Barnett, T. P., Dumenil, L., Schlese, U., Roeckner, E. and Latif, M., 1989, "The effect of Eurasian snow cover on regional and global climate variations", J. Atmos. Sci., 46, 661-686.
- Battisti, D. S. and Hirst, A. C., 1989, "Interannual variability in the tropical atmosphere-ocean model: influence of the basic state, ocean geometry and nonlinearity", J. Atmos. Sci., 45, 1687-1712.
- Behera, S. K., Krishnan R. and Yamagata, T., 1999, "Unusual oceanatmosphere conditions in the tropical Indian Ocean during 1994", Geophys. Res. Lett., 26, 3001-3004.
- Bhalme, H. N. and Jadhav, S. K., 1984, "The Southern Oscillation and its relation to the monsoon rainfall", *J. Climatol.*, **4**, 509-520.
- Bjerknes, J., 1969, "Atmospheric teleconnections from the equatorial Pacific", Mon. Weather Rev., 97, 163-172.
- Blandford, H. F., 1884, "On the connexion of the Himalayan snowfall with dry winds and seasons of drought in India", Proceedings of the Royal Society of London, 37, 1-23.
- Blanford, H. F., 1886, "Rainfall of India", Mem. India Meteorol. Dep., 2, 217-448.
- Boyaj, A., Ashok, K., Ghosh, S., Devanand, P. and Govardhan, D., 2017, "The Chennai extreme rainfall event in 2015: The Bay of Bengal connection", *Climate Dynamics*, 50, 7-8, 2867-2879.
- Cash, B. A., Barimalala, R., Kinter, J. L., Altshuler, E. L., Fennessy, M. J., Manganello, J. V., Molteni, F., Towers, P., Vitart, F., 2017, "Sampling variability and the changing ENSO-monsoon relationship", Clim. Dyn., 48, 11-12, 4071-4079.
- Chakraborty, A., 2018, "Preceding winter La Niña reduces Indian summer monsoon rainfall", Environ. Res. Lett., 13, 54030.
- Chang, C. P., Harr, P. and Ju, J., 2001, "Possible roles of Atlantic circulation on the weakening Indian monsoon rainfall-ENSO relationship", *Journal of Climate*, 14, 11, 2376-2380.
- Chen, G. and Tam, C. Y., 2010, "Different impact of two kinds of Pacific Ocean warming on tropical cyclone frequency over western North Pacific", Geophys. Res. Lett., 37, L01803.
- Chowdary, J. S., Parekh, A., Kakatkar, R., Gnanaseelan, C., Srinivas, G., Singh, P. and Roxy, M. K., 2016, "Tropical Indian Ocean response to the decay phase of El Nino in a coupled model and associated changes in south and east-Asian summer monsoon circulation and rainfall", Clim. Dyn., 47, 831-844, https://doi.org/10.1007/s00382-015-2874-9.
- Dai, A. and Wigley, T. M. L., 2000, "Global patterns of ENSO induced precipitation", Geophys. Res. Lett., 27, 1283-1286.
- Fadnavis, S., Roy, C., Ayantika, D. C, Sabin, T. P. and Ashok, K., 2017, "Potential modulations of pre-monsoon aerosols during El Niño", Climate Dynamics, 49, 7-8, 2279-2290, doi:10.1007/s00382-016-3451-6
- Feba, F., Ashok, K. and Ravichandran, M., 2018, "Role of changed Indo-Pacific atmospheric circulation in the recent disconnect between the Indian summer monsoon and ENSO", *Climate Dynamics*, 52, 3-4, 1461-1470, https://doi.org/10.1007/s00382-018-4207-2.

- Francis, P. A. and Gadgil, S., 2013, "A note on new indices for the equatorial Indian Ocean oscillation", J. Earth Sys. Sci., 122, 4, 1005-1011.
- Gadgil, S., 2003, "The Indian monsoon and its variability", *Annual Review of Earth and Planetary Sciences*, **31**, 429-467.
- Gershunov, A., Schneider, N. and Barnett, T., 2001, "Low-frequency modulation of the ENSO-Indian monsoon rainfall relationship: signal or noise?", J. Climate, 14, 2486-2492.
- Gill, A. E., 1980, "Some simple solutions for heat-induced tropical circulation", Quarterly Journal of Royal Meteorological Society, 106, 447-462.
- Goswami, B. N. and Shukla, J., 1984, "Quasi-periodic oscillations in a symmetric general circulation model", J. Atmos. Sci., 41, 20-37.
- Goswami, B. N. and Xavier, P. K., 2005, "Dynamics of "internal" interannual variability of Indian summer monsoon in a GCM", *Journal of Geophysical Research*, **110**, D24104.
- Guan, Z., Ashok, K. and Yamagata, T., 2003, "Summertime response of the tropical atmosphere to the Indian Ocean sea surface temperature anomalies", *J. Meteor. Soc. Japan*, **81**, 533-561.
- Hendon, H. H., Wheeler, M. C. and Zhang, C., 2007, "Seasonal dependence of the MJO-ENSO relationship", *Journal of Climate*, 20, 531-543.
- Jadhav, J., Swapna. P., Marathe. S. and Ashok, K., 2015 "On the possible cause of distinct El Niño types in the recent decades", Sci. Rep., 5, 17009.
- Jin, F. F., 1997a, "An equatorial ocean recharge paradigm for ENSO Part I: Conceptual model", J. Atmos. Sci., 54, 811-829.
- Joseph, P. V., 2014, "Role of Ocean in the Variability of Indian Summer Monsoon Rainfall", Surveys in Geophysics, 35, 3, 723-738,
- Ju, J. and Slingo, J., 1995, "The Asian summer monsoon and ENSO", Q. J. R. Meteorol. Soc., 121, 525, 1133-1168.
- Kao, H. Y. and Yu, J. Y., 2009, "Contrasting Eastern-Pacific and Central-Pacific Types of ENSO", J. Climate, 22, 615-632.
- Kawamura, R., 1998, "A possible mechanism of the Asian summer monsoon-ENSO coupling", J. Meteorol. Soc. Japan, 76, 1009-1027
- Kawamura, R., Uemura, K. and Suppiah, R., 2005, "On the recent change of the Indian summer monsoon-ENSO relationship", *SOLA*, 1, 201-204, doi:10.2151/sola.2005-052.
- Keshavamurthy, R. N., 1982, "Response of the atmosphere to sea surface temperature anomalies over the equatorial Pacific and teleconnections of the Southern Oscillation", *J. Atmos. Sci.*, **39**, 1241-1259.
- Kirtman, B. P. and Shukla, J., 2006, "Influence of the Indian summer monsoon on ENSO", *Quart. J. Metor. Soc.*, 126, 562, 213-239,
- Kripalani, R. H. and Kulkarni, A., 1997, "Climatological impact of El Nino/la Nina on the Indian monsoon: A new perspective", Weather, 52, 39-46.
- Krishnamurthy, L. and Krishnamurthy, V., 2014, "Influence of PDO on South Asian summer monsoon and monsoon-ENSO relation", Climate Dynamics, 42, 2397-2410.
- Krishnamurthy, V. and Goswami, B. N., 2000, "Indian monsoon-ENSO relationship on inter-decadal timescale", *Journal of Climate*, 13, 579-595.
- Krishnamurti, T. N., Martin, A., Krishnamurti, R., Simon, A., Thomas, A. and Kumar, V., 2013, "Impacts of enhanced CCN on the organization of convection and recent reduced counts of monsoon depressions July 2013", Climate Dynamics, 41, 1, 117-134.

- Krishnan, R. and Sugi, M., 2003, "Pacific Decadal Oscillation and variability of the Indian summer monsoon rainfall", *Climate Dynamics*, 21, 233-242.
- Krishnan, R., Kumar, V., Sugi M. and Yoshimura, J., 2009, "Internal Feedbacks from Monsoon-Midlatitude Interactions during Droughts in the Indian Summer Monsoon", J. Atmos. Sci., 66, 553-578, https://doi.org/10.1175/2008JAS2723.1.
- Krishnan, R., Venkatesan, C. and Keshavamurty, R. N., 1998, "Dynamics of upper tropospheric stationary wave anomalies induced by ENSO during the northern summer: A GCM study", *Proc. Indian Acad. Sci. Earth Planet Sci*, 107, 65-90.
- Kucharski, F., Bracco, A., Yoo, J. H. and Molteni, F., 2008, "Atlantic forced component of the Indian monsoon interannual variability", Geophys. Res. Lett., 35, L04706.
- Kug, J. S., Jin, F. F. and An, S. I., 2009, "Two-types of El Niño events: Cold Tongue El Niño and Warm Pool El Niño", J. Climate, 22, 1499-1515.
- Kumar, K. K., Rajagopalan, B. and Cane, M. A., 1999, "On the weakening relationship between the Indian Monsoon and ENSO", Science, 284, 5423, 2156-2159.
- Kumar, K. K., Rajagopalan, B., Hoerling, M., Bates, G. and Cane, M., 2006, "Unraveling the mystery of Indian monsoon failure during El Niño", Science, 314, 115-119.
- Larkin, N. K. and Harrison, D. E., 2005, "Global seasonal temperature and precipitation anomalies during El Niño autumn and winter", Geophys. Res. Lett., 32, L16705, doi:10.1029/2005GL022860.
- Lau, K. M. and Kim, K. M., 2006, "Observational relationships between aerosol and Asian monsoon rainfall and circulation", Geophys Res Lett., 33, L21810.
- Lau, N. C. and Nath, M. J., 2000, "Impact of ENSO on the variability of the Asian-Australian monsoons as simulated in GCM experiments", J. Climate, 13, 4287-4309.
- Lindzen, R. S. and Nigam, S., 1987, "On the role of sea surface temperature gradients in forcing low-level winds and convergence in the Tropics", J. Atmos. Sci., 44, 2418-2436.
- Marathe, S., Ashok, K., Panickal, S. and Sabin, T. P., 2015, "Revisiting El Niño Modokis", *Climate Dynamics*, **45**, 11-12, 3527-3545.
- Masumoto, Y. and Yamagata, T., "Response of the western tropical Pacific to the Asian winter monsoon: the generation of the Mindanao Dome", *Journal of Physical Oceanography*, 21, 1386-1398.
- Matsuno, T., 1966, "Quasi-geostrophic motions in the equatorial area", J. Meteor. Soc. Japan, 44, 25-43.
- Mujumdar, M., Kumar, Vinay and Krishnan, R., 2007, "The Indian summer monsoon drought of 2002 and its linkage with tropical convective activity over northwest Pacific", Clim. Dyn., 28, 743-758.
- Mujumdar, M., Preethi, B., Sabin, T. P., Ashok, K., Sajjad, S., Pai, D. S. and Krishnan, R., 2012, "The Asian summer monsoon response to the La Niña event of 2010", *Meteorol. Appl.*, 19, 216-225,
- Murakami, T. and Ding, Y. H., 1982, "Wind and temperature changes over Eurasia during the early summer of 1979", Journal of the Meteorological Society of Japan, 60, 183-196.
- Murtugudde, R., McCreary, J. P. and Busalacchi, A. J., 2000, "Oceanic processes associated with anomalous events in the Indian Ocean with relevance to 1997-1998", Journal of Geophysical Research: Oceans, 105, C2, 3295-3306.

- Navarra, A., Ward, M. N. and Miyakoda, K., 1999, "Tropical-wide teleconnection and oscillation I: Teleconnection indices and type I/type II states", *Quart. J. Roy. Meteor. Soc.*, 125, 2909-2935.
- Nigam, S., 1994, "On the dynamical basis for the Asian summer monsoon rainfall-El Niño relationship", J. Climate, 7, 1750-1771.
- Palmer, T. N., Brankovic, C., Viterbo P. and Miller, M. J., 1992, "Modeling interanual variations of summer monsoons", J. Climate, 5, 399-417.
- Pant, G. B. and Parthasarathy, B., 1981, "Some aspects of an association between the southern oscillation and Indian summer monsoon", *Arch Meteor Geophys BioKlimatol Ser B*, **29**, 245-251.
- Pant, G. B. and Rupa Kumar, K., 1997, "Climates of South Asia", J. Wiley and Sons, p317.
- Philander, S. G., 1985, "El Niño and La Niña", *J. Atmos. Sci.*, **42**, 2652-2662.
- Philander, S. G., 1990, "El Niño, La Niña and the Southern Oscillation", Academic Press, London, p289.
- Pottapinjara, V., Kumar, M. S. G., Sivareddy, S., Ravichandran, M. and Murtugudde, R., 2015, "Relation between the upper ocean heat content in the equatorial Atlantic during boreal spring and the Indian monsoon rainfall during June-September", *Int. J. Climatol.*, **36**, 2469-2480, https://doi.org/10.1002/joc.4506.
- Pradhan, P. K., Ashok, K., Preethi, B., Krishnan, R. and Sahai, A. K., 2011, "Modoki, IOD and Western North Pacific typhoons: Possible implications for extreme events", *J. Geophys. Res.*, 116, D18108.
- Raj, Y. E. A., Suresh, R., Sankaran, P. V. and Amudha, B., 2004, "Seasonal variation of 200 hPa upper tropospheric features over India in relation to performance of Indian Southwest and Northeast monsoons", *Mausam*, 55, 269-280.
- Rajeevan, M., Bhate, J., Kale, J. D. and Lal, B., 2006, "High resolution daily gridded rainfall data for the Indian region: Analysis of break and active monsoon spells, *Current Science*, 91, 3, 296-306.
- Rajeevan, M. and McPhaden, M. J., 2004, "Tropical Pacific upper ocean heat content variations and Indian summer monsoon rainfall", *Geophys. Res. Lett.*, 31, 18, L18203.
- Ramage, C. S., 1971, "Monsoon Meteorology (Vol. 15 of International Geophysics Series)", Academic Press, San Diego, CA, p296.
- Ramanathan, V., Chung, C., Kim, D., Bettge, T., Buja, L., Kiehl, J. T., Washington, W. M., Fu, Q., Sikka, D. R. and Wild, M., 2005, "Atmospheric brown clouds: impacts on South Asian climate and hydrological cycle", *Proc. Natl. Acad. Sci. USA*, 102, 5326-5333
- Rao, D. V. B., Ashok, K. and Yamagata, T., 2004, "A Numerical Simulation Study of the Indian Summer Monsoon of 1994 using NCAR MM5", J. Meteor. Soc. Japan, 82, 1755-1775
- Rao, Y. P., 1976, "Southwest Monsoon (meteorological monograph)", India Meteorological Department, New Delhi, p366.
- Rasmusson, E. M. and Carpenter, T. H., 1983, "The relationship between the eastern Pacific sea surface temperature and rainfall over India and Sri Lanka", Mon. Weather. Rev., 111, 517-528.
- Ratnam, J. V., Behera, S. K., Masumoto, Y., Takahashi, K. and Yamagata, T., 2010, "Pacific Ocean origin for the 2009 Indian summer monsoon failure", *Geophys. Res. Lett.*, 37, L07807.

- Rayner, N. A., Parker, D. E., Horton, E. B., Folland, C. K., Alexander, L. V., Rowell, D. P., Kent, E. C. and Kaplan, A., 2003, "Global analyses of sea surface temperature, sea ice and night marine air temperature since the late nineteenth century", J. Geophys. Res., 108, D14, 4407.
- Ropelewski, C. F. and Halpert, M. S., 1987, "Global and regional scale precipitation patterns associated with the El Niño Southern Oscillation", *Mon. Wea. Rev.*, **115**, 1606-1626.
- Saji, N. H., Goswami, B. N., Vinayachandran, P. N. and Yamagata, T., 1999, "A dipole mode in the tropical Indian Ocean", *Nature*, 401, 360-363.
- Sarangi, C., Kanawade, V. P., Tripathi, S. N., Thomas, A. and Ganguly, D., 2018, "Aerosol-induced intensification of cooling effect of clouds during Indian summer monsoon", *Nature Communications*, 9, 1, 3754.
- Shaman, Jeffrey and Tziperman, Eli, 2007, "The Summertime ENSO-North African-Asian Jet Teleconnection and Implications for the Indian Monsoons", Geophys. Res. Lett., 34, doi:10.1029/2006GL029143.
- Shukla, J. and J. M. Wallace, 1983, "Numerical simulation of the atmospheric response to equatorial sea surface temperature anomalies", J. Atmos. Sci., 40, 1613-1630.
- Shukla, J. and Paolina, D. A., 1983, "The southern oscillation and long range forecasting of the summer monsoon rainfall over India", *Mon. Weather Rev.*, 111, 1830-1837, doi: 10.1175/1520-0493.
- Sikka, D. R. and Gadgil, S., 1980, "On the maximum cloud zone and the ITCZ over India longitude during the Southwest monsoon", Mon. Weather Rev., 108, 1840-1853.
- Sikka, D. R., 1980, "Some aspects of the large-scale fluctuations of summer monsoon rainfall over India in relation to fluctuations in planetary and regional scale circulation parameters", *Proc. Indian Acad. Sci. Earth Planet Sci.*, 89, 179-195.
- Slingo, J. M. and Annamalai, H., 2000, "1997: The El Niño of the century and the response of the Indian summer monsoon", Mon. Weather Rev., 128, 1778-1797.
- Soman, M. K. and Slingo, J., 1997, "Sensitivity of the Asian summer monsoon to aspects of sea-surface-temperature anomalies in the tropical Pacific Ocean", Q. J. R. Meteor. Soc., 123, 309-336,
- Sreejith, O. P., Panickal, S., Pai, S. and Rajeevan, M., 2015, "An Indian Ocean precursor for Indian summer monsoon rainfall variability", Geophys. Res. Lett., 42, 9345-9354.
- Sridharan, S. and Muthusamy, A., 1990, "Northeast monsoon rainfall in relation to El Niño, QBO and Atlantic hurricane frequency", Vayu Mandal, 20, p1081.
- Suarez, M. J. and Schopf, P. S., 1988, "A delayed action oscillator for ENSO", J. Atmos. Sci., 45, 3283-3287.
- Tejavath, C. T., Ashok, K., Chakraborty, S. and Rengasamy, R., 2019, "A PMIP3 narrative of modulation of ENSO teleconnections to the Indian summer monsoon by background changes in the Last Millennium", *Climate Dynamics*, 1-17.

- Tyagi, Ajit and Pai, D. S., 2012, "Monsoon 2011 A Report", IMD Met. Monograph, Synoptic Meteorology No. 1/2012.
- Walker, G. T., 1923, "Correlation in Seasonal Variations of Weather, VIII: A Preliminary Study of World Weather", Mem. India Meteorol. Dep., 24, 75-131.
- Walker, G. T., 1924, "Correlation in seasonal variations of weather, IX: A further study of world weather", Memoirs of the India Meteorological Department, 24, 9, 275-333.
- Walker, G. T., 1928, "World weather", Q. J. R. Meteor. Soc, 54, 79-87.
- Wang, B., Wu, R. and Fu, X., 2000, "Pacific-east Asian teleconnection: How does ENSO affect east Asian climate?", Journal of Climate, 13, 1517-1536, doi:10.1175/1520-0442(2000)013.
- Wang, C., 2000, "On the atmospheric responses to tropical Pacific heating during the mature phase of El Niño", J. Atmos. Sci., 57, 3767-3781.
- Wang, C., Weisberg, R. H. and Virmani, J. I., 1999, "Western Pacific interannual variability associated with the El Niño-Southern Oscillation", J. Geophys. Res., 104, 5131-5149.
- Webster, P. J. and Yang, S., 1992, "Monsoon and ENSO: Selectively Interactive Systems", Quart. J. Roy. Meteor. Soc., 118, 877-926.
- Webster, P. J., Moore, A., Loschnigg, J. and Leban, M., 1999, "Coupled dynamics in the Indian Ocean during 1997-1998", *Nature*, 401, 356-360.
- Weisberg, R. H. and Wang, C., 1997, "A western Pacific oscillator paradigm for the El Niño-Southern Oscillation", Geophy. Res. Lett., 24, 779-782.
- Wu, R. and B. P. Kirtman, 2004, "The tropospheric biennial oscillation of the monsoon-ENSO system in an interactive ensemble coupled GCM", *Journal of Climate*, **17**, 1623-1640.
- Yadav, R. K., 2017, "On the relationship between east equatorial Atlantic SST and ISM through Eurasian wave", Climate Dynamics, 48, 1-2, 281-295, https://doi.org/10.1007/s00382-016-3074-y.
- Yanai, M., Li, C. and Song, Z., 1992, "Seasonal heating of the Tibetan Plateau and its effects on the evolution of the Asian summer monsoon", J. Meteor. Soc. Japan, 70, 319-351.
- Yanai, Michio, Wu, Guoxiong and Wang, Bin, 2006, "Effects of the Tibetan Plateau", *The Asian Monsoon*, 513-549,
- Yang, S., 1996, "ENSO-snow-monsoon associations and seasonal interannual predictions", *International Journal of Climatology*, 16, 2, 125-134, https://doi.org/10.1002.
- Yin, M. T., 1949, "A synoptic-aerologic study of the onset of the summer monsoon over India and Burma", *Journal of Meteorol.*, 6, 393-400.
- Zebiak, S. E. and Cane, M. A., 1987, "A model El Niño-Southern Oscillation", *Monthly Weather Review*, **115**, 2262-2278.
- Zhang, Y., Wallace, J. M. and Iwasaka, N., 1996, "Is climate variability over the North Pacific a linear response to ENSO?", *Journal of Climate*, 9, 1468-1478.





Emerging Skill in Multi-Year Prediction of the Indian Ocean Dipole

F. Feba^{1*}, Karumuri Ashok^{1*}, Matthew Collins² and Satish R. Shetye¹

¹ Centre for Earth, Ocean and Atmospheric Sciences, University of Hyderabad, Hyderabad, India, ² College of Engineering, Mathematics, and Physical Sciences, University of Exeter, Exeter, United Kingdom

The Indian Ocean Dipole is a leading phenomenon of climate variability in the tropics, which affects the global climate. However, the best lead prediction skill for the Indian Ocean Dipole, until recently, has been limited to ~6 months before the occurrence of the event. Here, we show that multi-year prediction has made considerable advancement such that, for the first time, two general circulation models have significant prediction skills for the Indian Ocean Dipole for at least 2 years after initialization. This skill is present despite ENSO having a lead prediction skill of only 1 year. Our analysis of observed/reanalyzed ocean datasets shows that the source of this multi-year predictability lies in sub-surface signals that propagate from the Southern Ocean into the Indian Ocean. Prediction skill for a prominent climate driver like the Indian Ocean Dipole has wide-ranging benefits for climate science and society.

Keywords: Indian Ocean (Dipole), decadal prediction, CanCM4, MIROC5, Southern Ocean, IOD and Southern Ocean, Antarctic Circumpolar Current (ACC), decadal prediction in tropics

OPEN ACCESS

Edited by:

Swadhin Kumar Behera, Japan Agency for Marine-Earth Science and Technology (JAMSTEC), Japan

Reviewed by:

Tomoki Tozuka, The University of Tokyo, Japan Benjamin Ng, CSIRO Oceans and Atmosphere, Australia

*Correspondence:

F. Feba feba.francis@outlook.com Karumuri Ashok ashokkarumuri@uohyd.ac.in

Specialty section:

This article was submitted to Predictions and Projections, a section of the journal Frontiers in Climate

Received: 05 July 2021 Accepted: 31 August 2021 Published: 27 September 2021

Citation:

Feba F, Ashok K, Collins M and Shetye SR (2021) Emerging Skill in Multi-Year Prediction of the Indian Ocean Dipole. Front. Clim. 3:736759. doi: 10.3389/fclim.2021.736759

INTRODUCTION

The Indian Ocean Dipole (IOD) is an inter-annual coupled ocean—atmosphere phenomenon in the tropical Indian Ocean that peaks during the boreal fall season (September to November; SON). Positive IODs are associated with anomalously warmer western Indian Ocean and anomalously cooler eastern Indian Ocean. Negative IOD events are associated with opposite anomalous sea surface temperatures (SSTs) across the Indian Ocean (Saji et al., 1999; Webster et al., 1999; Murtugudde et al., 2000). The IOD is a well-known driver of global climate (Saji and Yamagata, 2003). In addition to affecting the neighboring Maritime Continent to the east and East Africa to the west (Behera et al., 2005), the positive IOD events, for example, have been associated with reduced rainfall over western and southern Australia (Ashok et al., 2003; Ashok and Saji, 2007; Cai et al., 2011), enhanced seasonal Indian summer monsoon (ISM) rainfall (Ashok et al., 2001; Ashok and Saji, 2007), and climates of even distant regions of South America (Chan et al., 2008) and Europe (Hardiman et al., 2020). In addition to its own coupled dynamics (Gualdi et al., 2008; Yamagata et al., 2004; Behera et al., 2006; Ha et al., 2017; Tanizaki et al., 2017; Saji, 2018; Marathe et al., 2021), the IOD is suggested to be triggered by other inter-annual processes such as the El Niño–Southern Oscillation (ENSO), the dominant climate driver from the tropics.

Attempts to predict the IOD on a seasonal scale have been on-going for about two decades (Iizuka et al., 2000; Shinoda et al., 2004; Luo et al., 2007; Doi et al., 2016) and have met with relatively shorter lead time skills, the highest being of 4 months. This is in contrast to the 12–17 months of lead prediction skill for the ENSO as shown in recent studies (Barnston et al., 2012; Park et al., 2018; Tang et al., 2018). Several papers claim that prediction skills for the IOD and ENSO are linked and intertwined (Wajsowicz, 2005; Izumo et al., 2010; Luo et al., 2010).

1

The emerging discipline of decadal prediction, i.e., prediction of climate information for the near future, shows great promise for societal needs and economic policymakers. Decadal prediction lies between weather prediction and climate projection. Therefore, decadal prediction has to resolve initial value problems like in weather prediction and seasonal to inter-annual forecasts and climate variability and trends effective from boundary conditions, including slow varying oceanic processes, snow cover, and anticipated changes in anthropogenic greenhouse gases and aerosols (Meehl et al., 2009, 2014; Smith et al., 2013; Boer et al., 2016). Interestingly, the inter-annual ENSO and the IOD can also be modulated by decadal processes (Ashok et al., 2004; Tozuka et al., 2007). Such processes should enhance the decadal prediction skill of these inter-annual events.

Given the limited lead skill of the IOD on seasonal scales, its prediction at multi-year lead times is exceptionally challenging. Remarkably, in this study, we show that two model hindcasts from the CMIP5 (Coupled Model Intercomparison Project—Phase 5) decadal prediction datasets are found to show successful prediction skill for IOD events. These sets give us an opportunity to track the lead prediction skill of an event at a lead of up to 2 years.

DATA AND METHODS

Data

We have mainly used a sub-set of the decadal hindcast outputs from the CMIP5 decadal runs (Meehl et al., 2009, 2014; Taylor et al., 2012; Smith et al., 2013; Boer et al., 2016). These runs have anthropogenic and natural forcing in them, and comprise several independent decade-long ensemble-runs by each model. For example, the four members of the first ensemble are initialized in 1960 and run up to 1970 (Figure 1). Such runs are available with initial conditions from 1960 to 2011. Together, we have 51 ensemble members of decadal hindcasts for each model, each differing from the other in the initialization year (from 1960 to 2011). For each model, we average multiple ensembles with same initialization dates. These averages are referred to as the model hindcasts for the initial conditions of that particular year. The models, whose hindcasts we consider, are the CanCM4 (Merryfield et al., 2013), MIROC5 (Watanabe et al., 2010), BCC-CSM (Wu et al., 2013), and the GFDL (Delworth et al., 2006; Zhang et al., 2007) models. The output data from all the models are divided into 10 groups depending on the year after initialization (**Figure 1**). Yr1, yr2, yr3... indicate 1, 2, 3... year(s) after initialization.

We used Hadley Center Sea Ice and Sea Surface Temperature (HadISST; Rayner et al., 2003) and Ocean Reanalysis data from the European Center for Medium-Range Weather Forecasts (ORAS4; Balmaseda et al., 2013) for ocean temperatures. As for ENSO indices, we calculate the NINO3 and NINO4 indices as anomalies of SSTs in area averaged over the boxes 150–90°W, 5°S–5°N and $160^{\circ}E-150^{\circ}W$, $5^{\circ}S-5^{\circ}N$, respectively. We calculate the Indian Ocean Dipole Mode Index (IODMI) as the SST gradient between the western equatorial Indian Ocean (50–70°E and $10^{\circ}S-10^{\circ}N$) and the south-eastern equatorial Indian Ocean (90–110°E and $10^{\circ}S-0^{\circ}$). We take into consideration the

IODMI only during the months of September to November as the IOD peaks during this season.

Statistical Methods

We have carried out correlation and regression analysis. We have used the two-tailed Student's t-test to determine the significance of the correlation coefficients. We ascertained the robustness of the skills by applying a boot-strapping test for 1,000 simulations (using NCL) and found our results to be significant at 90% for up to 4 years. For verifying the skill of persistence for both the models and observations, we use the auto-correlation (Supplementary Figure 1). To illustrate briefly, say in the case of CanCM4, we correlate the predicted IODMI at lead 1 with that at lead 2 to get the persistence skill at lead 1. Similarly, the persistence skill at lead 2 is obtained by correlating the predicted IODMI at lead 0 with that at lead 2, and so on. We have used the Empirical Orthogonal Function (EOF) analysis technique (von Storch and Zwiers, 1999) to determine the dominant patterns of spatio-temporal variability in the equatorial Indian Ocean, as an additional analysis to compare the simulated IODs with the observations. The EOF analysis is a multivariate statistical technique to calculate the eigenvalues and eigenvectors of a spatially weighted anomaly covariance matrix. The corresponding eigenvalues quantify the variance percent explained by each pattern, which is, by definition, orthogonal to the other patterns.

To have an estimate of the inter-annual variability of IOD that could be attributed to the Southern Ocean (20°W:50°E; 60°S:40°S), we projected the IODMI on to the corresponding area-averaged subsurface temperatures (vertically averaged over 300–800 m depth), i.e., through a regression analysis, and measured the goodness-of-fit (figure not shown).

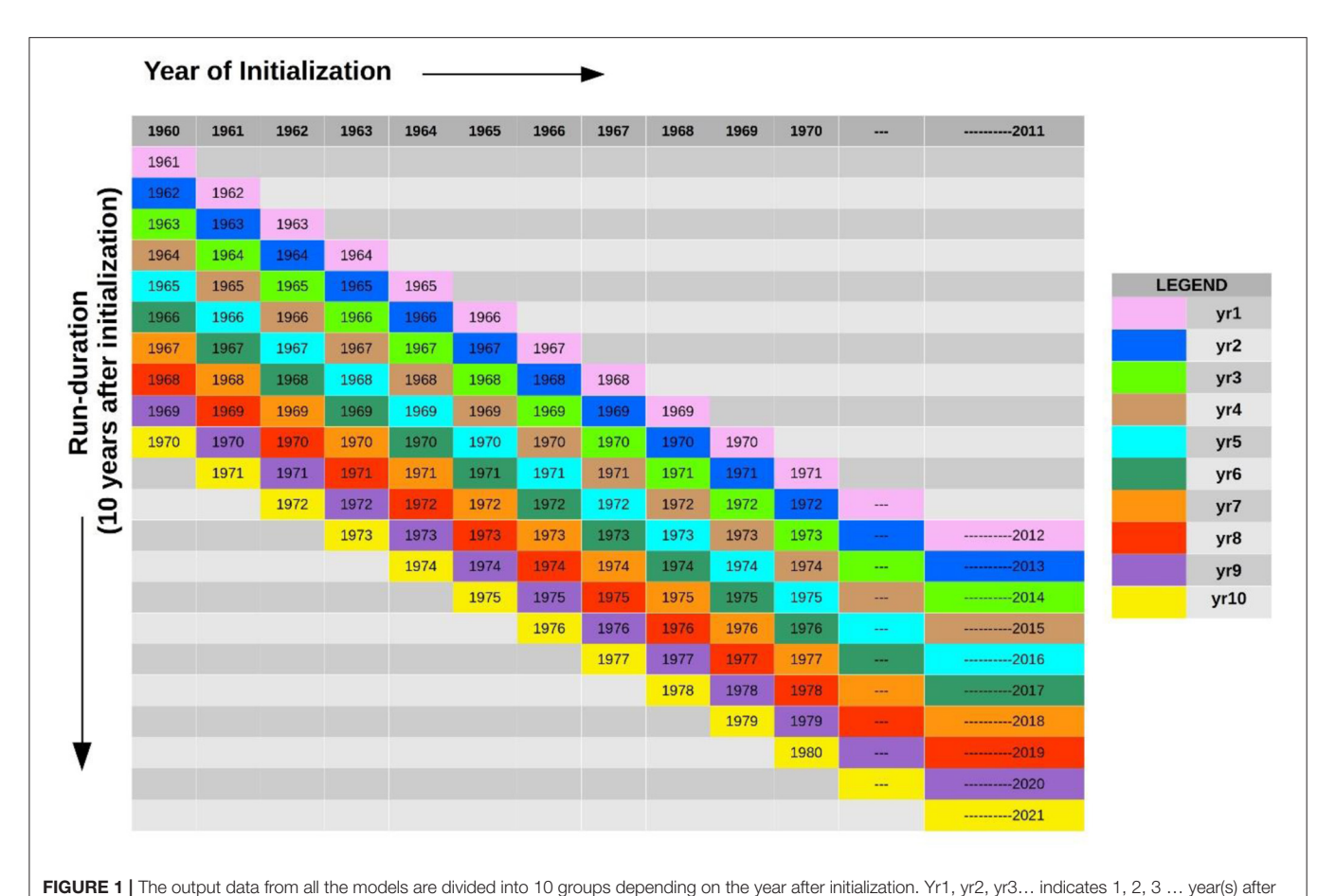
RESULTS

Lead Prediction Skills for ENSO and IOD

ENSO events peak during the boreal winter (through December), while the IOD events peak during boreal fall (September–November). Our analysis shows that the hindcasts analyzed in this study (**Figure 2A**) predict the peak NINO3 index (Trenberth, 1997) significantly at leads up to 12–13 months, in agreement with earlier studies (Sun et al., 2018; Pal et al., 2020).

Surprisingly, the hindcasts from the MIROC5 and CanCM4 predict the IODMI during the fall season with significant lead prediction skill for at least 2–3 years (**Figure 2B**). The skill levels for most of the lead times are not only statistically significant at the 95% confidence level from a two-tailed Student's *t*-test but also are better than persistence (**Supplementary Figure 1**). While the lead prediction skills of the IODMI from the CanCM4 fall below 95% confidence level at 4–5-year leads, these skill levels are still significant at a 90% confidence level. The MIROC5 also shows a weak skill for the eighth year, still significant at 80% confidence level.

It is noteworthy that this skill is present despite the maximum lead predictability of only 1 year for the NINO3 index in all the models. We also ascertain that the maximum lead time skill for the NINO4 is similar to those for the NINO3 index. The ISM



initialization, which is represented by individual colors.

rainfall is an ocean–atmosphere coupled phenomenon occurring every year from June to September bringing copious amount of rainfall over the Indian subcontinent. ISM is strongly influenced by ENSO and IOD, along with other factors. Our study shows that ISM has no predictability in the analyzed models, presumably due to model inadequacies in representing monsoon processes (figure not shown). Nevertheless, rainfall predictions could be improved by exploiting known statistical relationships between ENSO-ISM or IOD-ISM (Jourdain et al., 2013; Swapna et al., 2015; Dutta and Maity, 2018).

Fidelity of the Simulated IOD

To further ascertain whether the IODMI computed from the two hindcast datasets represents some of the observed features of the IOD (Yamagata et al., 2003), we compare the second leading simulated EOF modes of the SST from the hindcasts of MIROC5 and CanCM4 with that from the corresponding observations. **Figure 3**, derived from the EOF analysis at 1-year lead, shows that the models indeed capture the observed dominant IOD variance pattern associated with the EOF2 in terms of the location of the two centers of action. The simulated variance explained by this statistical mode from the MIROC5 is 12.2%, comparable with the corresponding observed value of 12% (Saji et al., 1999; Ashok et al., 2004). EOF2 of CanCM4 is 27.4%, which is higher than

the expected value as the dipole-like structure shows more spread in the eastern Indian Ocean (**Figure 3**). The simulated EOF1, associated with Indian Ocean Basin mode, and the corresponding variance explained are also realistic.

Source of the IOD Prediction Skill

A question arises as to what processes are responsible for the IOD predictability. Earlier studies have shown that the key component of improved decadal prediction lies in ocean physical processes, which internally generate decadal climate variability (Meehl et al., 2014; Farneti, 2017). Thus, the memory of the upper ocean (~800 m) provides an improved predictability of SST variability in models on decadal timescales (Yeager et al., 2012; Wang et al., 2014). Motivated by these, we looked for a source of predictability of IOD at several levels in the subsurface temperature (every 50 m). We found the maximum signal in the Southern Ocean at 300 to 800 m depth 7–10 years before the occurrence of the IOD event. From an analysis of the ORAS4 and SODA3 reanalysis datasets, we find a signal for the IODMI in the Southern Ocean. This is evidenced by significant correlations between depthaveraged 300-800 m temperatures in the Southern Ocean, which lead the IODMI by 10-6 years, respectively (Figure 4). The significant positive correlations in the Southern Ocean indicate that a positive temperature anomaly in the Southern Ocean leads

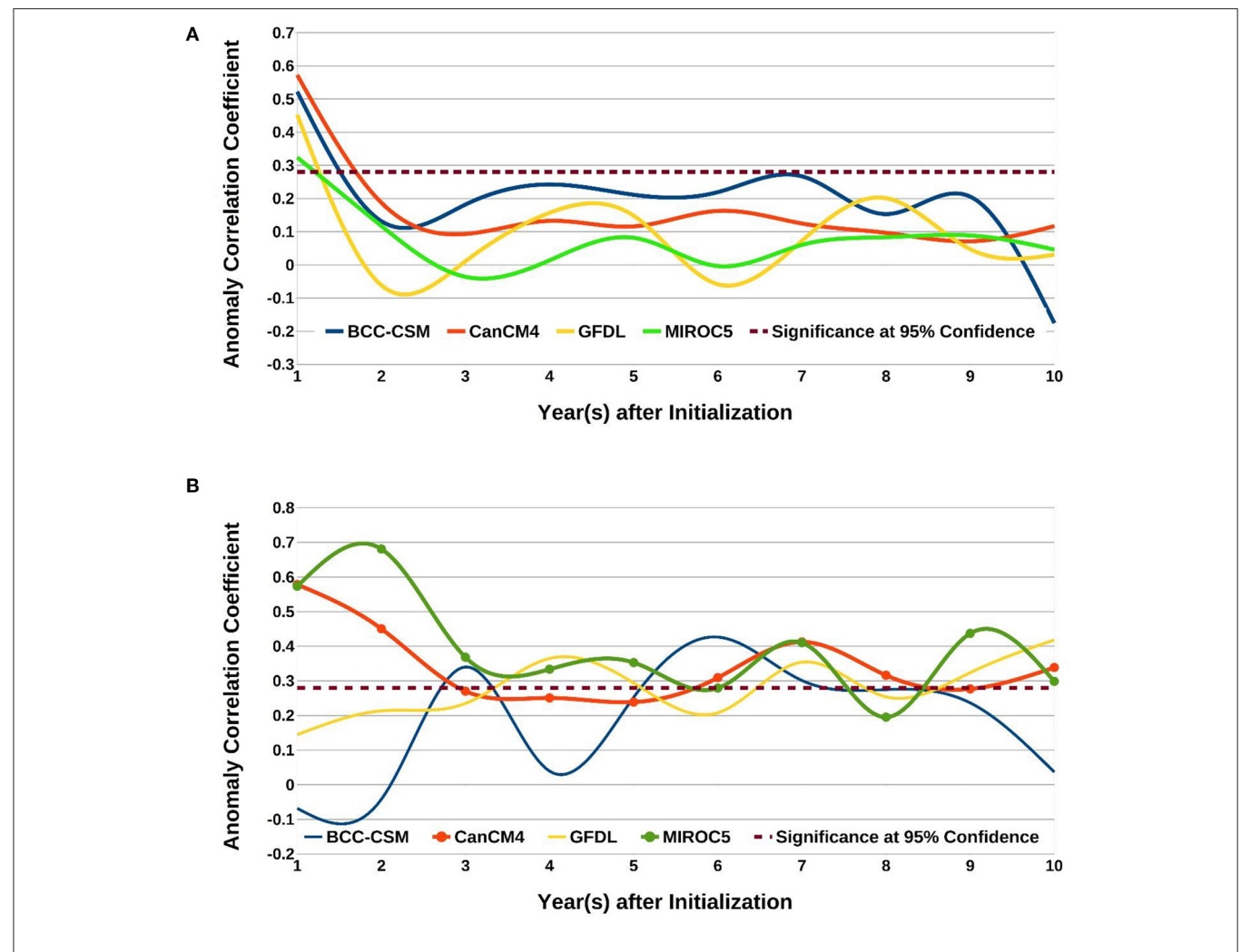


FIGURE 2 | (A) Anomaly correlations between observed NINO3 index with the corresponding predicted NINO3 index at different lead years for various models, shown in different colors. The significant correlation value at 95% confidence level is 0.27 and is shown by dashed lines. Details of how the correlations at different leads were obtained, from the sets of ~51 year-long decadal prediction runs with different initial years, are available from section Statistical Methods and Figure 1. (B) Same as (A) but for the IODMI. The lines with circles in (B) are the two models of interest for this study.

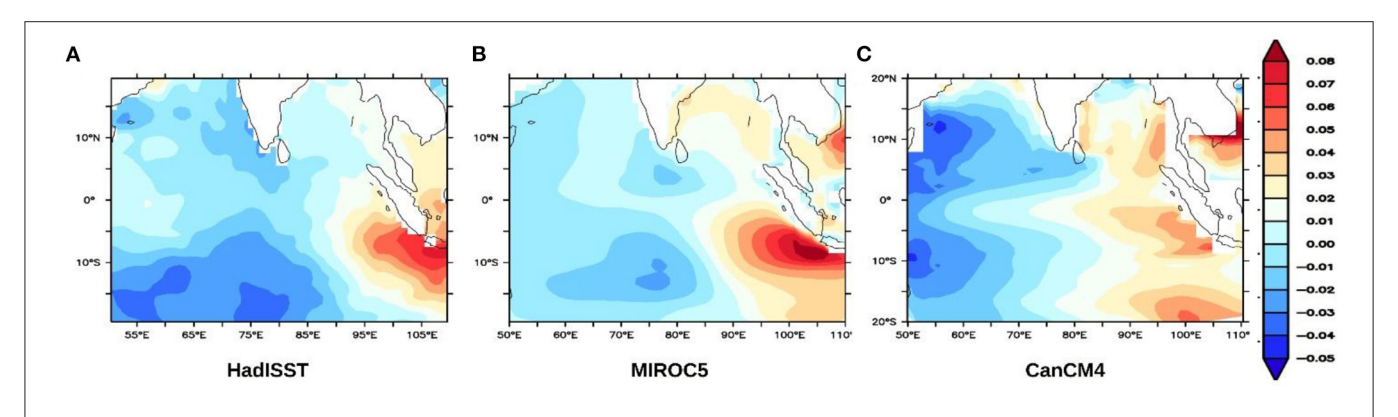


FIGURE 3 | The second mode from the EOF analysis of the tropical Indian Ocean SST, from (A) HadISST (1961–2011 period). (B,C) are the same as that of (A) but derived from MIROC5 and CanCM4 hindcasts for the same period (also see Supplementary Figure 2).

to a positive IOD event after 8-10 years, whereas a similar lead negative correlation coefficient in the Southern Ocean indicates a negative IOD event after such a time period. The signal leading the IODMI first appears in the sub-surface temperatures of the Southern Ocean just south-west of Africa between the depths of 300–800 m, 10 years before the occurrence of the IOD event. This signal is seen to propagate toward the east along the Antarctic Circumpolar Current (ACC, or West wind drift) to about 50-60°E about 6 years prior to the IOD event. From here, the signal in the heat content further propagates north, along the east of Madagascar, all the way to the Somali coast in a pathway that is coincident with the East Madagascar undercurrent (EMUC) an intermediate undercurrent at the depth of thermocline and below. The period of the propagation is in agreement with the EMUC as described by Nauw et al. (2008). The EMUC transports about 2.8 \pm 1.4 Sv of intermediate water equatorward. The signal upwells to the surface near Somalia (Somali upwelling) along with its propagation north (Figure 5).

The propagation of the signal from the deeper layers in the extra-tropics to the surface layers in the equatorial region can be explained by the Indian Ocean Meridional Overturning Circulation (IOMOC; Wang et al., 2014). The time period of the propagation is in agreement with the IOMOC. From the Somali coast, the lead heat content signal is seen to move east, reaching the central equatorial Indian Ocean 3 years before the IOD event. The signal remains in the equatorial Indian Ocean for the last 2-3 years before the occurrence of the IOD event (**Figure 6**). Furthermore, our correlation in **Figure 6** suggests an anomalous SST structure of opposite polarity in the equatorial Indian Ocean about a year before the occurrence of an IOD event. This is in conformation with Saji et al. (1999), who not only note a tight coupling between the intensity of the SST dipole anomaly and zonal wind anomaly but emphasize on a biennial tendency. The biennial tendency of the IOD is also noted by Meehl and Arblaster (2001), Ashok et al. (2003), etc. It is intriguing why the signal from the sub-surface at the equator does not manifest as an IOD event immediately. There are several studies that suggest potential drivers that can force an IOD such as the Indian summer monsoon, ENSO, and can account for the lead signals associated with the IOD with 1-2-year lead (Ashok et al., 2001; Ashok and Saji, 2007). As the current models do not show any lead skills of the Indian summer monsoon beyond a season, we can rule out that the long lead skills for the IODMI in the models come from the lead skills of monsoon or those related to ENSO (see Figure 2A). This might be explained by the fact that some IOD events are triggered by an atmospheric signal substantial enough to trigger the coupled evolution of the IOD (Shinoda et al., 2004; Saji, 2018) and hence this delay of 2-3 years.

A linear regression analysis carried out using HadISST and ORAS4 ocean temperature datasets (slope value = 0.46) indicates that the Southern Ocean signals at decadal lead explain about 18% of the inter-annual variability of IOD as suggested by a goodness-of-fit measure. To put it in perspective, ENSO, known as the most prominent driver of the Indian summer monsoon interannual variability, explains about 30% of the latter.

The source of decadal predictability for IOD in the MIROC5 and CanCM4 also apparently comes from the Southern Ocean (**Supplementary Figure 3**). We find statistically

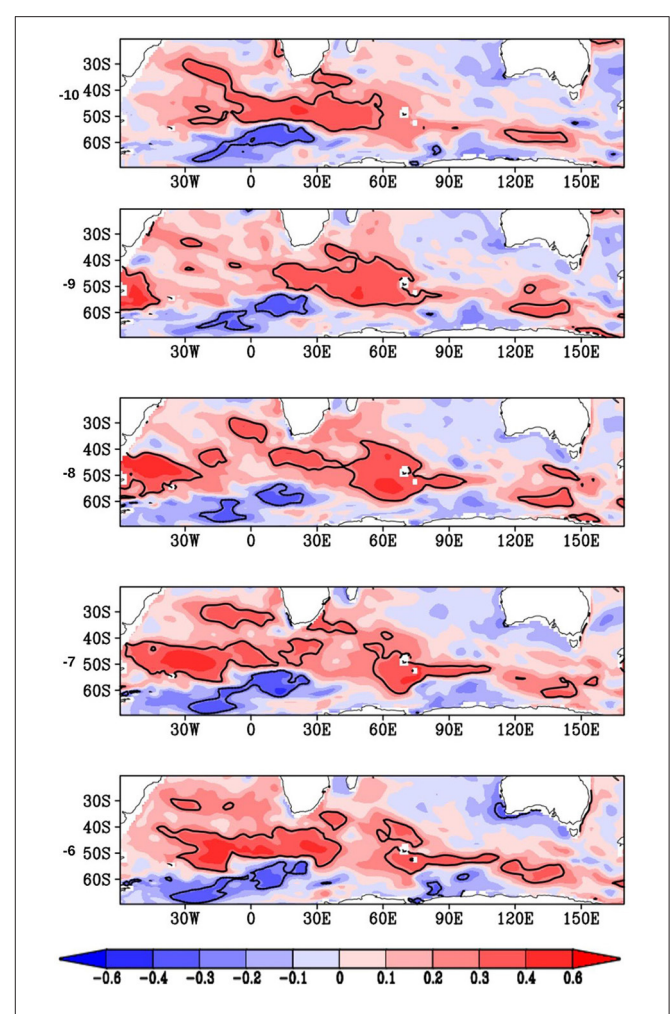


FIGURE 4 | Spatial distribution of the anomaly correlation of HadISST derived IODMI with vertically averaged subsurface temperatures from ORAS4 (over 300–800 m depth) from previous years averaged annually. The "lag number" is the years over which the IOD lags the Southern Ocean signal. In all panels, significant correlations at 95% confidence are shown as contour lines (value at 0.27)

significant anomaly correlations between the depth averaged from surface until ${\sim}800$ m hindcast heat content with the IODMI with the heat content leading at 10–5 years, conforming to our results from the reanalysis. The source of signal is the Southern Ocean for both the models, but the simulated signal path from here to the equatorial Indian Ocean are, however, weaker and remain unclear specifically in the MIROC5 model. However, the signals re-emerge finally 2–3 years before the occurrence of the simulated IOD. The models also do not capture the biennial tendency of the IOD as in observations. Further understanding of other possible factors affecting IOD variability on decadal scales is needed.

DISCUSSION

Our analysis of the CMIP5 decadal retrospective prediction products for the 1960–2011 period shows that two CMIP5 decadal prediction systems exhibit multi-year skill in predicting

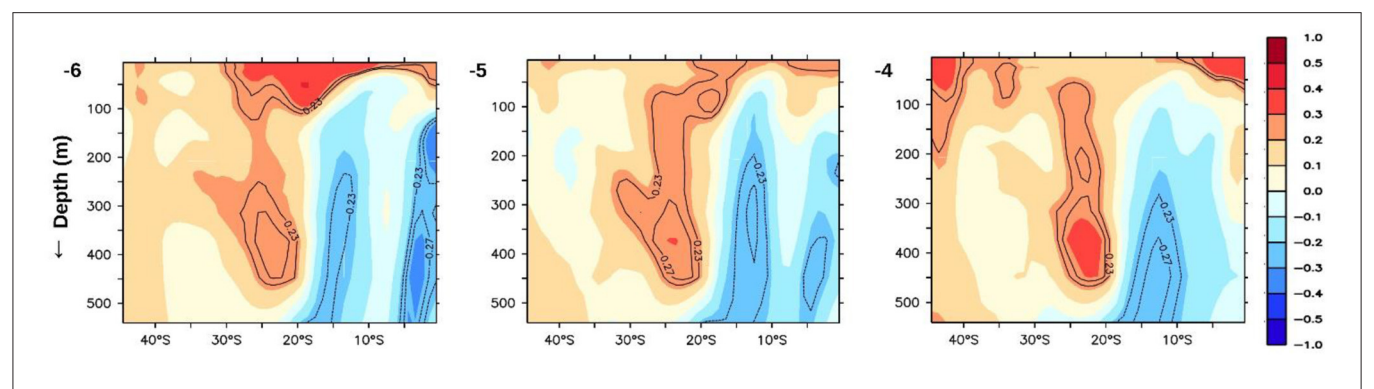


FIGURE 5 | Vertical distribution of anomaly correlation of IODMI with previous years' subsurface temperatures, averaged annually over longitudes 50–100°E. Significant correlations at 90% confidence (0.23) and at 95% confidence (0.27) are contoured.

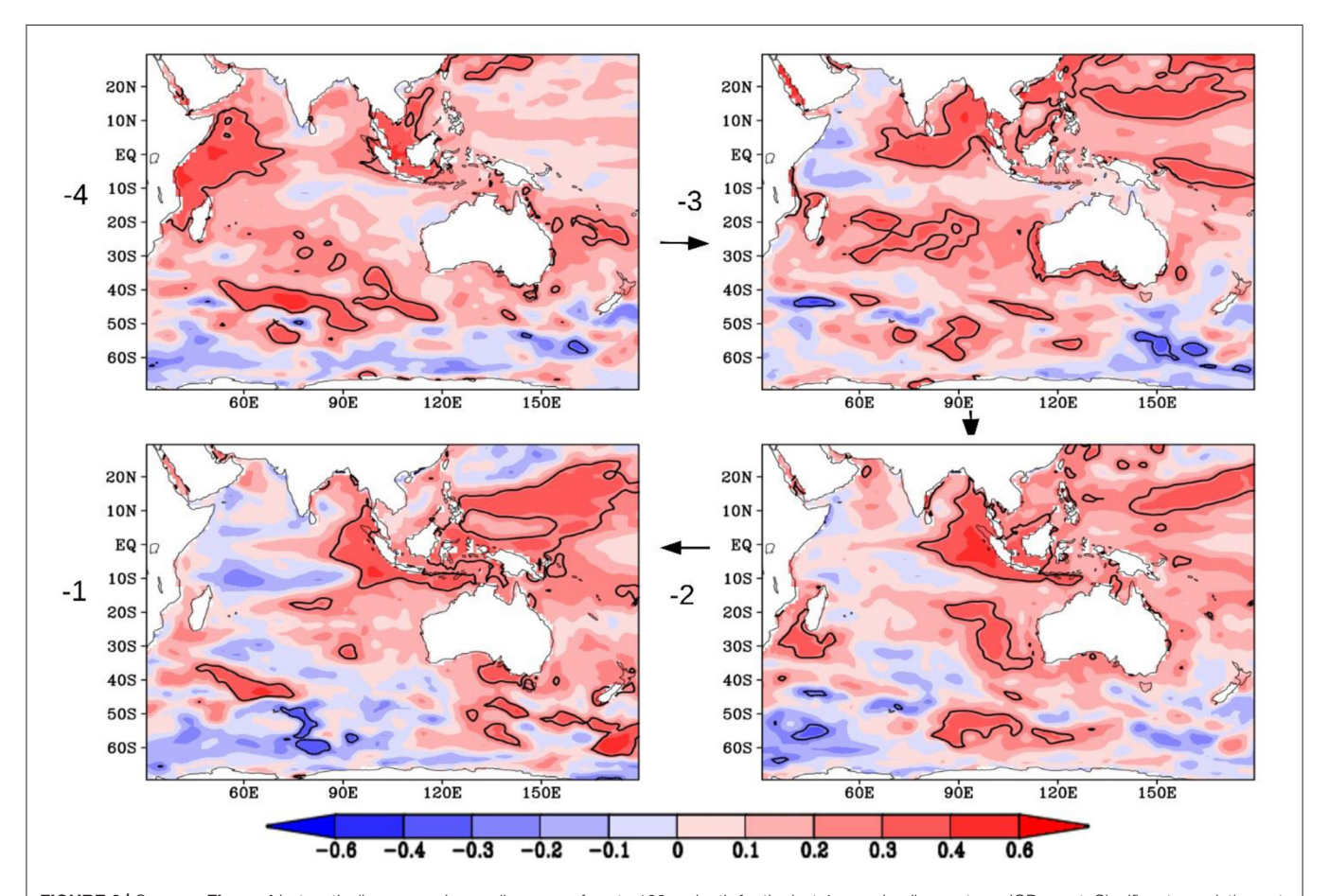


FIGURE 6 | Same as Figure 4 but vertically averaged annually over surface to 100 m depth for the last 4 years leading up to an IOD event. Significant correlations at 95% confidence are shown as contour lines (value at 0.27).

the IODMI, higher than the 17-month lead skills for the ENSO, a leading climate driver. The physical processes responsible for the skill levels seems to originate in the Southern Ocean up to a decade before emerging in the Indian Ocean, suggesting that this multi-year skill could be extended even further. To our knowledge, this is the first study to show decadal skill in predicting the IOD.

Skill levels for surface fields and, in particular, rainfall, are not statistically indistinguishable from zero. This is in common with long-term predictions of other climate phenomena (Scaife and Smith, 2018) and indicates the relative immaturity of this form of forecasting. It remains a challenge to both improve models and to fully exploit decadal prediction skill. Nevertheless, the potential for long-term planning in both public and private sector

organizations that could be facilitated by such skillful predictions is great.

DATA AVAILABILITY STATEMENT

The original contributions presented in the study are included in the article/**Supplementary Material**, further inquiries can be directed to the corresponding authors.

AUTHOR CONTRIBUTIONS

FF, KA, and MC formulated the hypothesis and co-wrote the manuscript. FF conducted the analyses. All authors reviewed the final version of the manuscript.

REFERENCES

- Ashok, K., Chan, W.-L., Motoi, T., and Yamagata, T. (2004). Decadal variability of the Indian Ocean dipole. Geophys. Res. Lett. 31:L24207. doi:10.1029/2004GL021345
- Ashok, K., Guan, Z., and Yamagata, T. (2003). Influence of the Indian Ocean Dipole on the Australian winter rainfall. Geophys. Res. Lett. 30:1821. doi:10.1029/2003GL017926
- Ashok, K., Guan, Z. Y., and Yamagata, T. (2001). Impact of the Indian Ocean Dipole on the relationship between the Indian monsoon rainfall and ENSO. Geophys. Res. Lett. 28, 4499–4450. doi: 10.1029/2001GL013294
- Ashok, K., and Saji, N. H. (2007). On the impacts of ENSO and Indian Ocean dipole events on sub-regional Indian summer monsoon rainfall. *Nat. Hazards*. 42, 273–285. doi: 10.1007/s11069-006-9091-0
- Balmaseda, M. A., Mogensen, K., and Weaver, A. T. (2013). Evaluation of the ECMWF ocean reanalysis system ORAS4. QJR Meteorol. Soc. 139, 1132–1161. doi: 10.1002/qj.2063
- Barnston, A. G., Tippett, M. K., L'Heureux, M. L., Shuhua, L., and DeWitt, D. G. (2012). Skill of real-time seasonal ENSO model predictions during 2002-11: is our capability increasing? *Bull. Amer. Meteor. Soc.* 93, 631–651. doi: 10.1175/BAMS-D-11-00111.1
- Behera, S., Luo, J., and Masson, S. (2005). Paramount impact of the Indian Ocean dipole on the East African short rains: a CGCM study. *J. Clim.* 18, 4514–4530. doi: 10.1175/JCLI3541.1
- Behera, S. K., Luo, J. J., Masson, S., Rao, S. A., Sakuma, H., and Yamagata, T. (2006). A CGCM study on the interaction between IOD and ENSO. *J. Clim.* 19, 1608–1705. doi: 10.1175/JCLI3797.1
- Boer, G. J., Smith, D., Cassou, C., Doblas-Reyes, F., Danbasoglu, G., Kirtman, B., et al. (2016). The decadal climate prediction project (DCPP) contribution to CMIP6. Geosci. Model. Dev. 9, 3751–3777. doi: 10.5194/gmd-9-3751-2016
- Cai, W. J., van Rensch, P., Cowan, T., and Hendon, H. H. (2011). Teleconnection pathways of ENSO and the IOD and the mechanisms for impacts on Australian rainfall. J. Climate. 24, 3910–3923. doi: 10.1175/2011JCLI4129.1
- Chan, S., Behera, S., and Yamagata, T. (2008). Indian Ocean dipole influence on South American rainfall. Geophys. Res. Lett. 35:L14SL12 doi: 10.1029/2008GL034204
- Delworth, T. L., Broccoli, A. J., Rosati, A., Stouffer, R. J., Balaji, V., Beesley, J. A., et al. (2006). GFDL's CM2 global coupled climate models. Part I: formulation and simulation characteristics. J. Climate. 19, 643–74. doi: 10.1175/JCLI3629.1
- Doi, T., Behera, S. K., and Yamagata, T. (2016). Improved seasonal prediction using the SINTEX-F2 coupled model. J. Adv. Model. Earth Syst, 8, 1847–1867. doi: 10.1002/2016MS000744
- Dutta, R., and Maity, R. (2018). Temporal evolution of hydroclimatic teleconnection and long-lead prediction of Indian summer monsoon rainfall using time varying model. Sci. Rep. 8:10778. doi: 10.1038/s41598-018-28972-z
- Farneti, R. (2017). Modelling interdecadal climate variability and the role of the ocean. Wiley Interdiscip. Rev. Climate Change. 8:e441. doi: 10.1002/wcc.441

FUNDING

FF thanks MC and NERC/MoES SAPRISE project (NE/I022841/1) for the travel grant to visit MetOffice, UK. FF acknowledges CSIR for the JRF & SRF fellowship. FF also thanks C T Tejavath for assistance in data processing.

SUPPLEMENTARY MATERIAL

The Supplementary Material for this article can be found online at: https://www.frontiersin.org/articles/10.3389/fclim. 2021.736759/full#supplementary-material

- Gualdi, S., Navarra, A., Guilyardi, E., and Delecluse, P. (2003). Assessment of the tropical Indo-Pacific climate in the SINTEX CGCM. Ann. Geophys. 46, 1–26 doi: 10.4401/ag-3385
- Ha, K.-J., Chu, J.-E., Lee, J.-Y., and Yun, K.-S. (2017). Interbasin coupling between the tropical Indian and Pacific Ocean on inter annual timescale: observation and CMIP5 reproduction. Clim. Dyn. 48, 459–475. doi: 10.1007/s00382-016-3087-6
- Hardiman, S. S., Dunstone, N. J., Scaife, A., Smith, D. M., Knight, J. R., Davies, P., et al. (2020). Predictability of European winter 2019/20: Indian Ocean dipole impacts on the NAO. Atmos. Sci. Lett. 21:e1005. doi: 10.1002/asl.1005
- Iizuka, S., Matsuura, T., and Yamagata, T. (2000). The Indian Ocean SST dipole simulated in a coupled general circulation model. *Geophys. Res. Lett.* 27, 3369–3372. doi: 10.1029/2000GL011484
- Izumo, T., Vialard, J., Lengaigne, M., de Boyer Montégut, C., Behera, S., Luo, J.J., et al. (2010). Influence of the state of the Indian Ocean dipole on following year's El Niño. *Nat. Geosci.* 3, 168–172. doi: 10.1038/ngeo760
- Jourdain, N. C., Sen Gupta, A., Taschetto, A. S., Ummenhofer, C. C., Moise, A. F., and Ashok, K. (2013). The Indo-Australian monsoon and its relationship to ENSO and IOD in reanalysis data and the CMIP3/CMIP5 simulations. Clim. Dynam. 41, 3073–3102. doi: 10.1007/s00382-013-1676-1
- Luo, J.-J., Masson, S., Behera, S., and Yamagata, T. (2007). Experimental forecasts of the Indian Ocean dipole using a coupled OAGCM. J. Clim. 20, 2178–2190, doi: 10.1175/JCLI4132.1
- Luo, J.-J., Zhang, R., Behera, S. K., Masumoto, Y., Jin, F.-F., Lukas, R., et al. (2010). Interaction between El Niño and extreme Indian Ocean dipole. J. Clim. 23, 726–742. doi: 10.1175/2009JCLI3104.1
- Marathe, S., Terray, P., and Karumuri, A. (2021). Tropical Indian Ocean and ENSO relationships in a changed climate. *Clim. Dynam.* 56, 3255–3276. doi:10.1007/s00382-021-05641-y
- Meehl, G., and Arblaster, J. (2001). The tropospheric biennial oscillation and Indian monsoon rainfall. *Geophys Res Lett.* 28, 1731–1734. doi: 10.1029/2000GL012283
- Meehl, G. A., Goddard, L., Boer, G., Burgman, R., Branstator, G., Cassou, C., et al. (2014). Decadal climate prediction an update from the trenches. *Bull. Am. Meteorol. Soc.* 95, 243–267. doi: 10.1175/BAMS-D-12-00241.1
- Meehl, G. A., Goddard, L., Murphy, J., Boer, G., Danabasoglu, G., Dixon, K. W., et al. (2009). Can It Be Skillful? Bull. Am. Meteorol. Soc. 90, 1467–1486. doi: 10.1175/2009BAMS2778.1
- Merryfield, W. J., Lee, W.-S., Boer, G. J., Kharin, V. V., Scinocca, J. F., Flato, G. M., et al. (2013). The Canadian Seasonal to interannual prediction system. Part I: models and initialization. *Mon. Wea. Rev.* 141, 2910–2945. doi: 10.1175/MWR-D-12-00216.1
- Murtugudde, R., McCreary, J. P., and Busalacchi, A. J. (2000). Oceanic processes associated with anomalous events in the Indian Ocean with relevance to 1997-98. *J. Geophys. Res.* 105, 3295–3306. doi: 10.1029/1999JC900294
- Nauw, J. J., van Aken, H. M., Webb, A., Lutjeharms, J. R. E., and de Ruijter, W. P. M. (2008). Observations of the southern East Madagascar Current

- and undercurrent and countercurrent system. J. Geophys. Res. 113:C08006. doi: 10.1029/2007JC004639
- Pal, M., Maity, R., Ratnam, J. V., Nonaka, M., and Behera, S. K. (2020). Long-lead prediction of ENSO modoki index using machine learning algorithms. Sci. Rep. 10:365. doi: 10.1038/s41598-019-57183-3
- Park, J. H., Kug, J. S., Li, T., and Behera, S. K. (2018). Predicting El Niño beyond 1-year lead: effect of western hemisphere warm pool. Sci. Rep. 8:14957. doi: 10.1038/s41598-018-33191-7
- Rayner, N. A., Parker, D. E., Horton, E.B., Folland, C. K., Alexander, L. V., Rowell, D. P., et al. (2003). Global analyses of sea surface temperature, sea ice, and night marine air temperature since the late nineteenth century. *J. Geophys. Res. Atmosp.* 108:4407. doi: 10.1029/2002JD002670
- Saji, N. H. (2018). "The Indian Ocean Dipole," in Oxford Research Encyclopedia of Climate Science, ed H. von Storch (Oxford: Oxford University Press).
- Saji, N. H., Goswami, B. N., Vinayachandran, P. N., and Yamagata, T. (1999). A dipole mode in the tropical Indian Ocean. *Nature* 401, 360–363. doi:10.1038/43854
- Saji, N. H., and Yamagata, T. (2003). Possible impacts 209 of Indian Ocean dipole mode events on global climate. Clim. Res. 25:151–169. doi: 10.3354/cr025151
- Scaife, A. A., and Smith, D. (2018). A signal-to-noise paradox in climate science. NPJ Clim. Atmos. Sci. 1:28. doi: 10.1038/s41612-018-0038-4
- Shinoda, H., Hendon, H., and Alexander, M. A. (2004). Surface and subsurface dipole variability in the Indian Ocean and its relation with ENSO. *Deep-Sea Res.* 51, 619–635. doi: 10.1016/j.dsr.2004.01.005
- Smith, D. M., Scaife, A. A., Boer, G. J., Caian, M., Guemas, V., Hawkins, E., et al. (2013). Real-time multi-model decadal climate predictions. *Clim. Dyn.* 41, 2875–2888. doi: 10.1007/s00382-012-1600-0
- Sun, Q., Bo, W. U., Zhou, T. J., and Yan, Z. X. (2018). ENSO hindcast skill of the IAP-DecPreS near term climate prediction system: comparison of full field and anomaly initialization. *Atmos. Oceanic Sci. Lett.* 11, 54–62, doi:10.1080/16742834.2018.1411753
- Swapna, P., Roxy, M. K., Aparna, K., Kulkarni, K., Prajeesh, A. G., Ashok, K., et al. (2015). The IITM earth system model: transformation of a seasonal prediction model to a long term climate model. *Bull. Am. Meteorol. Soc.* 96, 1351–1368. doi: 10.1175/BAMS-D-13-00276.1
- Tang, Y., Rong-Hua, Z., Ting, L., Wansuo, D., Dejian, Y., Fei, Z., et al. (2018).
 Progress in ENSO prediction and predictability study. *Natl. Sci. Rev.* 5, 826–839.
 doi: 10.1093/nsr/nwy105
- Tanizaki, C., Tozuka, T., Doi, T., and Yamagata, T. (2017). Relative importance of the processes contributing to the development of SST anomalies in the eastern pole of the Indian Ocean Dipole and its implication for predictability. *Clim. Dyn.* 49, 1289–1304. doi: 10.1007/s00382-016-3382-2
- Taylor, K. E., Stouffer, R. J., and Meehl, G. A. (2012). An overview of CMIP5 and the experiment design. Bull. Amer. Meteor. Soc. 93, 485–498. doi: 10.1175/BAMS-D-11-00094.1
- Tozuka, T., Luo, J. J., Masson, S., and Yamagata, T. (2007). Decadal modulations of the Indian Ocean Dipole in the SINTEX-F1coupled GCM. *J. Clim.* 20, 2881–2894. doi: 10.1175/JCLI4168.1

- Trenberth, K. E. (1997). The definition of El Niño. Bull. Am. Met. Soc. 78, 2771–2778. doi: 10.1175/1520-0477(1997)078<2771:TDOENO>2.0.CO;2
- von Storch, H., and Zwiers, F. W. (1999). Statistical Analysis in Climate Research (Cambridge: Cambridge University Press), 484.
- Wajsowicz, R. C. (2005). Potential predictability of tropical Indian Ocean SST anomalies. Geophys. Res. Lett. 32:L24702. doi: 10.1029/2005GL024169
- Wang, W., Zhu, X., Wang, C., and Köhl, A. (2014). Deep meridional overturning circulation in the Indian Ocean and its relation to Indian Ocean Dipole. J. Clim. 27, 4508–4520. doi: 10.1175/JCLI-D-13-00472.1
- Watanabe, M., Suzuki, T., O'ishi, R, Komuro, Y., Watanabe, S., Emori, S., et al. (2010). Improved climate simulation by MIROC5: mean states, variability, and climate sensitivity. J. Clim. 23, 6312–6335. doi: 10.1175/2010JCLI3679.1
- Webster, P. J., Moore, A., Loschnigg, J., and Leban, M. (1999). Coupled dynamics in the Indian Ocean during 1997-1998. Nature 401, 356–360. doi: 10.1038/43848
- Wu, T., Li, W., Ji, J., Xin, X., Li, L., Wang, Z., et al. (2013). Global carbon budgets simulated by the Beijing climate center climate system model for the last century. J. Geophys. Res. Atmos. 118, 4326–4347. doi: 10.1002/jgrd.50320
- Yamagata, T., Behera, S., Rao, S., Guan, Z. Y., Ashok, K., and Hameed, S. (2003).
 Comments on Dipoles, temperature gradients, and tropical climate anomalies.
 Bull. Am. Meteorol. Soc. 84, 1418–1422. doi: 10.1175/BAMS-84-10-1418
- Yamagata, T., Behera, S. K., Luo, J.-J., Masson, S., Jury, M., and Rao, S. A. (2004). "Coupled ocean-atmosphere variability in the tropical Indian Ocean," in: Earth Climate: The Ocean-Atmosphere Interaction, eds. C. Wang, S.-P. Xie, and J. A. Carton (Washington, DC: AGU), 189–212.
- Yeager, S., Karspeck, A., Danabasoglu, G., Tribbia, J., and Teng, H. (2012). A decadal prediction case study: late twentieth century North Atlantic Ocean heat content. J. Clim. 25, 5173–5189. doi: 10.1175/JCLI-D-11-00595.1
- Zhang, S., Harrison, M. J., Rosati, A., and Wittenberg, A. T. (2007). System design and evaluation of coupled ensemble data assimilation for global oceanic climate studies. *Monthly Weather Rev.* 135, 3541–3564. doi: 10.1175/MWR3466.1

Conflict of Interest: The authors declare that the research was conducted in the absence of any commercial or financial relationships that could be construed as a potential conflict of interest.

Publisher's Note: All claims expressed in this article are solely those of the authors and do not necessarily represent those of their affiliated organizations, or those of the publisher, the editors and the reviewers. Any product that may be evaluated in this article, or claim that may be made by its manufacturer, is not guaranteed or endorsed by the publisher.

Copyright © 2021 Feba, Ashok, Collins and Shetye. This is an open-access article distributed under the terms of the Creative Commons Attribution License (CC BY). The use, distribution or reproduction in other forums is permitted, provided the original author(s) and the copyright owner(s) are credited and that the original publication in this journal is cited, in accordance with accepted academic practice. No use, distribution or reproduction is permitted which does not comply with these terms.